The Role of Histone Variant H3.3 in Cortical Development

by

Owen Funk

A dissertation submitted in partial fulfillment
of the requirements for the degree of
Doctor of Philosophy
(Human Genetics)
in the University of Michigan
2021

Doctoral Committee:

Associate Professor Kenneth Y. Kwan, Chair
Associate Professor Dawen Cai
Associate Professor Shigeki Iwase
Associate Professor Stephen Parker
Professor Bing Ye

Owen H. Funk

ofunk@umich.edu

ORCID iD: 0000-0001-6524-6958

Acknowledgements

There are too many people to thank for helping me through my entire PhD career, but I'll try and thanks as many as I can. I thank my dear partner Bree Doering for all the care and encouragement throughout the years, for the countless adventures and quiet nights in, and for the endless patience with all my complaints and problems. I couldn't have done any of this without the love and support of my family, my parents Ray and Kate and sister Emma encouraged me all along the way. I thank my dear friends Jacob Johnson, Alison Ho, Daniel Kowalsky, Paloma Garcia and Andrew Schwartz. You were invaluable friends throughout the PhD process, from Genetics 541 to a wedding in Taiwan.

I thank the entire Kwan lab, members past and present for teaching me every day and creating the best possible lab environment that kept me coming back, even on weekends, holidays and late nights. Thanks to Adel and Yaman Qalieh for teaching me just about everything I know about Python, R, and Unix, and for fielding my endless computational questions day or night. Thanks to Jason Keil and Dan Doyle, you've been incredible colleagues and friends, and destined for great things. Thanks to Mandy for endless encouragement and time spent teaching me all the technical skills I have.

I thank my mentor and friend Ken Kwan, who believed in me from the start, and had I not met Ken in a Yale coffee shop in 2013 I would not be in science today. His obvious passion and enthusiasm for science was inescapable, and was an exceptional

example to strive towards. I've been fortunate to have numerous fantastic mentors over my life, but none that cared as much about my success and growth as Ken, and I owe a great deal of any accomplishment in science to him. He gave me the tools to think critically about the brain and genome, and his boundless curiosity inspires me to do thoughtful, meaningful science every day.

Many thanks to everyone in department of human genetics for creating an exceptional learning environment, and constantly challenging me to think deeper and work harder with their inspiring science. I thank my thesis committee, Dr. Bing Ye, Dr. Dawen Cai, Dr. Stephen Parker, and Dr. Shigeki Iwase for invaluable advice and feedback in driving this project forward, and for the patience and understanding to help me switch gears from my original plan and still put together an impactful body of work.

Table of Contents

List of Figures

List of Abbreviations

bp	base pairs
CP	Cortical plate
dKO	Double knockout
dKO-E	Double knockout via *Emx1*^{Cre}
dKO-N	Double knockout via *Neurod6* ^{Cre}
dKO-R	Double knockout via *Rbp4* ^{Cre}
L2-4	Layers 2-4
L5	Layer 5
L6	Layer 6
NPC	Neural progenitor cell
PTM	Post translational modification
RD	Replication dependent
RI	Replication independent
SP	Subplate
SV	Structural variants
SVZ	Subventricular zone
VZ	Ventricular zone

Abstract

The vast amount of information contained in the genome is organized and packaged by chromatin into a cell's nucleus. This chromatin is composed of protein complexes called nucleosomes, made up of histone proteins that can regulate accessibility and functionality of the underlying DNA. Canonical histones are synthesized and deposited during S-phase in a replication-coupled manner, meeting the demand for a massive number of new histones to package the newly synthesized DNA. There are also multiple variant histones, and these variants are thought to have different impacts on the DNA they bind. These variants can be deposited DNA synthesis-independently and provide replacement histones in terminally post-mitotic cells, including neurons. Encoded by two separates genes *H3f3a* and *H3f3b*, H3.3 is expressed throughout the cell cycle, and incorporates preferentially at enhancers, promoters, and gene bodies, suggestive of a function in gene regulation. H3.3 is known to play a role in developmental processes, including neural crest cell differentiation, gametogenesis, and zygotic genome activation. In the brain, silencing of H3.3 genes by RNA interference leads to deficits in neuronal layer distribution, activity- and environmental enrichment-induced gene expression, and memory

Here, I leverage stage-dependent deletion of H3.3 genes from: 1) cycling neural progenitor cells, 2) neurons immediately after terminal mitosis, or 3) several days later, revealing the first post-mitotic days to be a critical window for *de novo* H3.3. Despite ubiquitous expression of H3.3 throughout cell types and the cell cycle, newborn cortical

neurons undergo substantial *de novo* accumulation of H3.3 after becoming terminally post-mitotic. Deletion of H3.3 prior to this critical window abrogated this accumulation and had a profound impact on the establishment of the neuronal transcriptome. H3.3 is known to play a role in cell state transition, and the genes found to be most affected were typically upregulated across development, and often associated with a bivalent or “poised” promoter in neural progenitors. Coincident with these transcriptomic changes, I observed severe deficits in the formation of cortical axon tracts, including agenesis and misrouting of key intracortical connections and complete loss of the cortical spinal tract. Neuronal identity was also affected, and the typical laminar identity of deep-layer projection neurons failed to undergo normal refinement, resulting in mixed identities.

After H3.3 accumulation within this developmental window, co-deletion of *H3f3a* and *H3f3b* caused progressive loss of H3.3 over several months without significant disruption of the transcriptome. The loss of H3.3 was not accompanied by an observable decrease in overall H3 levels or in H3 PTMs. Through this work I uncovered the potential existence of a non-H3.3 source of H3 that can compensate for the loss of H3.3 once the neuronal transcriptome is established, but not before.

My work uncovers an active role of H3.3 in establishing transcriptional landscape and molecular identity in developing neurons immediately post-mitosis that is distinct from its role in maintaining histone H3 levels over the neuronal lifespan. These findings lead to further questions on the importance of H3.3 vs. histone turnover, and has important implications for histone variant regulation of developmental processes.

Chapter 1 Cortical Neurogenesis

Thesis Overview

My doctoral research explores the roles the histone variant H3.3 plays in shaping neuronal development in the cerebral neocortex. In the first chapter, I lay out current understanding of the exquisite organization of the cortex, as well as a brief overview of the developmental processes responsible for its formation. In chapter two, I highlight key differences in canonical and non-canonical H3, as well as the impact these differences have on their respective functions and the resulting chromatin profiles once incorporated into DNA-bound nucleosomes. In chapter three, I present my research efforts on the effects of H3.3 deletion from the developing cortex using conditional knockout mouse models. I find that H3.3 plays an active role during a critical developmental window in which it is important for developmental acquisition of neuronal transcriptome, identity, and axonal projection. In chapter four, I expand upon my initial findings, investigating the role of H3.3 several days after exit from the cell cycle and into late maturity. These experiments define a distinct role for H3.3 in maturing neurons, where it is largely dispensable for the major phenotypes discovered in chapter three, but plays a long-term role maintaining H3 levels over the neuronal lifespan. Through this work I also uncover a surprising finding that in H3.3 knockout neurons, H3.3 is progressively depleted whereas overall H3 levels are maintained, suggesting an alternative source of post-mitotic H3.

Chapter five concludes with thoughts and perspectives on my exploration of distinct H3.3 roles within neurons, as well as possible avenues of future research.

Organization of the Neocortex

The higher cognitive functions that define humans as a unique species, including speech and language, decision making, and emotional and social processing, are centered in the neocortex, which is thought to be an important advance in mammalian evolution (1). The emergence of these higher functions during evolution was accompanied by structural changes in the neocortex, and the acquisition of areal specializations. Disordered cortical development has been implicated in many pathologies including schizophrenia, bipolar disorder, autism, and pediatric cancer. Understanding the fundamental mechanisms of neuronal development remains a goal at the forefront of research efforts and will enable a greater understanding of the genesis of humans' remarkable capabilities, as well as the different ways development can be disrupted.

Structural

The brain, and in particular the cortex have undergone an incredible expansion across evolutionary time in mammals and to a greater extent in primates. The neocortex underlies not only remarkable motor and sensory capabilities, but also some of our most distinctly human cognitive functions. To accomplish these complex and diverse tasks, it has developed exquisite organization and connectivity, both within and beyond the cortex. The cortex is organized into six cytoarchitechtonically distinct horizontal layers (**Fig. 1.1**) (2-4). Within each of these six layers, there is stereotypical connectivity to other cortical and subcortical structures, dictating the many functions of individual layers. There is

further tangential arealization of the cortex, primarily associated with separation of functions: motor, sensor and association (5, 6).

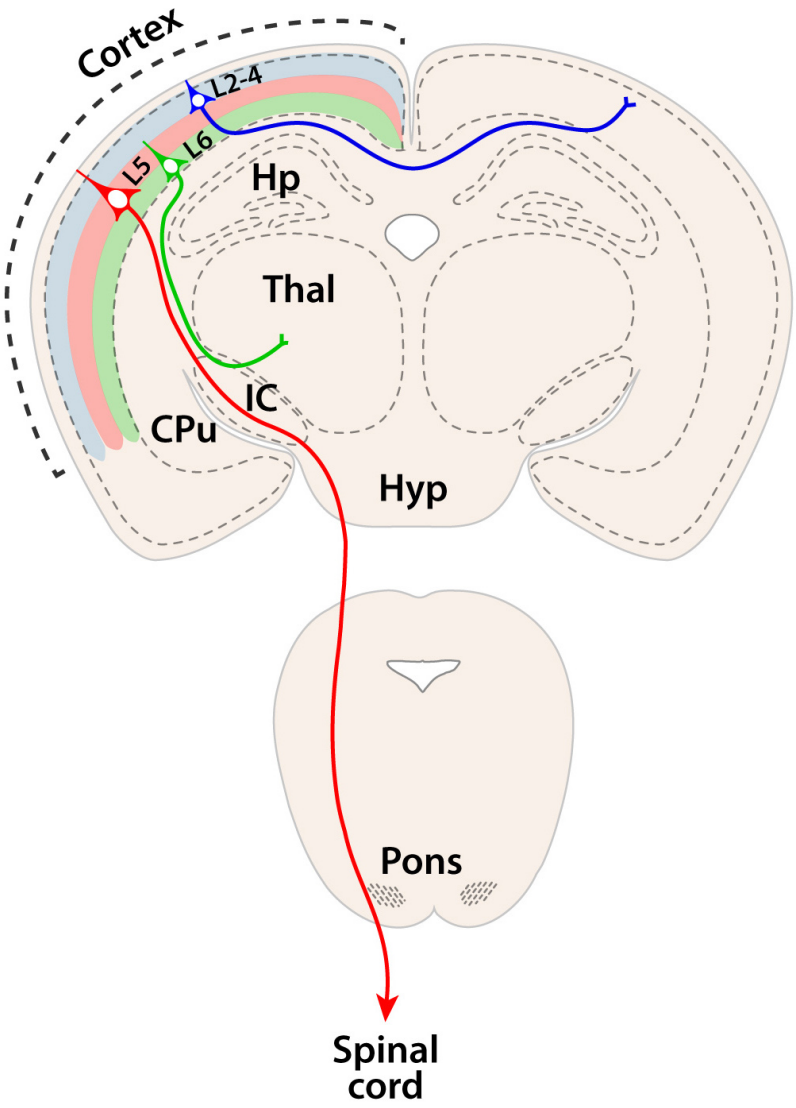

Figure 1.1 The six-layered neocortex enables complex connectivity

The neocortex occupies the outermost layer of the brain, composed of six horizontal laminae, with stereotypical connectivity. Upper layers (L2-4) from cortico-cortical connections, connecting the hemispheres dorsally through the corpus callosum (blue axon) and more ventrally through the anterior commissure. Deep layers (L5-6) project corticofugally outside the cortex, allowing for communication with the rest of the body.

Hp: hippocampus, Thal: thalamus, IC: internal capsule, CPu: caudate putamen, Hyp: hypothalamus, L2-4: layer 2-4, L5: layer 5, L6: layer 6

Cell Types

Given the vast array of functions the cortex serves, the cells within this organ display a similar myriad of identities (7, 8). The neurons that reside within the cortex fall into two broad classification, excitatory glutamatergic neurons and inhibitory GABAergic neurons (9, 10). Excitatory neurons make up the majority of neurons within the cortex and project long-range axonal connections that link the cortex to itself as well as other brain regions. Most of cortical glutamatergic neurons are highly polarized pyramidal cells, with a single apical dendrite extending dorsally, several smaller basal dendritic outgrowths, and a single axon extending ventrally from the base of the cell and into the white matter (11). To ensure proper function of these projection cells, inhibitory neurons project locally and synapse onto excitatory cells to exert a modulatory effect. Within inhibitory neurons there are also many classifications of cells, from chandelier to basket neurons and others, each with their own unique connectivity, morphology, and function (12, 13).

The cortex is home to several non-neuronal cell types as well. Oligodendrocytes provide the myelin sheath to nearby neurons, insulating their axons in segments (14). Microglia serves as the brain's macrophages, clearing cellular debris as well as pruning synapses during development (15, 16). Astrocytes play a broad supportive role, facilitating synaptic function, protecting neurons from oxidative stress and controlling the blood brain barrier (17).

Connections

The organizing principles of the cortex include not only the cell types within each area, but also their connectivity (**Fig. 1.1**) (18-20). Upper-layer neurons, those in layers 2-4, form intracortical connections within the ipsilateral hemisphere and to the

contralateral hemisphere via the corpus callosum (21, 22). Intracortical neurons also form the anterior commissure, another corticocortical connection connecting the lateral cortical hemispheres as well as the amygdala (23). Layer 5 cells project primarily to a number of subcortical targets; striatum, thalamus, brainstem, and spinal cord forming the corticospinal tract (21). Most layer 6 cells project to the thalamus, through the corticothalamic tract. Miswiring of these circuits is thought to contribute to neurodevelopment disorders (24) and the study of tract formation and regulation remains an important topic in the field.

Development

In the mouse, cortical neurogenesis begins around embryonic day (E)11 and continues until day E17 (**Fig. 1.2**). Early neurodevelopment is characterized by symmetrically dividing neural progenitor cells (NPCs), which are restricted to the ventricular zone (VZ) (25). Starting at E11 some of these NPCs transition to radial glia, and begin the process of asymmetrical division, in which one daughter cell goes on to become a neuron and the other maintains its proliferative capacity (26, 27). This division is accompanied by migration of the two cells, with the newborn neuron migrating dorsally along radial glial scaffolds to settle into the nascent cortical plate (CP) and the NPC remaining in the VZ.

This formation of the CP happens in an inside-out fashion. The first-born neurons form the transient preplate, which then splits into the marginal zone and subplate, a ventral layer involved in directing the flow of newborn neurons into the six horizontal laminae. The next wave of cortical neurons born migrates into layer 6, followed by a subsequent round that migrates past the L6 neurons to form layer 5. This continues with

the newborn neurons traveling dorsally past the older, deeper layers until all six are formed, around day E17. After the excitatory neurons are specified, neurogenesis from cortical NPCs switches to gliogenesis, giving rise primarily to astrocytes (**Fig 1.2**).

Once formed during asymmetrical division, projection neurons begin the processes of migration and differentiation. Initially they travel upward, through the sub ventricular zone (SVZ) and intermediate zone en route to their final location along scaffolding formed by radial glial processes (28, 29). Newly post-mitotic, neurons undergo a series of dramatic transcriptional changes that instigate the transition to their destined morphology, connectivity, and function (30-32). While the excitatory neurons arise from progenitors residing in the VZ and migrate dorsally, inhibitory neurons are born in the ganglionic eminences, and migrate tangentially to integrate into the developing cortex (33, 34).

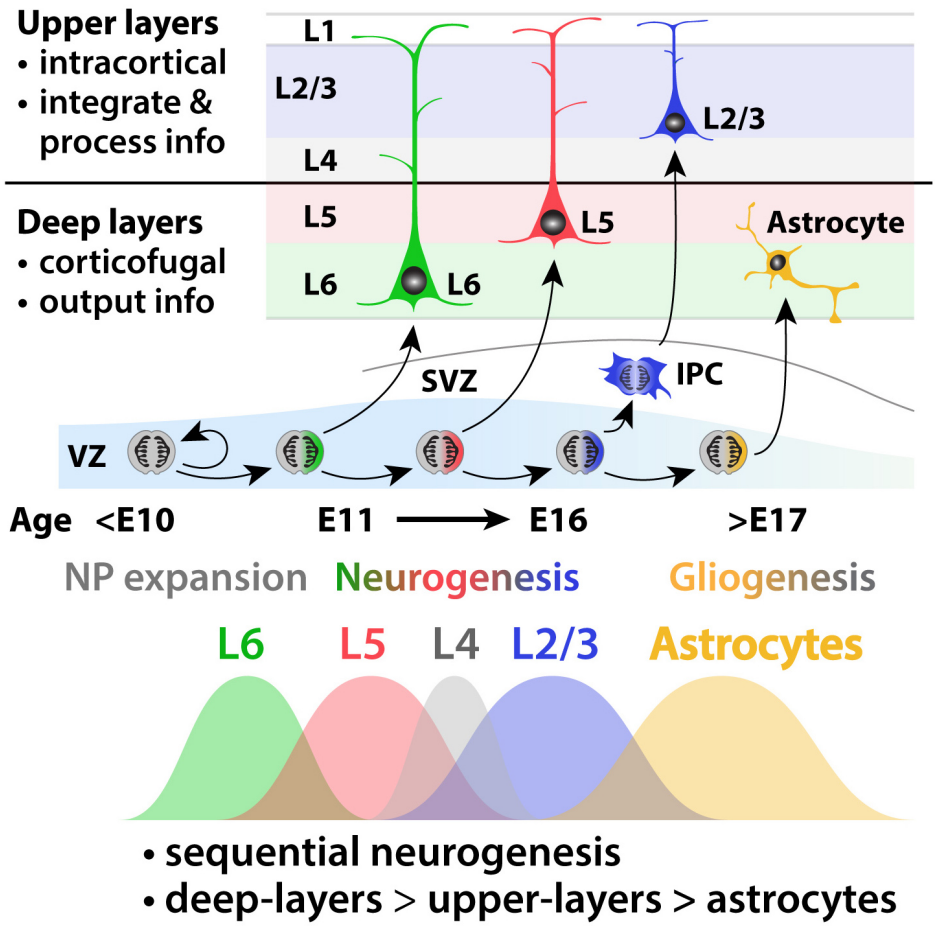

Figure 1.2 The neocortex develops by sequential neurogenesis

Neural Progenitor Cells (NPCs) first divide symmetrically (<E11) to expand the total pool of stem cells in the brain. These NPCs then transition to asymmetric division, producing one neuron and one stem cell in a process termed sequential neurogenesis. Cortical neurons are born in an inside-out manner, with L6 being generated first, followed by L5, L4 and so on. As they are born, these cells migrate dorsally passed the older, deeper layered to form more ventral layers. After the formation of L2, the NPC pool transitions to gliogenesis.

L1: layer 1, L2/3: layer 2/3, L4: layer 4, L5: layer 5, L6: layer 6, VZ: ventricular zone, SVZ: subventricular zone, IPC: intermediate progenitor cell

Acquisition of Neuronal Identity

The mechanisms and timing of neural fate specification are still an active topic of research. Some of the primary differentiators are transcription factors exclusive to layers and cell types, and their expression is thought to play a large part in the specification of different populations of neurons (**Figure 1.3**). Many of these factors have also been found to be key drivers of characteristic connectivity and function of their respective cell types, without which laminar organization and brain function can be disrupted (35-39).

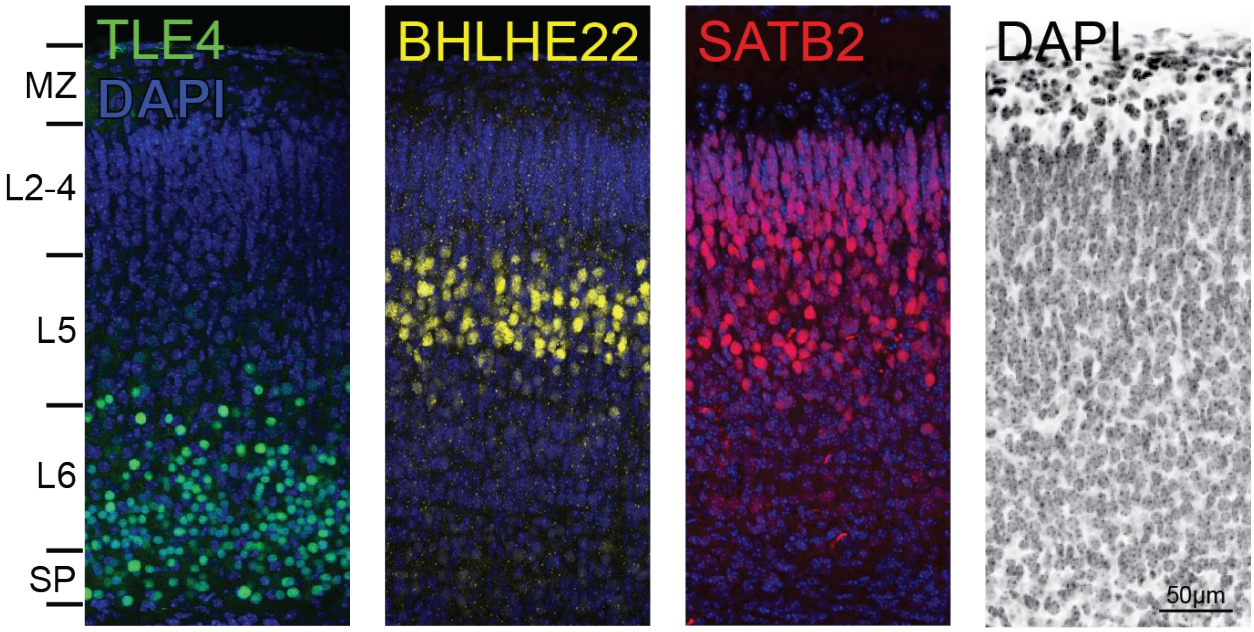

Figure 1.3 Cortical layer markers help define distinct regions

The Cortex is divided into six cytoarchitectonically distinct laminae, and each layer has stereotypic connectivity and function. The cells that populate these layers express transcription factors and other genes that are unique to one or several layers, and often help to define that layers functionality. *Tle4* is exclusive to layer 6 neurons, *Bhlhe22* to layer 5 cells, and *Satb2* is found to label almost all upper layer, 2-4 cells as well as many of the large corticofugal neurons of layer 5.
MZ: Marginal Zone, SP: Subplate

Differentiation

The time immediately following the terminal mitosis is an important period of molecular identity acquisition and refinement for new neurons (40, 41). Epigenetic modifications and chromatin remodeling are thought to contribute to rewiring the transcriptome to establish cellular identity during neurogenesis (42, 43). Early work suggested that NPCs underwent progressive fate restriction, limiting the potential cell types they could produce as neurogenesis progressed. Recent work has called this idea into question via heterochronic transplantation studies, demonstrating an ability for late-development progenitors to regain the ability to produce early-development neurons (44). Intermediate progenitors, however, have been shown to be fate restricted, suggesting that in some cell types there is indeed a point at which they become irreversibly committed. Thus, the well-choreographed set of triggers that determine temporal cell fate in the cortex allows some flexibility up to a point. Even once fate-restricted, there remains post-mitotic refinement in neurons that continues to shape and mature cellular identity.

Refinement

Even after a neuron becomes post-mitotic and starts to express neuronal specific factors, its fate is not set in stone. Post-mitotic refinement processes continue to operate to fine tune layer identity. For example, newly born deep-layer neurons co-express Layer 5 (L5) and Layer 6 (L6) markers at first, and over the first post-mitotic days undergo refinement to acquire their distinct identities (45, 46). This process is mediated in part by SOX5, without which laminar identity is mixed and axonal routing are affected (40). This refinement was also observed in human induced subplate cells that co-expressed disparate cell-type markers past their final division, before undergoing refinement towards

a single fate (47). The mechanisms behind this refinement are still being explored but may involve extra-cellular signaling based on the surrounding environment and changes to the chromatin architecture.

Neuronal cell fate is specified and refined at multiple stages, at the level of NPC, intermediate progenitors, and even after the neurons is born (48). Chromatin remodeling enzymes and complexes are known to play a role in the differentiation of neurons (49). The SWI/SNF remodeling complex can be composed of different set of subunits in different cell types, lending specificity to its function. In the brain, it has been found that during the transition from NPC to neurons, the ATPases Brg and Brm are replaced with BAF45a/b in SWI/SNF (50). This incorporation is necessary for the transition to post-mitotic neurons, and positions chromatin remodeling as critical step in the differentiation process.

Chapter 2 Histone Variant H3.3

Histone Variants

The human genome is made up of six billion base pairs (bp) that must be condensed into a micron scale nucleus. Nucleosomes are the primary substrate on which the DNA is packaged, wrapping the genome into many subdomains to achieve a level of compaction compatible with nuclear size. These nucleosomes are eight membered protein complexes responsible for not only packaging and compaction, but also a fundamental level of regulation of the underlying DNA. Once wrapped around nucleosomes, DNA is protected, not only from damage but also from various cellular factors. To affect the underlying DNA, nucleosomes must be moved, via sliding, exchange, or eviction. This turnover process and to what extent it controls gene regulation is still poorly understood. The manner in which nucleosomes are altered, either through physical displacement or chemical modification of specific amino acid residues is extensively studied to understand this process of genetic regulation on top of the sequence identity of the genome itself.

The nucleosome is composed of two sets of four separate protein subunits termed histones. These histones, H2a, H3b, H3 and H4, form an octamer that facilitates wrapping of DNA in increments of approximately 146 bp. These octamers are built sequentially, first by a pair of H3-H4 dimers combining to form an H3-H4 tetramer. This is followed by binding to the DNA strand, and then recruiting two H2a-H2b dimers to form the full 8

membered complex. Nucleosomes are further connected to each other by the linker histone sub-unit H1 that stabilizes nucleosomes connections as well as the DNA between nucleosomes. Individual histones are made up of two primary regions, the histone fold domain, made up of three α-helical regions that form histone-histone interactions and the unstructured N-terminal tail (51). This tail has several residues that can be post translationally modified through methylation, acetylation, phosphorylation, or even modification by neurotransmitters such as dopamine or serotonin (52, 53). There are dozens of different varieties of these post translational modifications (PTMs) fall within the N-terminal tail that in combination act as regulators of chromatin state and dynamics. These modifications can be added, removed, or interpreted by writer, eraser, and reader enzymes that effect transcriptional regulation and DNA repair (54). The mechanism of action for PTMs is varied and intensely studied, but generally these modifications can attract or repel various cofactors or chromatin “readers” that interact specifically with modified histones. These readers can then recruit further molecular complexes catalyzing cellular processes like DNA repair or transcription. Additionally, histone PTMs can affect greater chromatin super-structure, condensing or relaxing DNA binding by nucleosomes, and influencing intra-chromosomal connections and partitioning. PTMs can function in concert, and the vast number of possible PTM combinations (the “histone code”) create a highly dynamic and exquisitely orchestrated system by which the genome is regulated.

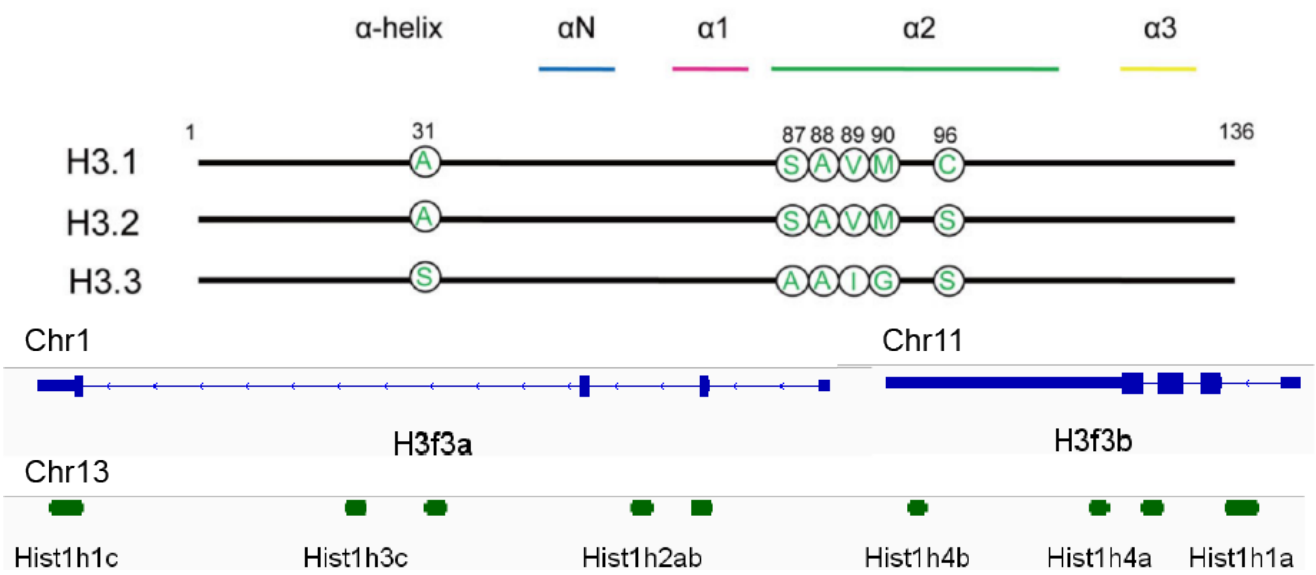

Figure 2.1 Protein and genome level structure of H3 variants

H3.3 varies from canonical histones by 4 or 5 amino acids; S31, A87, A88, A89, G90 and S96. Histone H3.3 is encoded by two genes that make the same protein, *H3f3a* and *H3f3b* with introns and a long polyA+ 3' UTR. Canonical histones are produced by arrays of genes, the Hist1 cluster is displayed. These genes are unspliced, and contain a short stem-loop that is not polyadenylated.

Canonical H3

Within eukaryotes, there exists two broad classifications of histones: the replication-dependent (RD) canonical versions and replication-independent (RI) histone variants. H3.1 and H3.2 are the replication-dependent canonical H3 proteins, each of which are encoded by clusters of multiple-copy genes (**Fig. 2.1**). H3.1 and H3.2 differ by only one amino acid (C96 or S96) but this difference has not been conclusively linked to any separate function between the two. Unlike most mRNAs, canonical histone genes lack introns and are unspliced, terminating in a small stem-loop structure without a polyA tail (55). This stem loop is made up of a 26 nucleotide sequence, with a 4 bp loop and 6 bp stem structure. While the sequence itself can be somewhat variable between species, this secondary structure is remarkably conserved. This conservation extends to non-metazoan species leading to interesting questions about the evolutionary conservation of this regulatory mechanism (56). The stem-loop is also proceeded by the Histone Downstream Element (HDE), another regulatory binding site that interacts with the U7 snRNA and FLASH. During replication, mRNA binding factors bring together locally clustered arrays of histone genes into close physical proximity to form the Histone Locus Body (HLB), coordinating expression from the entire array of genes while also coupling transcription and post-transcriptional processing (57).

Canonical histone mRNAs are thought to be quite transient, and quickly degraded once the cell exits S-phase along with many of the processing proteins involved in canonical histone synthesis. Supporting this idea, cytoplasmic levels of canonical histones were found to rapidly decline in conjunction with inhibition of DNA replication (55). As the cell exists S-phase, RD transcripts are appended with a short poly-uridine

tail, which is subsequently bound by LSM ring proteins that recruit exosomes, resulting in transcript degradation (58). Furthermore SLBP, a primary regulator of RD histone expression, is phosphorylated for degradation by CDK1 (59). This process of “cleaning up” after RD histone synthesis is thought to be important for regulating histone pool levels as to not overwhelm the cell with excess unbound histones. Histones are highly basic proteins, and when left unchecked they form aggregations, interact aberrantly with acidic cellular components, and lead to widespread cytotoxicity (60). As such, the rapid increase and decrease of histone levels is tightly regulated, and pools of non-nuclear histones are constantly bound by a series of chaperone factors (61).

The H3.3 Variant

In contrast to the canonical H3 variants, histone variant H3.3 is replication independent and expressed throughout the cell cycle. H3.3 is encoded by two genes, *H3f3a* and *H3f3b*, which express mRNAs that contain introns, undergo splicing, and are polyadenylated. *H3f3a* and *H3f3b* produce the same identical protein, yet have divergent untranslated regions (**Fig. 2.1**) (62-64). Whether these genes perform separate functions and what those distinct functions may be are still being debated, but some differences in tissues expression have been noted (65, 66). H3.3 plays many roles within the genome, depending on the genomic context into which it incorporates, and the PTMs it acquires thereafter. Originally, H3.3 was thought to mark active regions of the genome, as it is enriched at gene bodies and promoter and found carrying activating marks like H3K36me3 and H3K72Ac (67-69). Recent work has shed light onto the role of H3.3 in heterochromatic regions as well, where it is found decorated with the repressive PTM H3K9me3 (68). H3.3 is found to also play a role in formation of telomeric and centromeric

chromatin, as well as the repression of repetitive elements like ERVs and L1 (70-72). How H3.3 differs from its canonical counterparts is still an active field of study.

At the protein level, H3.3 differs from canonical histone at only four or five residues, 31, 87, 89, 90 and 96. 87, 89 and 90 reside in the α2 helix of the histone-fold domain and primarily dictate interactions between soluble H3 and its various chaperone proteins. H3.3 is thought to be the sole partner for the chaperones HIRA and DAXX, both of which function to deposit H3.3 replication independently. The H3.3-specific S31 residue can be phosphorylated, and this modification has been attributed to several functions that differentiate H3.3 from H3.1/2. H3.3S31Phos was originally identified as a marker for centromere boundaries in late metaphase cells (73). More recently, it has been shown to be involved in activating transcription, via interactions with SETD2 mediated H3K36me3 and eviction of transcriptional repressor ZMYND11. Further study into the functionality of the S31 substitution is required, but as the lone difference in the N-terminal tail from that of canonical histones, it is a likely contributor to differences between canonical H3 and H3.3.

Although H3.3 is expressed outside of S-phase and is thought to provide the primary source of histone 3 in non-dividing cells, it is expressed throughout the cell-cycle and has been shown to play important roles in development. Despite rapid and massive canonical histone synthesis in S-phase, H3.3 still constitutes a significant portion of total H3, with some estimates as high as 25% even in replicating cells (74), although this is likely subject to tissue type and developmental stage variability. In quiescent or permanently post-mitotic cells, H3.3 takes over as the predominate source of H3, reaching saturating levels with age, about a year in neurons (75, 76). This enrichment of

H3.3 accompanies rewiring of transcriptional programs marked by an initial enrichment of H3.3 at promoters, enhancers, and gene bodies of newly active, cell-type specific genes (77). Furthermore, H3.3 has been shown to play an important role in the establishment of bivalent domains within stem cells (78). These domains, marked by co-occupancy of repressive and activating histone PTMs, are important for facilitating cell fate transitions as differentiation proceeds across development. H3.3's role in genome integrity is also important during development for proper formation and stabilization of the telomere and centromere, without which karyotypic abnormalities and embryonic death result (74, 79, 80). Due to its replication-independent nature, H3.3 eventually replaces all H3 in the genome in non-diving cells, although how much of this is due to passive replacement or active biological function is still unknown (75, 81). Given that it will eventually occupy the entire genome, ascribing a specific role to H3.3 is context dependent, and requires differentiating between the biochemical properties of the molecule and the biological process of histone turnover. In the adult brain, H3.3 is thought to play a role in plasticity-based remodeling and induction of activity-dependent gene expression (76, 82). Given this wide variety of roles, the context, modification, and turnover of H3.3 are important factors when considering the function of H3.3.

Histone H3 chaperones

Due to the modular nature of nucleosomes, histone variant incorporation represents an important layer of regulation, a process mediated by histone chaperones. Free histones are charged molecules that left unchecked, can form aggregates or unregulated interactions with DNA. Chaperone proteins are thus responsible for specific targeting of canonical and variant histones to the genome, and can effect regulation by

selective incorporation. Due to the protein differences in canonical and non-canonical H3, there are different collections of chaperone and factors that control assembly into nucleosomes and deposition onto DNA. Canonical histone deposition is DNA-synthesis dependent, and occurs at the replications fork through the chaperone CAF1, which interacts directly with the PCNA sliding clamp (83). Although often described as replication-dependent, canonical H3 deposition has also been observed at sites of DNA-damage outside of S-phase, but is still coupled to DNA synthesis (84). Other exceptions to the replication-dependent moniker are discussed in Chapter 5.

H3.3 is also known to be incorporated through the synthesis-coupled pathway, and interacts readily with CAF1 (85). However, outside of S-phase there are additional complexes that mediate H3.3 incorporation into chromatin. The histone regulator A (HIRA) complex deposits H3.3 in genomic regions associated with activating histone marks, and is involved in recruitment of RNAPII (86). The ATRX/DAXX complex has been found to localize H3.3 to heterochromatic regions of the genome, and in particular has been shown to play an important role in centromere and telomere formation (87, 88). Recently, DAXX-mediated H3.3 deposition has also been found to play a role in silencing of ERVs and other repetitive elements, adding to the list of biological process influenced by H3.3 (70). Although H3.3 was originally thought to be an activating mark, through the study of chaperone proteins, it is now clear that H3.3 interactions with HIRA or DAXX mediate active or repressive functions, more so that histone variant itself.

H3 deposition begins with H3 dimerizing with H4, followed by binding of anti-silencing factor 1 (ASF1). ASF1 then takes this heterodimer into the nucleus, likely through the help of importin proteins. Once localized, it then hands off the dimer to CAF1,

HIRA, or DAXX, which facilitates formation of the H3-H4 tetramer on the DNA strand. Finally, a pair of H2a-H2b dimers is added to the bound H3.3-H4 tetramer to form the complete 8-membered nucleosome.

Post-Translation Modifications (PTMs)

The N-terminal tail of histone proteins, and in particular histone H3, has several characteristic residues that can be chemically modified, resulting in changes to nucleosome stability, histone-DNA binding, or histone-enzyme interaction (89, 90). Addition or subtraction of methyl, acetyl, phosphoryl, or ubiquitin can fundamentally change the accessibility of DNA underlying the chromatin containing these marks and is one of the primary mechanisms of chromatin-based transcriptional and structural control. In addition to classic marks, there have recently been a number of alternative modifications to histones described, with additions of benzoyl, serotonin, dopamine, homocysteines and more found to have potential roles in chromatin based regulation (91, 92).

Histone Turnover

Once incorporated into nucleosomes, histones are not simply static packaging molecules. Their incorporation, eviction, recycling, and replacement all play roles in regulating the chromatin and transcriptional dynamics of the underlying DNA. The removal and deposition process may play fundamental roles in regulation. However, the importance of dynamics versus histone variants are difficult to untangle empirically.

Eviction

The DNA-nucleosome interaction is quite strong, and chromatin-bound DNA is folded into higher order structures that further restrict access. Therefore, to enable access to the genome, nucleosomes must be actively displaced for any transactions on DNA. Chromatin remodelers are the primary effectors of nucleosome eviction (93). There are numerous enzymes that can catalyze the removal of histones, typically in an ATP-dependent fashion, and many have specificity for specific histone variants (94). They function by disassembling the nucleosome, completely or partially, to allow for the binding of factors or passage of polymerases. Disassembly can happen completely (the entire nucleosome) or partially (only the H2a-H2b tetramer is ejected), but it is always the first step in the process (95). In partial disassembly, the H3-H4 nucleosome remains along their PTMs, to maintain the epigenetic state previous to turnover. Complete disassembly removes the nucleosome entirely, and in the brain was found to potentially involve proteasomal degradation (76). This would remove any PTMs and thus can functionally reset the genomic region, allowing for rewriting of the chromatin landscape. Importantly, partial disassembly can permit the passage of RNA polymerase. Thus, transcription can proceed while the H3-H4 tetramer remains bound (96).

Recycling

Complete eviction, which requires replacement of the H3-H4 dimers, is rare during transcriptional elongation, and can result in H3 histones being recycled in transcribed gene bodies and thus the continued presence of H3 PTMs on the recycled histones (96). In fact, there is evidence that some marks of active transcription like H3K36me3 discourages the exchange of histones, thus maintaining the active mark on active genes

(97). This quick recycling of the resident histones can happen co-transcriptionally through factors associated with the transcriptional complex.

Replacement

Even though overall replacement rate is low in the gene body, in higher organisms transcriptional elongation is still linked to canonical H3 replacement with H3.3 (98). This would imply that as a gene becomes highly transcriptionally active, repeated polymerase passage eventually leads to H3 replacement by H3.3 via turnover. This is mediated by HIRA, although whether histone replacement stimulates transcription or is the consequence of elongation is unclear. Turnover does affect other pieces of the transcriptional process; the turnover rate in promoters and enhancers is much higher (99). Increased H3.3 turnover is often concurrent with differentiation or changes in cell states, and is present in “poised” regions of stem cells (100). A high rate of histone turnover is thought to increase accessibility of enhancer and promote regions, allowing for the binding of transcription factors and polymerases to the transiently unbound DNA. What the mechanisms are that instigate this increased turnover and whether they precede or proceed factor binding are still being explored.

Functional Consequences of H3.3 Deficiency

Being one of the fundamental units of chromatin organization, there has been much study surrounding Histone 3, as well as the replication independent variant H3.3. Given its fundamental nature, however, deletion or disruption studies have proved difficult, with only a few examples. The consequences of H3.3 deficiency vary widely, based upon a number of factors including species, disruption strategy, tissue(s) affected, and even variability between laboratory groups. Individual *H3f3a* or *H3f3b* knockouts also

resulted in discordant data on the importance of the individual genes responsible for H3.3 production (74, 101, 102).

Germline

The Magnuson lab generated *H3f3a/H3f3b* null mice and found early embryonic lethality and severe growth retardation (79). In whole embryo knockouts using a conditional allele and *Sox2*^{Cre}, embryos died around day E6.5. Interestingly, the transcriptome of these embryos was relatively unaffected, and a majority of the defects manifested as cell cycle arrest and karyotypic abnormalities (79). Consistent with other literature suggesting H3.3 roles in transcriptional fidelity and developmental programming, it seems likely that in total nulls the cytogenetic toxicity manifests first, and that any reported changes to the transcriptome are not immediate and require longer times to develop. Alternatively, H3.3 may play a limited role in transcriptional regulation this early in development, and not until later does enrichment in active regions begin. Interestingly, in this study the single gene KOs, *H3f3a* or *H3f3b*, were normal and viable, although the assays used were limited to overt morphological growth and may have missed some more subtle effects noted in other publications.

A constitutive germline *H3f3b* knockout from another group resulted in strong developmental defects and semi-lethality (74). Further investigation of this mouse found widespread ectopic distribution of CENP-A, the centromeric H3 variant, and gross karyotypic abnormalities. This study adds further evidence to importance of H3.3 in genome stability, as well as its role in centromere formation and chromosomal segregation (74). Intriguingly, this study also found hyper phosphorylation of S31 in KO MEF cell lines, along with a reduced, but not proportional reduction of H3 Lysine

modifications. They noted that the *H3f3b* null mice were all infertile, and that *H3f3b* KO in spermatozoa was accompanied by an increase in the repressive H3K9me3 mark, as well as increased apoptosis (103).

HIRA and DAXX, the two primary chaperones for H3.3, have also been knocked out in mice, with similar embryonic lethality at E9.5 (104, 105). This might imply both replication-independent deposition pathways are important in development, as H3.3 double knockouts die sooner than either chaperone individually, but closer investigation would be necessary to tease apart the mechanisms involved in these pathways.

In vitro

Combined *H3f3b* KO and *H3f3a* KD via shRNA in mouse embryonic fibroblasts led to slowed proliferation, karyotypic and nuclear defects, and cell death (106). However, much like the *Sox2* conditional knockout, this study found the transcriptome to be relatively intact, again suggesting that in developing cells the genome integrity function of H3.3 is more important than its role in transcriptional regulation. In mouse embryonic stem cells, H3.3 depletion led to reduced histone turnover and altered H3K27 methylation, particularly around promoters of developmentally regulated genes, and led to altered differentiation potential (78), suggesting a requirement for H3.3 in H3K27 methylation-mediated gene regulation.

H3.3 has been found to play a critical role not only in differentiation, but also in cellular reprogramming. In *Xenopus* nuclear transfer experiments, H3.3 incorporation was found to be an important and early step in reprogramming the somatic cell to an oocyte (107). In reprogramming of iPSCs, H3.3 was found to act as both a barrier to the changing of cell fate, as well as an integral part of reprogramming (108). Without H3.3, cells more

readily changed state, but failed to remain in a differentiated state, more easily sliding back to an undifferentiated one. Interestingly, they also found relatively little effect on already established cellular identity, suggesting that H3.3 in this context is more important to cell fate transition, rather than maintenance. Together, these works position H3.3 as an important factor in cell state transition and rewiring of the transcriptome. These insights help explain the role of H3.3 in differentiation and its connection to cancer when mutated.

Brain

In adult mouse brain, H3.3 KD was found to decrease overall synaptic connectivity, and led to a reduction in spine density and number (76). This study also found alterations to activity dependent gene transcription and other plasticity adjacent genes. Altering H3.3 dynamics in the nucleus accumbens or ventral tegmental area were also found to affect behavior, increasing vulnerability to depressive-like symptoms and association with cocaine-self administration (82, 92, 109). shRNA mediated KD of H3.3 in electroporated neurons resulted in decreased proliferation and premature terminal differentiation (110). However, genetic KO experiments in the embryonic brain, in particular stage-dependent genetic manipulations, are still necessary to untangle the full extent of H3.3's impact on neurodevelopment.

H3.3 in Human Disease

There are a number of epigenetic regulators implicated in cancer etiology, including chromatin readers, writers, and erasers. Histone marks governing gene expression are important safeguard against cancer transformation, and any disruption to epigenetic regulation can pose a risk. Histone proteins themselves are also implicated in the development of cancers, and there exists several characteristic mutations, particularly

in H3. Among the most common cancer-associated mutations in H3.3 are K27M and G34R/G34V. These missense mutations happen at a much higher frequency in *H3f3a* and *H3f3b* compared to canonical histones and lead most commonly to pediatric glioblastoma in the case of K27M, present in as much as one third of all tumors sampled (111). Diffuse intrinsic pontine glioblastoma (DIPG) has been strongly linked to H3.3 mutation, with over 70% carrying the K27R mutation (112). Most mutant H3-associated tumors were also accompanied by p53 or other tumor suppressor mutations. Notably, these appear to be dominant H3 mutations, as most tumors were heterozygous for the mutant allele. Giant cell tumors of the bone (GCTB) and chondroblastoma are also strongly linked to H3.3 and G34R/V mutations, with as much as 90% of sampled tumors containing alterations to G34 (113).

The mechanism behind these mutations is largely thought to be driven by changes to PTMs on mutant histones, and the resulting transcriptional effects. H3K27 is a well-known site for modification, primarily by methyltransferases, and in H3K27M mutant cells, global H3K27me levels are decreased as much as 65% (114) while H3K27Ac is somewhat increased (115). Furthermore, the H3K27M protein has been shown to have increased interactions with EZH2, potentially disrupting normal PRC2-mediated regulation (115, 116). While G34 is not known to be modified itself, it lies very close to H3K36, another well-known site of post translation modification. It therefore seems likely that amino acid changes, especially from a small non-polar residue like glycine to a larger, charged one like arginine, could cause steric hindrance to chromatin interacting enzymes. Indeed, G34R cells show a relative reduction in H3K36me levels (111, 117). There exists some divergence in the incidence of K27M vs G34 mutations in *H3f3a* and *H3f3b* genes,

likely due to sequence level differences that predispose each gene to different missense mutations. One recent study implicated *H3f3a* in microcephaly (118) although this study identified L62 as the causative mutation. While not a known substrate for modification, this does sit close to K64, which has been reported to be methylated and acetylated (119). Whether K64 modifications are altered or how this mutation impacts brain development remain unknown. *H3f3b* has been linked specifically to K36M mutations and chondroblastoma, whereas *H3f3a* has not (113).

Mutations to histone proteins can cause imbalances to activating or repressive marks, and this disruption is thought to precipitate cancerous transformation. G34R was found to result in dramatic upregulation of the oncogene N-Myc (120). H3.3 is also known to play a role in telomere and centromere formation through ATRX/DAXX, and disruption of these processes could lead to chromosomal abnormalities or higher order chromatin defects that pose a potential risk for disease. Indeed, ATRX and DAXX themselves are also often found to be mutated in similar cancers (88).

The link between oncohistones and neoplasia is still being explored, but in light of revelations in my work as well as others about the importance of H3.3 in differentiation, the inability to transition from a dividing state to a quiescent or terminally post-mitotic one may indeed contribute to transformation. Alternatively, if somatic mutation in histone genes lead to a regression in differentiated tissue to a more “stem-like” state, this could also be a plausible link between H3.3 mutation and cancer. Extensive research is required to define the exact mechanisms at play, but basic research into histones and histone variant function in development will be critically important.

Summary and Overview of Thesis

The objective of this thesis is to define the functions of H3 variant H3.3 in the developing neocortex. Chromatin biology has become central to our concept of normal brain development. It is also a key contributor to many neurodevelopmental and neuro-oncological disorders. Studies into brain chromatin often focus on chromatin remodeling enzymes and the post-translational marks they affect. The influences of histone proteins and their variants on the process of brain development are still being explored, and it is my aim to add to that growing body of knowledge with this work.

In this work, I find a substantial increase in H3.3 levels in newly born neurons as they integrate into the nascent cortical plate. Using a conditional knockout model, I co-deleted *Hf3fa* and *H3f3b* from newly post-mitotic neurons as well as earlier in NPCs and found highly similar phenotypes including perinatal lethality. Transcriptomic analyses showed widespread changes to gene expression, particularly in genes upregulated across neuronal differentiation and those with bivalent TSSs in early development. These changes were accompanied by deficits in the acquisition of neuronal identity and misexpression of cortical layer markers. Conditional knockout mice also suffered from defects in axonal projection and lacked several major axon tracts. I further investigated the effects of H3.3 deletion several days after the final mitosis and found none of the major defects seen in early deletions. Due to the longevity of these mice, I was able to further explore the function of H3.3 in aging cells, and discovered a slow, progressive removal of the H3.3 over time. My work uncovered evidence for a potentially underappreciated source of H3 in post-mitotic neurons and established an early role for H3.3 in establishing the neuronal transcriptome that is distinct from its role later in life.

This work is an important addition to the literature on the impacts of chromatin function on neurodevelopment, and the importance of H3.3 in histone turnover. In the final chapter, I contextualize these findings and lay out future research avenues.

Chapter 3 H3.3 is Required for Cortical Neuron Developmental Processes

Abstract

Cortical development is associated with a number of molecular and morphological changes. Many of these changes are associated with by modification of the chromatin structure in developing neurons. Here I found a substantial accumulation of H3.3 in neurons as they exit the cell cycle and migrate to the nascent cortical plate. Stage-dependent deletion of H3.3 genes from cycling neural progenitor cells and neurons immediately after terminal mitosis revealed the first post-mitotic days as a critical window for *de novo* H3.3. I further characterized defects in neuronal subtype identity and axon pathfinding in H3.3 KOs. Together, this work outlines the importance of post-mitotic H3.3 synthesis and deposition in the normal development of cortical neurons.

Results

H3.3 is ubiquitously expressed in the developing brain

H3.3 protein is encoded by *H3f3a* and *H3f3b*, which are thought to be broadly expressed in all tissues (61, 69). To confirm the expression of H3.3 genes throughout the cortex I used single nuclei (sn)RNA-seq data from wildtype embryonic day (E)14.5 cortex to explore transcript levels. Of the 9,300 cells assayed that met stringent quality control for snRNA-seq, a median of 2,642 genes were detected per cell. Clustering by Seurat (121) revealed 18 groups that encompassed the full complement of known cell types in

embryonic cortex (**Fig. 3.1 A**). High *H3f3a* and *H3f3b* expression levels were found in all types of NPCs, including radial glial cells (RGCs) and intermediate progenitor cells (IPCs), as well as post-mitotic neurons at various stages of maturation (**Fig. 3.1 A**). Each of the 18 cell types expressed *H3f3a* and *H3f3b* (**Fig. 3.1 A**). At the level of single cells, *H3f3a* was detected in 9,113/9,300 cells (98.0%) and *H3f3b* was detected in 9,132/9,300 cells (98.2%), although cells without H3.3 genes were likely a result of dropouts. Consistent with bulk and scRNA-seq of the developing human cortex (122, 123), this data indicated that *H3f3a* and *H3f3b* were likely ubiquitously expressed in the developing cortex. This is further consistent with previous reports that *H3f3a* and *H3f3b* are expressed throughout the cell cycle and in all tissues (69, 124).

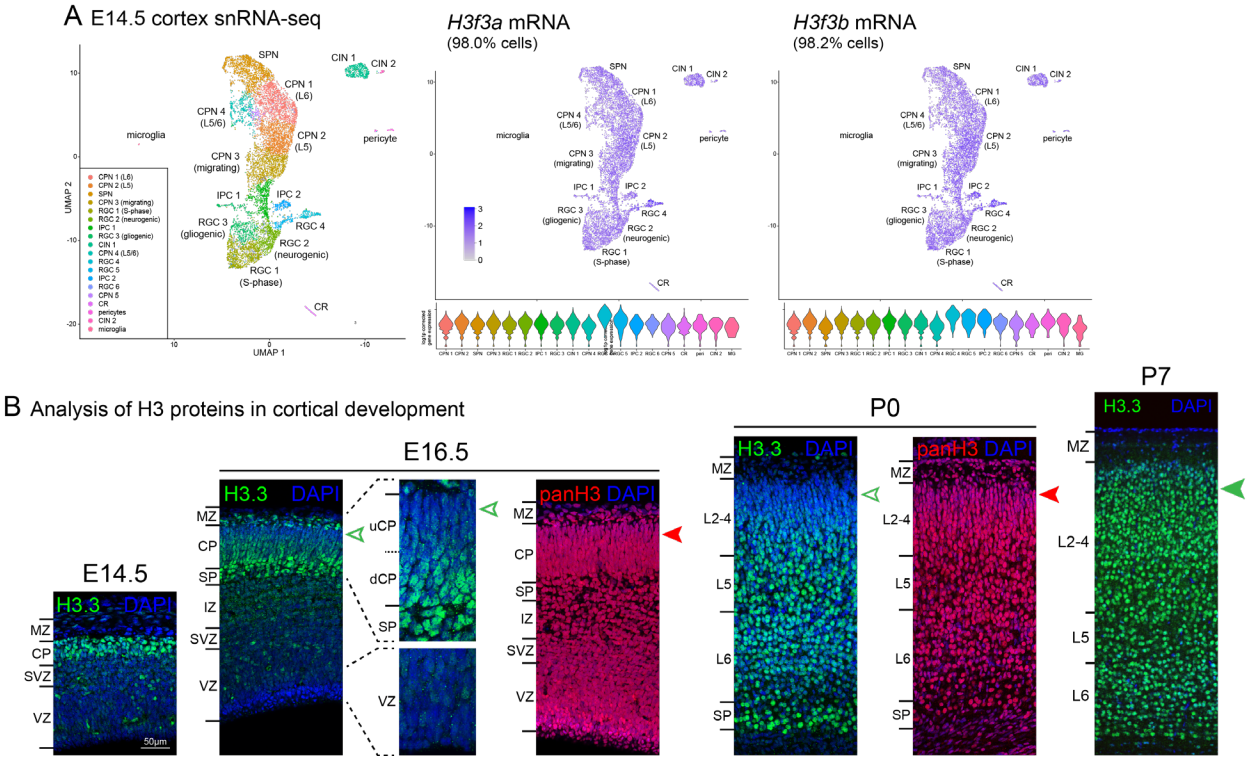

Figure 3.1 Post-mitotic accumulation of histone H3 variant H3.3 in cortical neurons and genetic manipulation of H3.3 genes *H3f3a* and *H3f3b*.

(A) Single nuclei (sn)RNA-seq of wildtype E14.5 cortex visualized by Uniform Manifold Approximation and Projection (UMAP). *H3f3a* and *H3f3b* mRNA was present in each of the 18 identified cell clusters and in 98.0% and 98.2% of cells, respectively. (B) Analysis of variant H3.3 protein and panH3 protein in cortical development by immunostaining. On embryonic day E14.5 and E16.5, low levels of H3.3 (green) were present in the germinal zones, ventricular zone (VZ) and subventricular zone (SVZ), composed largely of cycling neural progenitor cells (NPCs). High levels of H3.3 were present in cortical plate (CP), composed largely of post-mitotic neurons. Within the E16.5 CP and the postnatal day (P)0 cortical layers, higher levels of H3.3 were present in the early-born neurons of the subplate (SP) and deep layers, compared to the late-born neurons of the upper layers (open arrowheads). PanH3 (red) was broadly present in cortical layers and showed no preference for early-born neurons. High levels of panH3 were present in late-born upper layer neurons (solid arrowhead).

H3.3 is substantially accumulated in post mitotic neurons

To assess H3.3 protein levels in individual cells, I used H3.3-specific immunostaining on embryonic wildtype cortex. H3.3 is found primarily within nucleosome complexes, most of which are tightly bound by DNA and some even more tightly bound by heterochromatin. To achieve IHC staining of this mark I employed a number of antigen retrieval techniques, primarily treatment with hydrochloric acid and mild heat treatment at 37°C. At E14.5, SOX2+ NPCs in ventricular zone (VZ) and subventricular zone (SVZ) were characterized by lower levels of H3.3 proteins (**Fig. 3.1 B**). In contrast, post-mitotic neurons in the cortical plate (CP) were characterized by relatively higher H3.3 levels, suggesting that H3.3 accumulation increased post-mitotically as neurons finished their migration and integrated into the CP. At E16.5, H3.3 levels in NPCs remained low. In post-mitotic neurons, however, H3.3 levels began to show a layer-dependent gradient; higher in deeper portions of the cortex and lower in more superficial parts (**Fig. 3.1 B**). In the developing cortex, excitatory neurons are generated sequentially (subplate neurons → deep layer neurons → upper layer neurons) and settle in the cortex in an inside first, outside last manner (125, 126). At E16.5, the earliest born subplate (SP) and lower layer (L5/L6) neurons were characterized by the highest levels of H3.3, the next-born neurons of the deep CP showed comparatively lower levels of H3.3, and the most recently-born upper CP neurons had the lowest levels of H3.3 (**Fig. 3.1 B**). This gradient suggested that H3.3 accumulation occurred progressively over several days after exit from the cell cycle. In contrast to H3.3 specific staining, pan-H3 staining was uniform throughout the cortex, without the gradient seen in H3.3 (**Fig. 3.1 B**). The high level of pan-H3 staining in NPCs, in which H3.3 staining was low, was consistent with canonical H3 (H3.1 and

H3.2) deposition in cycling cells, and continued normal levels of H3 containing nucleosomes despite H3.3 deletion (127, 128). At P0, the latest born cortical neurons, located at the upper edge of L2/3, were characterized by low H3.3 staining, but similar pan-H3 staining compared to the earlier-born deep layer neurons (**Fig. 3.1 B**). Importantly, by P7, the layer gradient in H3.3 staining had disappeared; both deep and upper layer neurons were characterized by high levels of H3.3 (**Fig. 3.1 B**). This finding suggested that the layer difference in H3.3 levels at E16.5 and P0 (**Fig. 3.1 B**) reflected the age of neurons since final mitosis, and that by P7, late-born upper layer neurons have had sufficient time to reach H3.3 levels similar to earlier-born deep layer neurons.

To directly quantify H3.3 levels from the time of neuronal birth, I labeled wildtype embryos with a pulse of thymidine analog EdU at E13.5, and tracked labeled cells 2h, 24h, 3 days, 5 days, or 6 days later. I found that in S-phase cells labeled by a 2h pulse of EdU, H3.3 was present only at low levels (**Fig. 3.2 A**). Over the next 6 days following neuronal birth, H3.3 levels progressively increased in lower-layer EdU-labeled neurons (**Fig. 3.2 B**). Together, our data indicated that although *H3f3a* and *H3f3b* were expressed throughout the cell cycle, H3.3 histone accumulation in neurons significantly increased post-mitotically over several days following the final mitosis (**Fig. 3.2 B**). Together these data show a remarkable increase in H3.3 accumulation following the terminal mitosis in neuronal development.

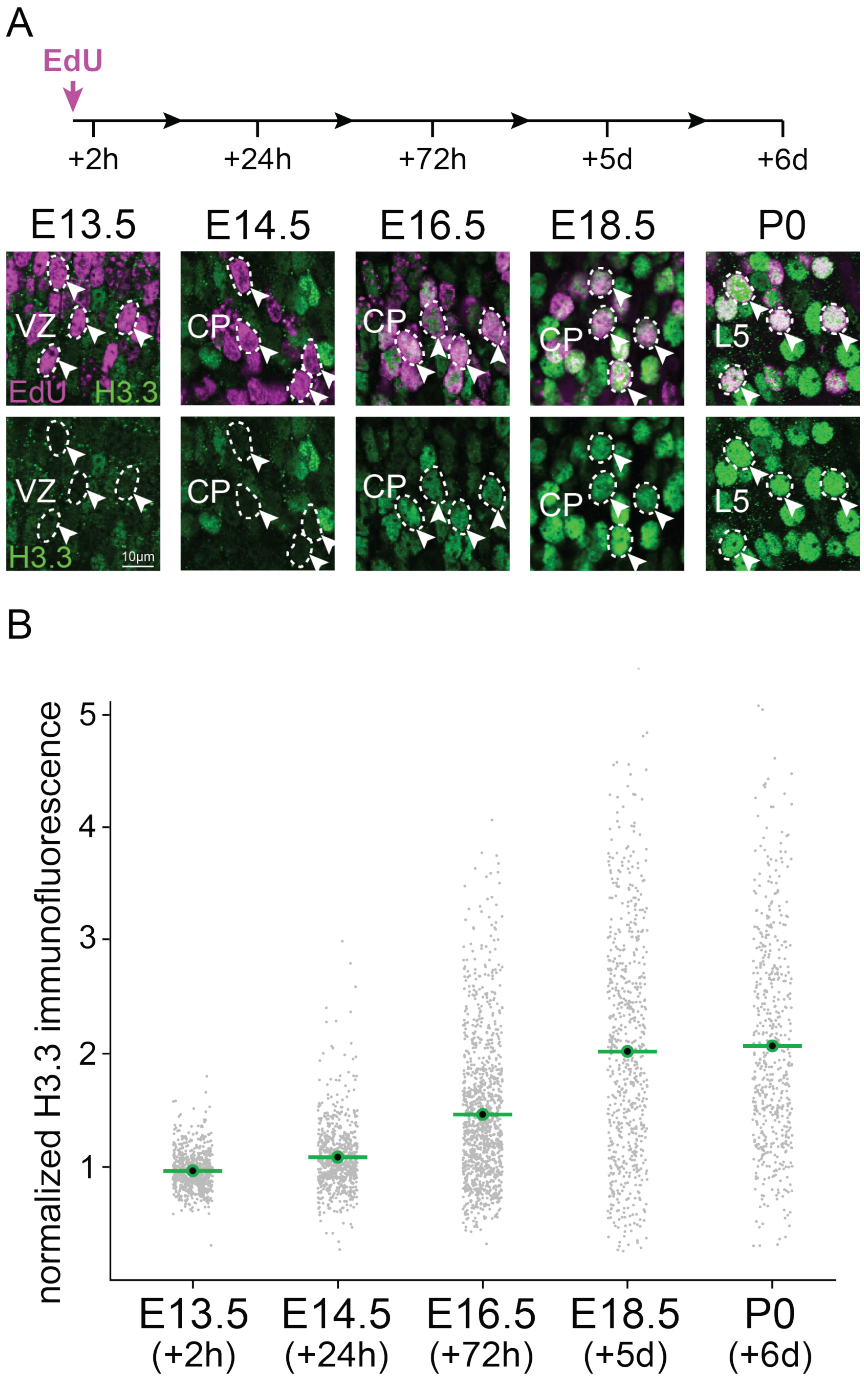

Figure 3.2 Quantification of H3.3 accumulation in post-mitotic neurons

(A) Temporal analysis of H3.3 accumulation. Neurons born on E13.5 were labeled by a single pulse of 5-Ethynyl-2´-deoxyuridine (EdU). EdU-labeled neurons (magenta, arrowheads) were analyzed by H3.3 immunostaining (green). (B) Quantitative analysis of immunofluorescence revealed a progressive increase in H3.3 levels over the first post-mitotic days (one-way ANOVA with Tukey's post-hoc test).

Conditional deletion of *H3f3a* and *H3f3b* from the developing cortex

There have been several studies exploring the consequences of H3.3-gene knockout in many contexts. Constitutive co-deletion of *H3f3a* and *H3f3b* leads to peri-implantation lethality by E6.5 in mice (79) and zygotic knockdown of both genes leads to a significant decrease in successful blastulation (129). To study the roles of H3.3 in cortical development, I leveraged conditional alleles of *H3f3a* and *H3f3b* (130). These alleles were each designed with a reporter; Cre recombination of the *H3f3a* floxed allele would delete *H3f3a* and turn on Venus reporter expression, whereas Cre recombination of the *H3f3b* floxed allele would delete *H3f3b* and turn on Cerulean reporter expression (**Fig. 3.3 C**) (130). To distinguish potential H3.3 functions in post-mitotic neurons versus cycling NPCs prior to final neurogenic mitosis, I used two complementary Cre lines for conditional deletion. First, to assess the role of post-mitotic H3.3 deposition, I used *Neurod6*^{Cre} (*Nex*^{Cre}), which mediates recombination in new-born excitatory neurons after terminal mitosis, without affecting NPCs (131). Second, to assess the role of the comparatively lower levels of H3.3 in NPCs, I used *Emx1*^{Cre}, which mediates recombination in cortical NPCs starting at E10.5 (132), prior to the onset of neuronogenesis. Published patterns of CRE expression were confirmed in these lines at E14.5 (**Fig. 3.4 B**), and the cell-type specificity and efficiency of Cre-mediated H3.3 floxed allele recombination by reporter expression (**Fig. 3.4 C**).

The resulting double H3.3 gene conditional knockouts, *Neurod6*^{Cre}*;H3f3a*$^{f/f}$;*H3f3b*$^{f/f}$ (dKO-N) and *Emx1*^{Cre}*;H3f3a*$^{f/f}$;*H3f3b*$^{f/f}$ (dKO-E) were born alive. Both dKO-N and dKO-E, however, were characterized by complete early postnatal lethality within several hours of live birth accompanied by absence of milk spot, which suggested an inability to suckle. In

contrast, mice with one or more wildtype allele of H3.3 gene, either *H3f3a* or *H3f3b*, were not affected by early lethality; they lived into adulthood, were fertile as adults, and did not show any observable phenotypes.

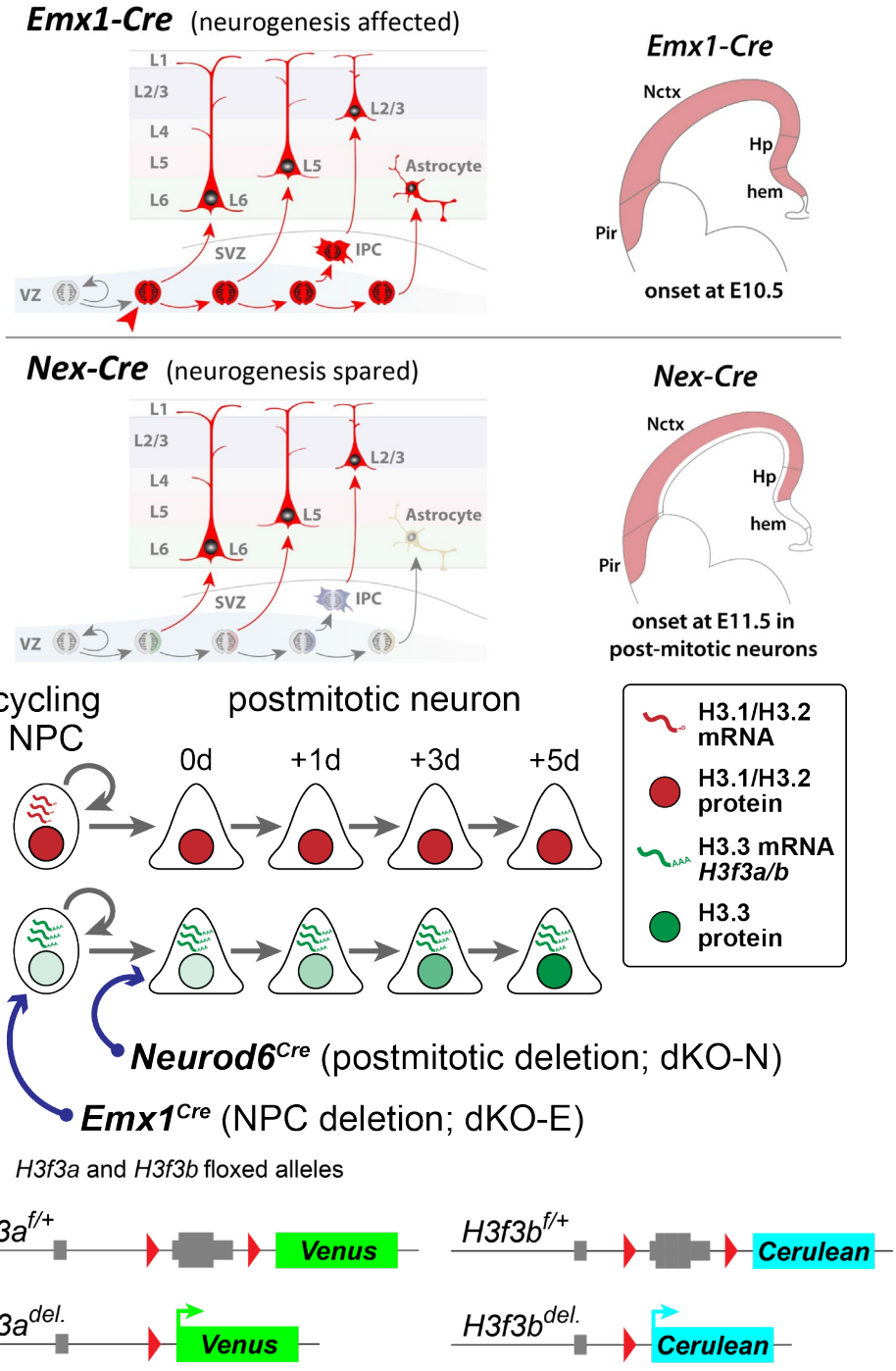

Figure 3.3 Cre expression in *Emx1*^{Cre} and *Neurod6*^{Cre} and the timing of H3

Emx1^{Cre} is expressed in the NPCs of the developing cortex, beginning at E10.5. *Neurod6*^{Cre} (*Nex*^{Cre}) is expressed in cortical neurons immediately after they become post-mitotic and is absent from NPCs. Canonical histone genes stop being transcribed after the neurons become post mitotic, while H3.3 is expressed throughout the cell cycle. Therefore, in postmitotic cells, H3.3 accumulates to saturating levels over time. (C)

Schematic of the H3f3a and H3f3b floxed alleles. The H3.3 coding sequences were flanked by loxP sites and followed by fluorescent reporter genes Venus (H3f3a) or Cerulean (H3f3b)

L1: layer 1, L2/3: layer 2/3, L4: layer 4, L5: layer 5, L6: layer 6, VZ: ventricular zone, SVZ: subventricular zone, IPC: intermediate progenitor cell, Pir: piriform cortex, Nctx: neocortex, Hp: hippocampus.

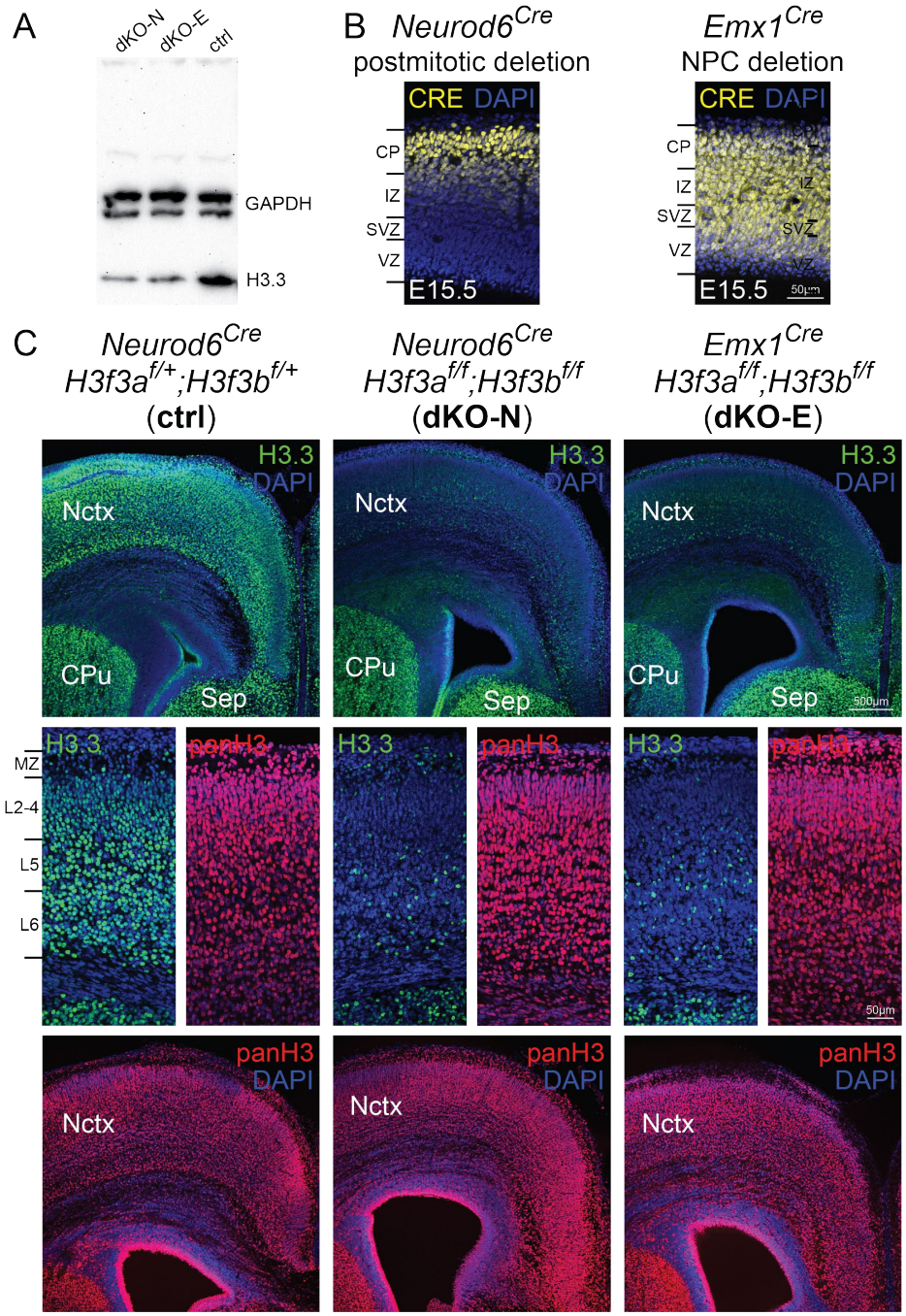

Figure 3.4 H3.3 protein levels in conditional double knockout cortex.

(A) Western blot of H3.3 protein levels showed a similar reduction in dKO-N and dKO-E. (B) Immunofluorescence of Cre confirmed expression patterns of *Neurod6*^{Cre} and *Emx1*^{Cre}. (C) Analysis of H3 proteins in P0 control (ctrl) and double H3.3 gene conditional knockouts, *Neurod6*^{Cre};*H3f3a*$^{f/f}$;*H3f3b*$^{f/f}$ (dKO-N) and *Emx1*^{Cre};*H3f3a*$^{f/f}$;*H3f3b*$^{f/f}$ (dKO-E). In both dKO-N and dKO-E, H3.3 (green) was largely lost from neocortex (Nctx) but preserved in caudate putamen (CPu) and septum (Sep). The levels of panH3 (red) were unaffected in dKO-N or dKO-E.

Deletion of H3.3 genes is not cell autonomously lethal

Previous studies have established H3.3 to be critical for blastulation and embryonic development (79, 130). To assess the phenotypic consequences of H3.3 loss in the developing brain, I employed conditional *H3f3a*/*H3f3b* co-deletion and analyzed the mutants at P0. Whole mount P0 brains showed no significant loss of cortical tissue in dKO-N or dKO-E, whereas quantification of cortical thickness revealed a minor reduction (p-value = .0427 for dKO-N and .0214 for dKO-E) (**Fig. 3.5**). Importantly, despite loss of H3.3 from cortical neurons, both dKO-N and dKO-E were characterized by an abundance of reporter-expressing cells (**Fig. 3.6 A**), indicating that loss of H3.3 did not cause widespread cell loss at P0. This finding was consistent with immunostaining for cleaved caspase 3 (CC3), a marker of apoptosis, and phospho-(p)KAP1 (TRIM28), a marker of DNA double-strand breaks (**Fig. 3.6 B**). Together, these data showed that loss of H3.3 from cortical neurons in dKO-N and dKO-E did not cause extensive cell lethality or DNA damage.

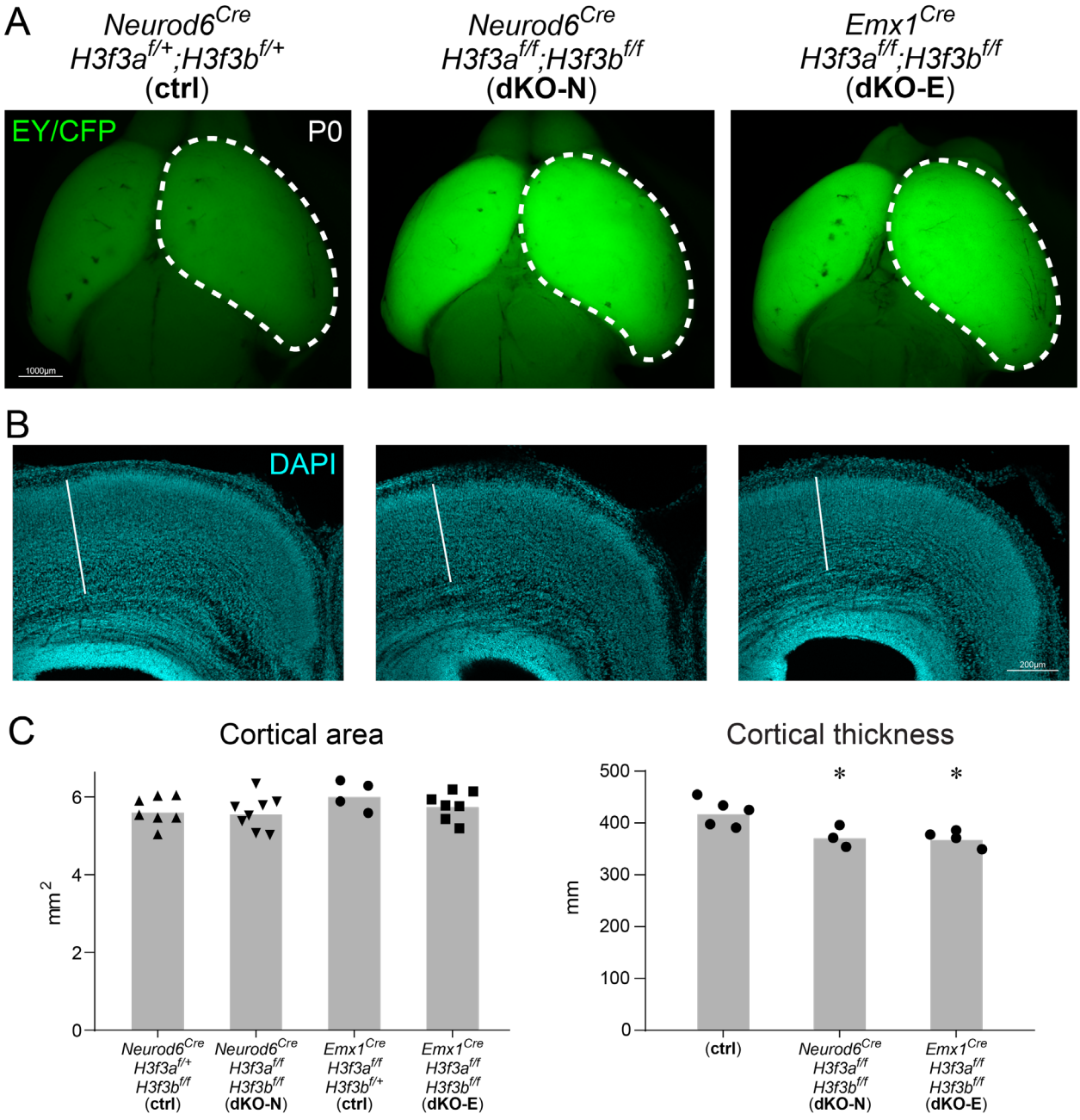

Figure 3.5 Cortical volume and thickness in H3.3 conditional knockouts

(A) Dorsal view of whole mount P0 ctrl, dKO-N, and dKO-E brains. (B) Coronal sections of P0 ctrl, dKO-N, and dKO-E stained by DAPI (cyan). (C) quantitative analysis of cortical hemisphere area and cortical thickness (data are mean, one-way ANOVA with Tukey's post-hoc test*, $p < 0.05$).

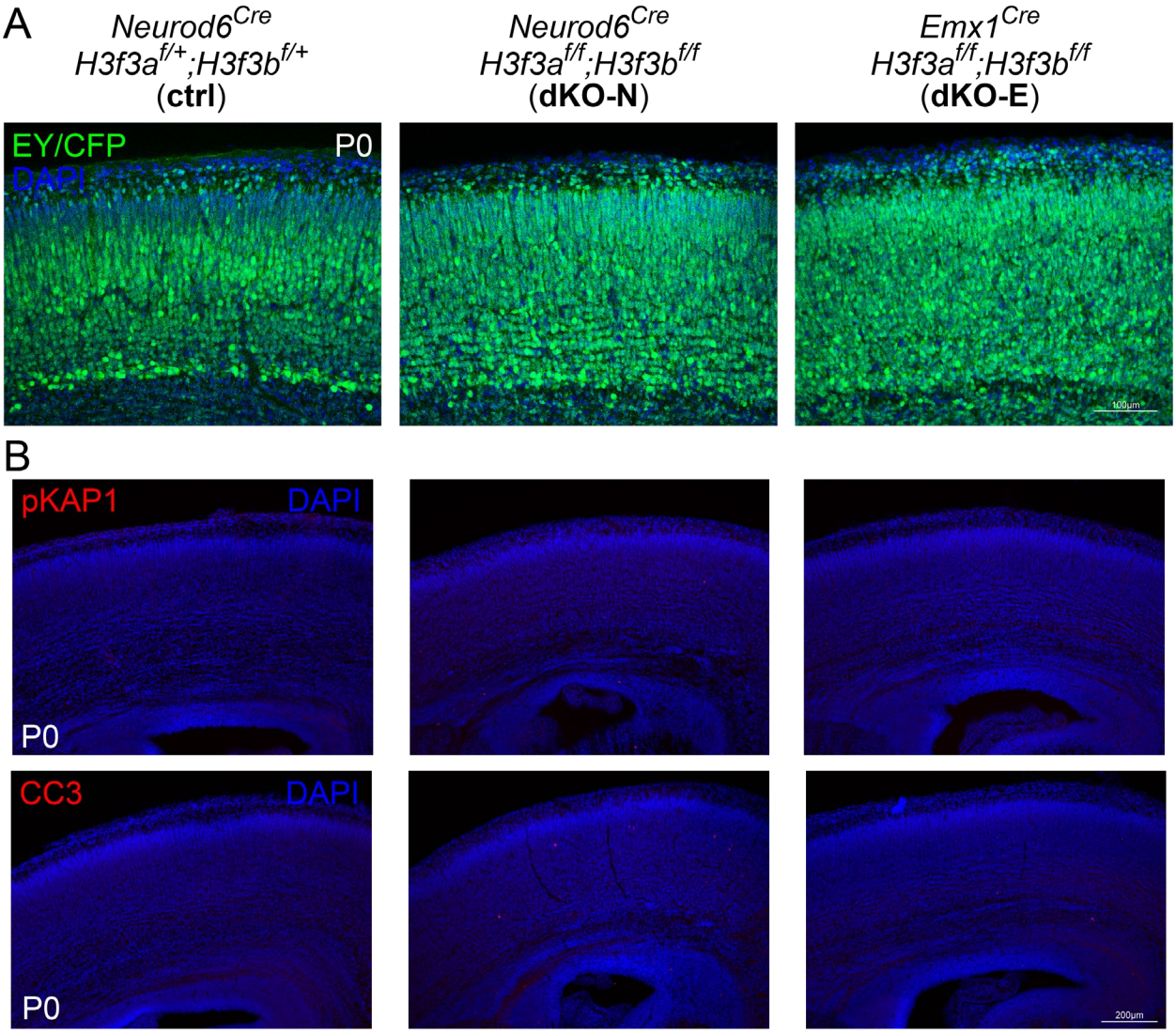

Figure 3.6 H3.3 deletion is not cell-autonomous lethal in NPCs or neurons

(A) Reporter gene expression by EGFP immunostaining (Venus or Cerulean: EY/CFP, green) on P0 coronal sections. An abundance of reporter-expressing cells were present in both dKO-N and dKO-E cortex. (B) Immunostaining of DNA double strand break marker pKAP1 (red) and apoptosis marker cleaved caspase 3 (CC3, magenta) revealed no significant DNA damage or cell death in P0 dKO-N or dKO-E.

H3.3 is necessary for acquisition of the neuronal transcriptome

H3.3 can contribute to transcriptional regulation by selective incorporation into gene bodies, promoters, or enhancers (133-135). H3.3 also carries gene regulatory PTMs, including H3K4me3 and H3K27me3 (136, 137). To assess the potential transcriptional roles of post-mitotic H3.3 incorporation in neurons, I studied the consequences of post-mitotic *H3f3a* and *H3f3b* co-deletion by transcriptomic analyses of dKO-N and littermate control cortices at P0. I generated sequencing libraries for unique molecular identifier (UMI) RNA-Seq by Click-seq (138). In UMI RNA-seq, individual cDNA molecules barcoded by the addition of a UMI tag such that PCR-amplified reads can be de-duplicated after sequencing, which enabled highly quantitative measurements of expression levels (139, 140). Differential gene expression was analyzed using edgeR (141). This revealed significant changes meeting a stringent FDR of < 0.01 in 948 genes in cKO-N compared to control (**Fig. 3.7 A**). Of these differentially regulated genes (DEGs), 579 were significantly downregulated ($log_2FC < 0$) and 369 were significantly upregulated ($log_2FC > 0$).

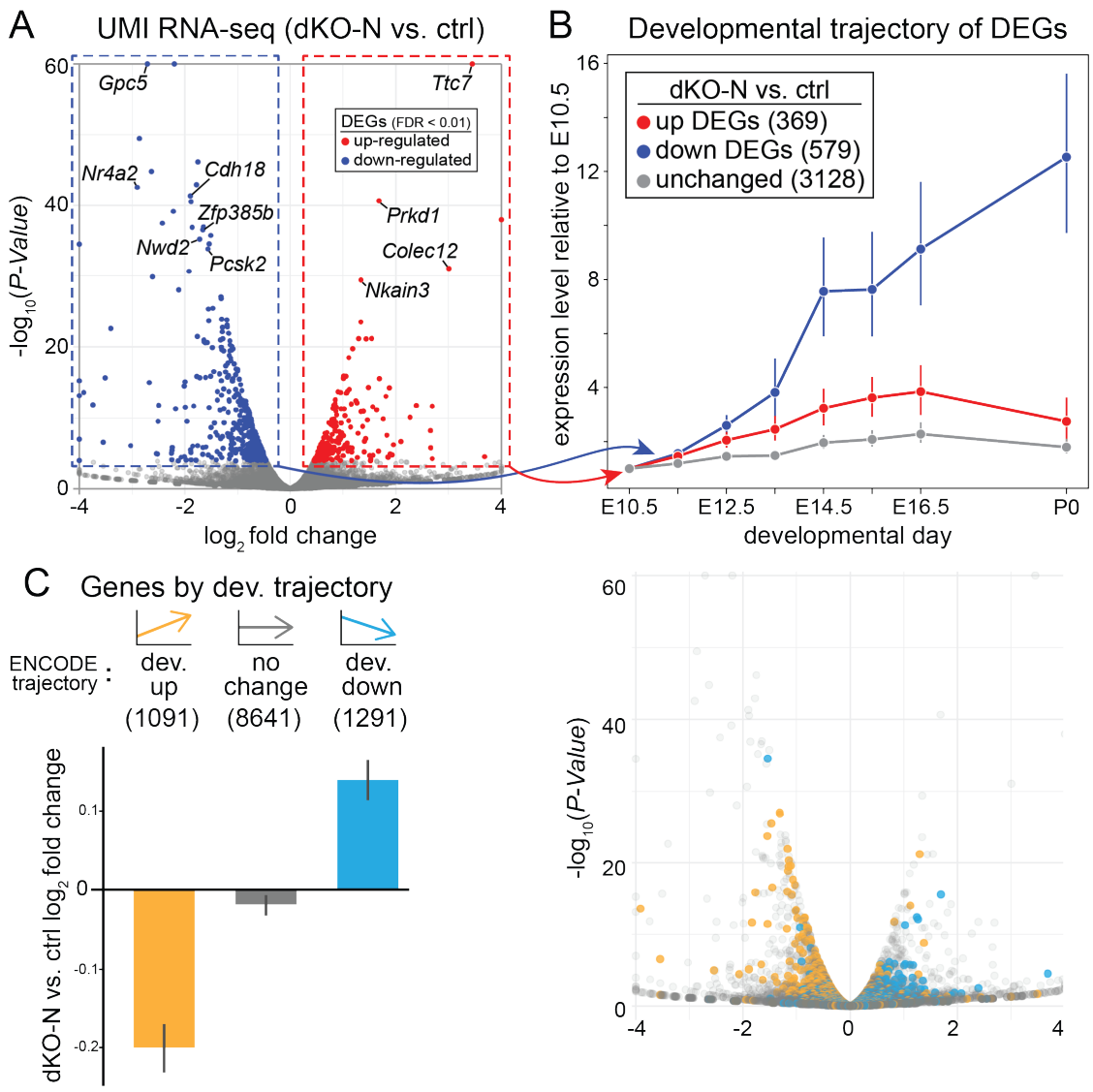

Figure 3.7 Acquisition of the neuronal transcriptome following H3.3 deletion

(A) Volcano plot of UMI RNA-seq comparing P0 cortex of dKO-N to control. For each gene, *P* value was calculated with likelihood ratio tests and false discovery rate (FDR) was calculated using the Benjamini-Hochberg procedure. Of 948 differentially expressed genes (DEGs, FDR < 0.01), 579 were significantly down-regulated (blue dots) and 369 were significantly up-regulated (red dots). (B) The developmental expression trajectories of dKO-N DEGs and 3128 unchanged genes based on ENCODE RNA-seq data of wildtype mouse forebrain. Expression trajectories were normalized to E10.5 levels. Genes downregulated in dKO-N were characterized by a progressive increase in expression across embryonic forebrain development. (C) Genes were categorized based on developmental trajectory using logistic regression on the ENCODE wildtype forebrain RNA-seq data. Genes that normally increase in expression over the course of embryonic

development (dev. up, slope > 2, pval < 0.01) were significantly downregulated in dKO-N. Developmentally up and down genes are then labeled on the dKO-N volcano plot.

The early post-mitotic accumulation of H3.3 coincided with an important period of molecular identity acquisition and refinement for new neurons (40, 41). To determine whether co-deletion of H3.3 genes affected the developmental establishment of the transcriptional landscape, I intersected genes that were significantly downregulated (579), upregulated (369), or unchanged (3128, FDR > 0.9, $-0.1 < \log_2FC < 0.1$, $\log_2CPM > 1$) in dKO-N with wildtype embryonic forebrain gene expression data from ENCODE at multiple developmental timepoints (E10.5 to P0) (142). This revealed in downregulated DEGs an overrepresentation of genes with a strongly positive developmental trajectory (i.e. a progressive increase in expression across normal forebrain development) (**Fig. 3.7 B**). This enrichment, which was absent from genes that were unchanged in dKO-N, suggested that following neuronal *H3f3a*/*H3f3b* co-deletion, some genes that normally increase in expression during development failed to do so. I confirmed this finding by using logistic regression on the ENCODE data to identify all genes that normally increase over the course of embryonic forebrain development (i.e. with a significantly positive trajectory; slope > 2, pval < 0.01) (**Fig. 3.7 C**). As a group, these genes were significantly downregulated in dKO-N, consistent with a role for H3.3 in upregulating neuronal genes to establish the transcriptome post-mitosis. Genes that normally decrease over development (i.e. with a significantly negative trajectory; slope < -2, pval < 0.01) were moderately increased in dKO-N, whereas genes that maintained expression levels across development were broadly unaffected (**Fig. 3.7 C**). Together, these data indicated that transcriptomic defects following neuronal *H3f3a*/*H3f3b* deletion included specific deficits in the developmental acquisition of the neuronal transcriptome.

H3.3 can influence gene expression via regulatory PTMs. To determine whether the differentially expressed genes following neuronal *H3f3a*/*H3f3b* deletion were preferentially marked by certain histone H3 PTMs, I used ENCODE ChIP-seq data from wildtype E10.5 to P0 forebrain for intersectional analyses (142). This revealed that downregulated DEGs in dKO-N are characterized by dynamic PTM shifts over normal forebrain development. At earlier timepoints (e.g. E10.5) they are associated with both H3K27me3 and H3K4me3 (**Fig. 3.8 A**), which together mark a bivalent chromatin state that can be resolved into active transcription or repressive silencing (143-145). As development progressed, H3K4me3 enrichment is maintained at these genes, but H3K27me3 enrichment is progressively reduced, indicating that these genes are normally resolved into a transcriptionally active chromatin state over embryonic development (**Fig. 3.8 A**). These included top dKO-N differentially expressed genes like *Nwd2* and the neuronal differentiation markers like *Rbfox3* (*NeuN*) (**Fig. 3.8 B**). Together, these data suggest that in the absence of *de novo* H3.3 in neurons, bivalent genes that normally resolve into active transcription over the course of cortical development did not developmentally upregulate their transcription, thus resulting in reduced expression levels in P0 dKO-N compared to control.

To determine whether the lower levels of H3.3 within dividing NPCs has additional contribute to gene regulation, I analyzed the P0 cortical transcriptome of dKO-E, in which *H3f3a*/*H3f3b* were co-deleted from cycling NPCs. This revealed in dKO-E 1934 DEGs, of which 964 were significantly downregulated and 970 were significantly upregulated compared to control (**Fig. 3.9 A**). Although the number of genes meeting FDR < 0.01 was higher in dKO-E compared to dKO-N, differential gene expression analysis (**Fig. 3.9 B**)

and analysis of hypergeometric distributions (**Fig. 3.9 C**) revealed significantly overlapping transcriptomic changes between dKO-E and dKO-N. In support of this, the genes that were differentially expressed in dKO-E were remarkably consistent in expression change directionality in dKO-N (**Fig. 3.9 D**). Similarly, the genes that were differentially expressed in dKO-N were also comparably changed in dKO-E. Thus, these analyses revealed significantly overlapping gene expression changes following *H3f3a*/*H3f3b* deletion from NPCs prior to final mitosis or from neurons post-mitosis. Together, our transcriptomic results support an important post-mitotic role for H3.3 accumulation in the developmental establishment the neuronal transcriptome.

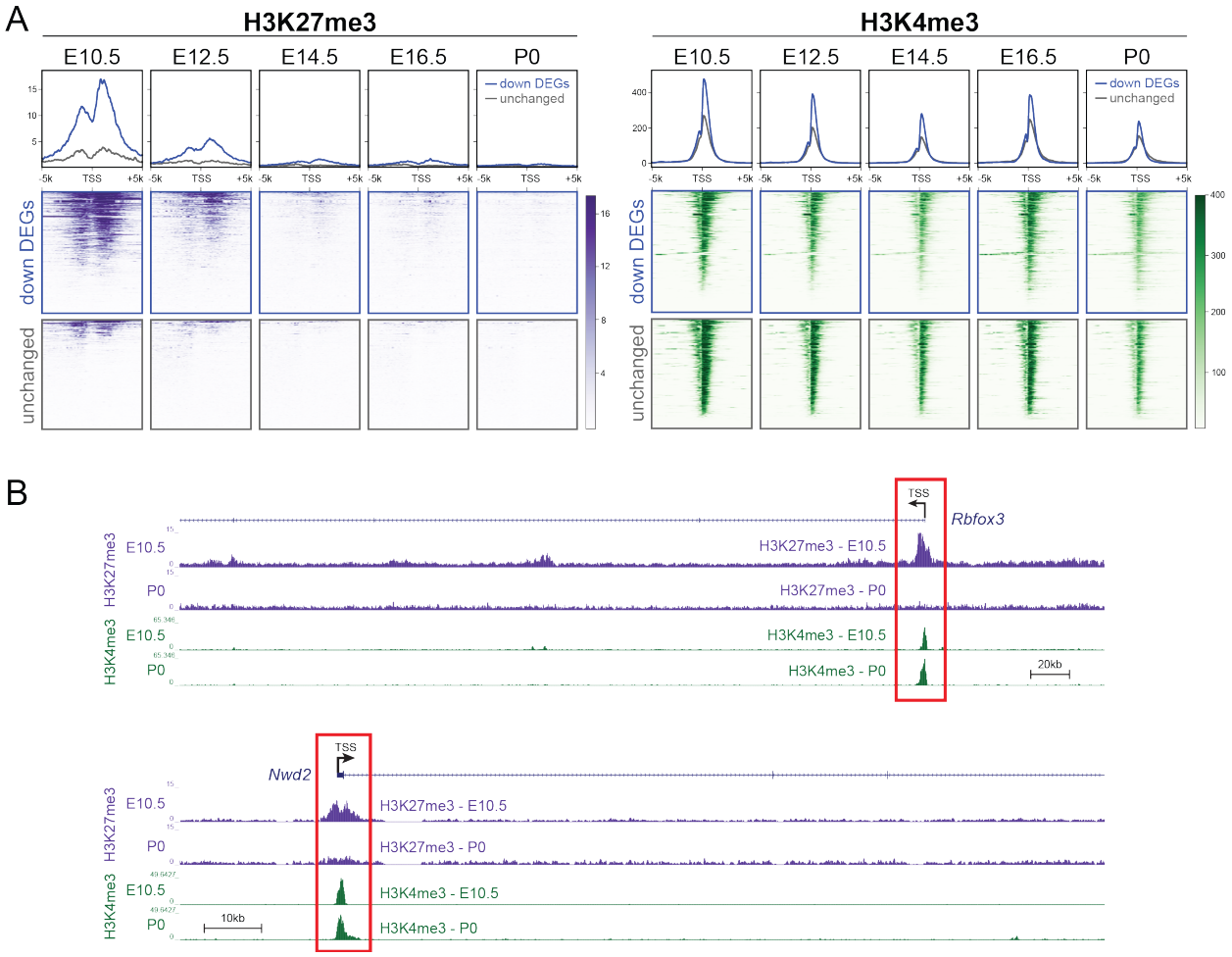

Figure 3.8 Genes affected by H3.3 deletion are associated with developmentally resolved bivalent TSSs

(A) The developmental H3 post-translational modification (PTM) trajectories of dKO-N downregulated and unchanged genes based on ENCODE mouse forebrain ChIP-seq data. Genes downregulated in dKO-N (blue traces) are normally characterized by a progressive decrease in H3K27me3 enrichment (indigo), but not in H3K4me3 enrichment (dark green), across forebrain development.

(B) UCSC Genome Browser tracks of ENCODE E10.5 and P0 forebrain ChIP-seq data. At E10.5, H3K27me3 (purple) and H3K4me3 (green) were both present at the transcription start site (TSS) of dKO-N downregulated DEGs *Rbfox3* and *Nwd2*. At P0, high H3K4me3 persisted at these loci whereas H3K27me3 levels have decreased. These bivalent loci have appear to have resolved to active chromatin over embryonic forebrain development.

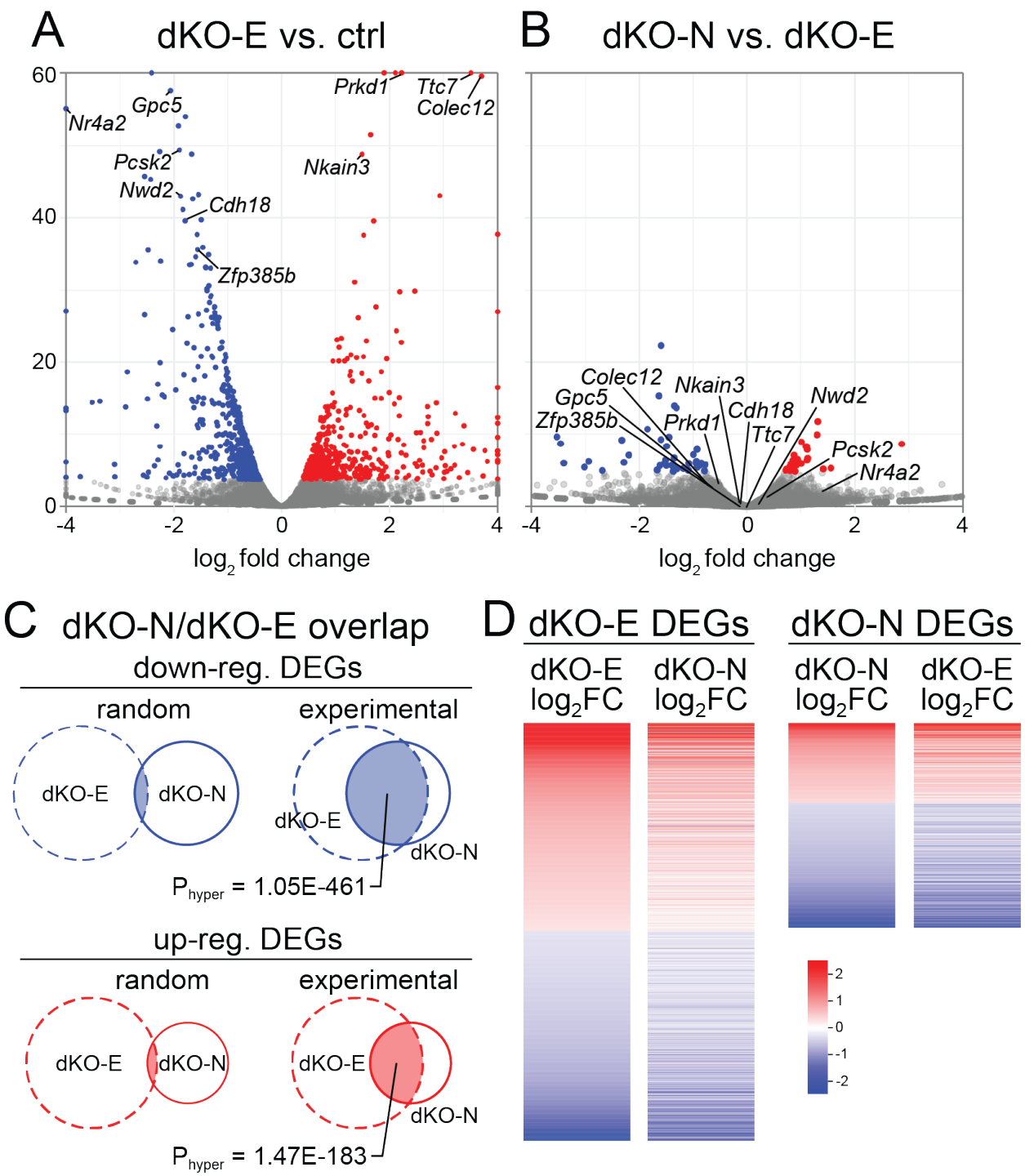

Figure 3.9 Acquisition of the neuronal transcriptome after H3.3 deletion from NPCs

(A) Volcano plot comparing P0 cortex of dKO-E to control (B) Volcano plot comparing dKO-N to dKO-E (F). DEGs are indicated as in A. (G) Experimental overlap of dKO-N and dKO-E DEGs compared to random overlap based on hypergeometric probability. (H) Heatmap of dKO-N and dKO-E DEGs based on log_2FC. dKO-N and dKO-E DEGs showed highly congruent expression change directionality.

Defects in layer identity following H3.3 deletion

The cerebral cortex is specified into six cytoarchitectonically distinct laminae, each with a characteristic composition of molecularly defined neurons (19, 21). To assess whether the transcriptional deficits following *H3f3a* and *H3f3b* co-deletion accompanied altered development of cortical laminae, I first used immunostaining for RBFOX3 (NEUN), a neuronal differentiation marker (146). In P0 control, RBFOX3 immunostaining was present in all cortical layers but more intensely labeled L5 and subplate (SP) neurons (**Fig. 3.10 A**). In both dKO-N and dKO-E, RBFOX3 immunostaining was reduced in all cortical layers, and the intense labeling of L5 and SP neurons was lost (**Fig. 3.10 A**). I next used layer markers to assess layer-dependent molecular identities. In control, BCL11B (CTIP2) showed intense staining in L5 neurons and moderate staining in L6 neurons in a highly stereotyped pattern (39, 40) (**Fig 3.10 B**). In both dKO-N and dKO-E, however, this stereotypic distinction was lost; although BCL11B staining was correctly present in deep layers, a clear differential staining between L5 and L6 was absent. This change was accompanied by additional disruptions of deep-layer marker expression. In control P0 cortex, intense BHLHE22 staining was present in L5 neurons, whereas TLE4 staining was restricted to L6 neurons (**Fig. 3.10 C**). In both dKO-N and dKO-E, the L5 staining of BHLHE22 was lost, whereas TLE4 staining extended beyond L6 and was aberrantly present in L5 (**Fig. 3.10 C**). Thus, the identities of deep-layer cortical neurons were perturbed following *H3f3a*/*H3f3b* co-deletion. Notably, these laminar phenotypes were indistinguishable between dKO-E and dKO-N, suggesting that the requirement for H3.3 in layer-dependent gene expression is post-mitotic.

Neuronal identity is defined by combinatorial gene expression (147). I therefore assessed the molecular specification of neurons using BCL11B and TLE4 co-immunostaining (**Fig. 3.11 A**), and BCL11B and TBR1 co-immunostaining (**Fig. 3.11 B**). In P0 control cortex, L6 neurons were intensely labeled by TLE4 and TBR1 and weakly labeled by BCL11B, whereas L5 neurons were characterized by intense BCL11B labeling and an absence of TLE4 and TBR1, similar to previous reports (37, 39, 148). In dKO-N, however, L5 and L6 neurons were strongly co-labeled by BCL11B and TLE4 (**Fig. 3.11 A**) and BCL11B and TBR1 (**Fig. 3.11 B**). Thus, in the absence of *de novo* neuronal H3.3, deep-layer neurons did not acquire fully distinct L5 versus L6 identities.

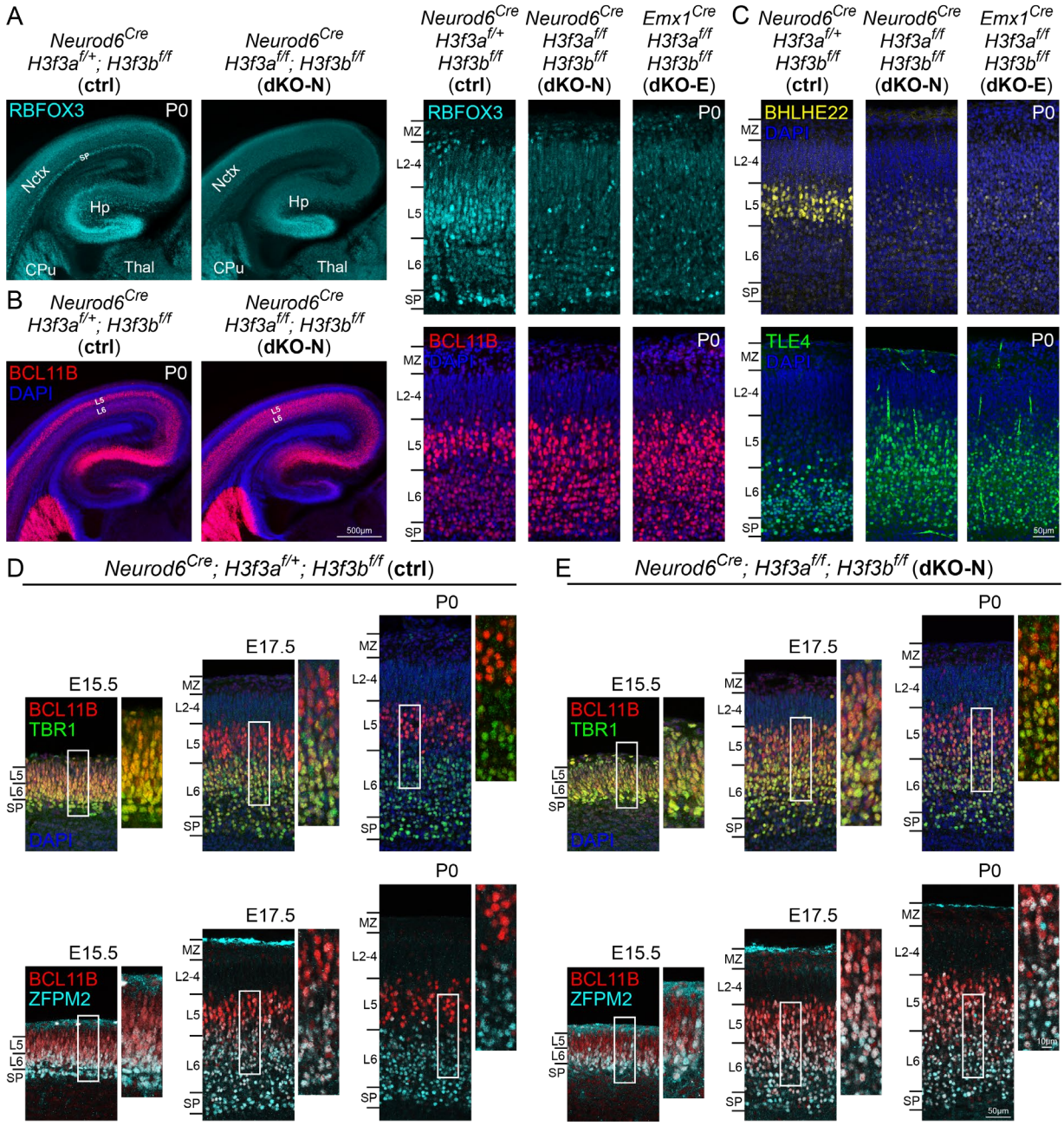

Figure 3.10 Disrupted establishment of layer-dependent neuronal identities following *H3f3a* and *H3f3b* co-deletion.

(A) In P0 control cortex, RBFOX3 (NEUN, cyan) immunostaining was present in all cortical layers and intensely labeled L5 and SP neurons. In dKO-N and dKO-E cortex, RBFOX3 expression was decreased compared to control and intense staining of L5 and SP neurons was absent. (B) In P0 ctrl, BCL11B (CTIP2, red) showed intense staining in L5 neurons and moderate staining in L6 neurons in a stereotyped pattern. In dKO-N and dKO-E, the differential BCL11B staining between L5 and L6 was lost. (C) In P0 ctrl, BHLHE22 (yellow) immunostaining intensely labeled L5 neurons, and TLE4 (green) immunostaining was restricted to L6 neurons. In dKO-N and dKO-E, intense L5 staining of BHLHE22 was lost, and TLE4 staining was aberrantly present in L5. (D and

E) Post-mitotic refinement of deep-layer neuronal identities was analyzed in E15.5, E17.5, and P0 cortex by layer marker co-staining. In control (D), TBR1(green)- or ZFPM2(FOG2, cyan)-labeled L6 neurons abundantly co-expressed BCL11B (red) at E15.5. TBR1- or ZFPM2-labeled L6 neurons have begun to downregulate BCL11B at E17.5 and largely did not express high levels of BCL11B by P0. In dKO-N (E), BCL11B was co-expressed with TBR1 or ZFPM2 at E15.5 in a manner similar to control. Abundant marker co-expression, however, persisted at E17.5 and P0. Deep-layer neurons maintained a developmentally immature, mixed L5/L6 molecular identity in dKO-N until P0.

Hp, hippocampus; Thal, thalamus

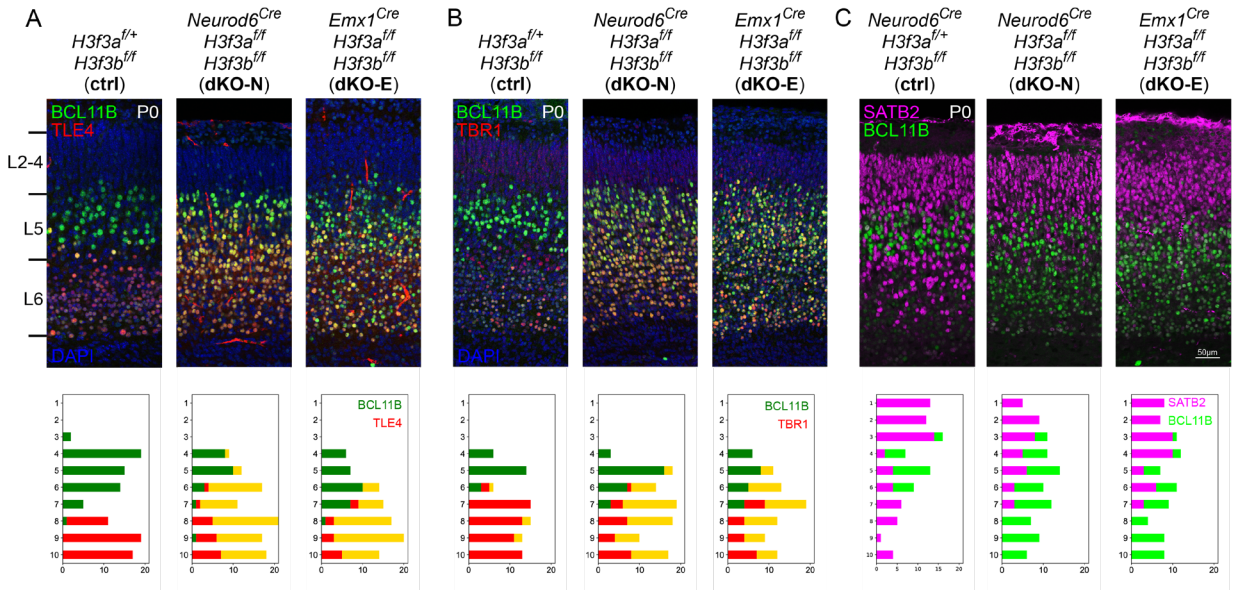

Figure 3.11 Co-expression of deep-layer markers in H3.3 dKO cortex

(A and B) Coronal sections of P0 ctrl, dKO-N, and dKO-E analyzed by layer marker co-immunostaining. In control, L6 neurons were intensely labeled by TLE4 (red, A) and TBR1 (red, B) and weakly labeled by BCL11B (green), and L5 neurons showed intense BCL11B labeling and an absence of TLE4 and TBR1. In dKO-N and dKO-E, L5 and L6 neurons were abundantly co-labeled by BCL11B and TLE4 (A), and BCL11B and TBR1 (B). (C) Coronal sections of P0 ctrl, dKO-N, and dKO-E analyzed by SATB2 (magenta) and BCL11B (green) co-immunostaining. In control, SATB2 and BCL11B labeled largely non-overlapping neurons, with only a small proportion of neurons showing co-labeling. In dKO-N and dKO-E, this distinction was maintained, and upper layer neurons did not misexpress BCL11B.

Defects in cortical axon projection following H3.3 deletion

The axonal projections of cortical neurons are linked to their laminar identities (18-20). To assess whether axonal phenotypes accompanied the transcriptomic and layer identity changes following *H3f3a*/*H3f3b* co-deletion, I analyzed cortical axon tracts in P0 cortex (**Fig. 3.12 A**). In control cortex, immunostaining of L1CAM, an axon marker, revealed axons traversing white matter (WM) below cortical plate (CP) (**Fig. 3.12 B**). L1CAM also labeled the trajectory of the corpus callosum (CC), which normally connects the left and right cortical hemispheres (**Fig. 3.12 B**). *H3f3a* and *H3f3b* co-deletion from neurons (dKO-N) or NPCs (dKO-E) led to a marked loss of white matter thickness, and complete agenesis of corpus callosum (**Fig. 3.12 B**). Next, I leveraged the Cre-dependent fluorescent reporters expressed from the *H3f3a* and *H3f3b* floxed loci to analyze axon tracts. In both dKO-N and dKO-E, the anterior commissure (AC), which normally connects lateral cortical regions, failed to cross the midline and was misrouted towards the hypothalamus (**Fig. 3.12 C**). In addition to intracortical tracts, corticofugal tracts were also disrupted. In both dKO-N and dKO-E, corticofugal axons projected into the caudate putamen (CP) and innervated the internal capsule (IC) (**Fig. 3.12 D**), where corticofugal axons normally coalesce before diverging towards their respective subcortical targets(21, 149). Thus, efferent axons were able to extend out of the cortex in the absence of H3.3. Beyond the internal capsule, however, corticofugal axons showed deficits in reaching their subcortical targets in both dKO-N and dKO-E. Analysis of the corticothalamic tract, which was abundantly visible in control, revealed a near complete absence of cortical axons reaching the dorsal thalamus (**Fig. 3.12 D**). Similarly, analysis of the corticospinal tract (CST) also revealed an absence of axons that reached the level of the pons or

beyond (**Fig. 3.12 E**). I further analyzed the axons of hippocampal pyramidal neurons (**Fig. 3.13 A**). In both dKO-N and dKO-E, hippocampal axons projected into the fimbria, but failed to innervate the fornix. These deficits accompanied alterations in hippocampal organization (**Fig. 3.13 B** and **C**). Together, these data revealed a requirement for H3.3 in the formation of both intracortical and corticofugal tracts, especially in enabling axons to reach their final targets in the contralateral hemisphere or in subcerebral brain structures. Importantly, these axonal defects were phenotypically indistinguishable between dKO-N and dKO-E, indicating that the requirement for *de novo* H3.3 accumulation in axon tract development is largely post-mitotic.

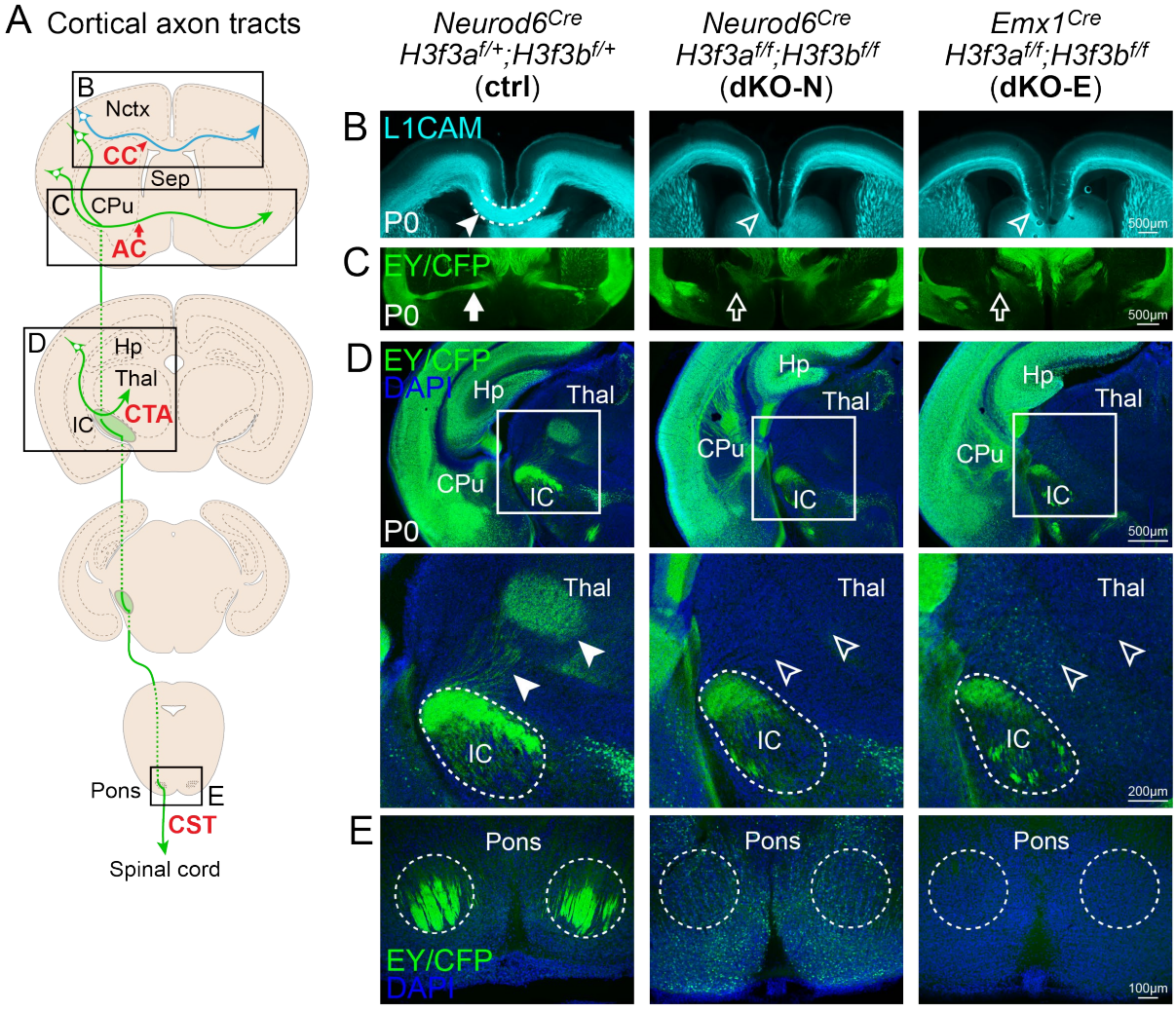

Figure 3.12 Defective axon tract development following *H3f3a* and *H3f3b* co-deletion.

(A) A schematic of major cortical axon tracts. (B) L1CAM (cyan) staining of P0 ctrl, dKO-N, and dKO-E cortex. dKO-N and dKO-E were characterized by a loss of white matter thickness and complete agenesis of corpus callosum (CC, arrowheads). (C-E) Cre-dependent fluorescent reporters expressed from the *H3f3a* and *H3f3b* floxed loci were detected by EGFP immunostaining of EYFP and ECFP residues and used to analyze axon tracts in P0 ctrl, dKO-N, and dKO-E cortex. (C) EY/CFP (green) reporter staining revealed failed midline crossing of the anterior commissure (AC, arrows) and misrouting of anterior commissure axons to the hypothalamus in dKO-N and dKO-E. (D) In dKO-N and dKO-E, corticofugal axons reached the internal capsule (IC), but the corticothalamic tract (CTA, arrowheads) did not form. (E) Analysis of the corticospinal tract (CST) revealed an absence of axons that reached the level of the pons in dKO-N and dKO-E.

CC, corpus callosum; AC, anterior commissure; CTA, corticothalamic tract; CST, corticospinal tract; IC, internal capsule

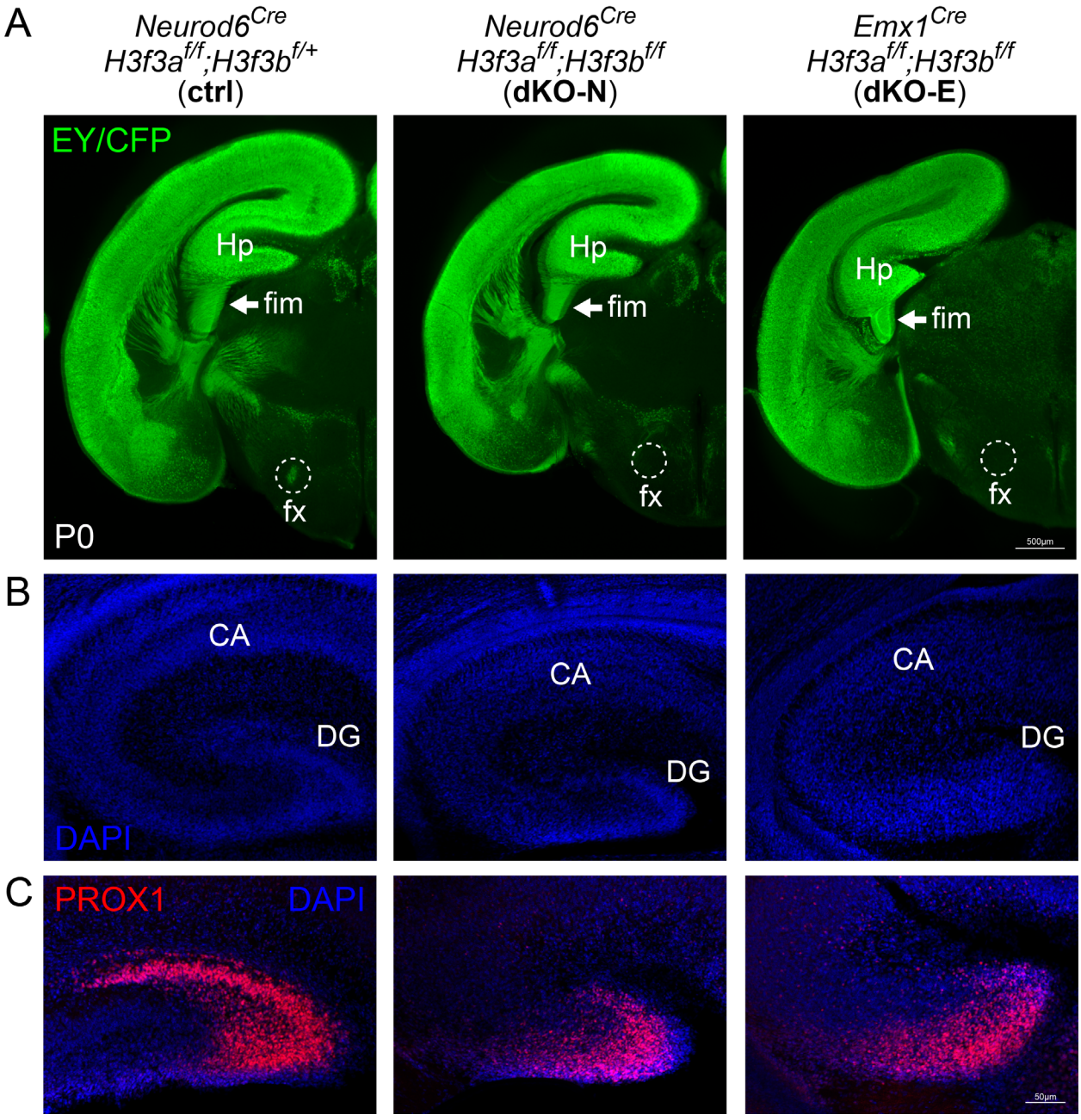

Figure 3.13 Fornix defects and hippocampal dysplasia following *H3f33a/H3f3b* co-deletion

(A) Axon analysis by EGFP immunostaining of Cre-dependent reporters (EY/CFP, green). In P0 control, EY/CFP-labeled axons from hippocampus (Hp) extended through the fimbria (fim) and innervated the fornix (fx). In dKO-N and dKO-E, hippocampal axons projected into fimbria (arrows) but failed to innervate fornix (dashed outlines). (B) DAPI staining (blue) of P0 hippocampus revealed dysplasia of cornu ammonis (CA) and dentate gyrus (DG) in dKO-N and dKO-E. (C) PROX1 immunostaining (red) of P0 hippocampus revealed disorganization of dentate gyrus cells in dKO-N and dKO-E.

Discussion

Accumulation of H3.3 in newly born neurons

After undergoing asymmetric cell division and migrating into the cortical plate, recently post-mitotic neurons begin a massive transition in gene expression and cellular function. Through immunofluorescence I observed a stark difference in the amount of H3.3 protein in the nascent cortical plate in comparison to cells in the VZ, SVZ, and IZ. This would suggest that after the final mitosis, the neuronal genome becomes significantly enriched with newly synthesized H3.3. Conditional deletion of H3.3 from neurons by *Neurod6*^{Cre} affects cells only after they become post-mitotic, and resulted in a lack of H3.3 throughout the cortical plate. Thus, expression of H3.3 in NPCs, which is preserved in dKO-N, is insufficient to drive normal accumulation of H3.3 in neurons. Any H3.3 mRNA carried over from NPCs appears to be insufficient to drive production, and *de novo* H3.3 synthesis and deposition in neurons is required. H3.3 is known to play a role in maintaining H3 levels in the cell, and eventually reaches saturating levels over time (75, 76). This process occurs much slower than the rapid accumulation in post mitotic neurons I observed. H3.3 is known to be enriched at active regions of the genome and found decorated with transcriptionally activating PTMs (69, 150). Furthermore H3.3 turnover has been linked to open chromatin accessibility, as well as the activation of regulatory elements like enhancers and promoters (134, 150). Given the great accumulation of H3.3 associated with differentiation in neurons, it seems likely that H3.3 plays a key role in the activation of developmentally regulated genes. Given the large amount of transcriptional rewiring and chromatin reorganization necessary for cell fate transition, this H3.3

accumulation would need to rapidly affect much of the genome. Indeed, H3.3 has been found to play a critical role during development in several instances (79, 108, 110).

It has been proposed that when H3.3 is depleted, histone turnover stalls (76). In all of the dKO brains I analyzed, I found normal levels of total H3, and no appreciable cell death. This would agree with a model in which H3.3 depletion inhibits histone turnover, as there was no evidence for widespread loss of nucleosomes or apoptosis in the affected cells. Further experimentation to specifically track histone turnover, as well as genomic localization of H3.3, would help to determine if turnover is indeed impaired in dKO neurons.

While H3.3 does possess the unique S31 residue, the biochemical differences between it and canonical H3 are few, and their significance is contested. It has been proposed that H3.3 specific chaperones can directly recruit chromatin remodelers, thus connecting H3.3 deposition to chromatin modifying enzymes (78, 151). Another possibility is that this replacement functionally “resets” histone marks, allowing for a new chromatin landscape to be established. Alternatively, the act of turnover itself can increase accessibility to the underlying DNA (150). As histones are removed and replaced, buried motifs are uncovered and can be bound by regulatory factors. My work showed clear deficits in the dKO-N mice when H3.3 is removed immediately after the final division, but the causative mechanisms that lead to the observed phenotype remain to be discovered. Currently, the chromatin field still lacks consensus on whether it is H3.3 specific PTMs, H3.3 genomic loci, or increased turnover associated with H3.3 that is most important for its observed functions.

A single H3.3 allele is sufficient for cortical development

Somewhat surprisingly, I found that a single H3.3 allele, either *H3f3a* or *H3f3b* was sufficient for normal development, and these one-of-four allele mice showed no defects or major observable phenotypes. This is contrasted to other studies, in which single gene deletions (*H3f3a* or *H3f3b*) resulted in defects (74, 101, 102), however these studies were not conducted on cortical neurons, and it seems likely that at least in this context either gene is sufficient to drive the rapid accumulation across embryonic development. Compensatory upregulation of either gene was difficult to establish, as the transgenic mouse model used replaces the endogenous locus with a pre-spliced *H3f3a* CDS, but overall H3.3-transcript levels were roughly comparable between conditions. Canonical histone expression was not detected, likely due to the lack of a polyA tail that precluded polyT priming during library construction, and due to the synthesis-linked natured of canonical histone production. How exactly a single allele is able to compensate for loss of the others, and whether either H3.3 producing gene plays a specialized role in cortical neurons requires further experimentation, initial inspection suggests that transcriptomicly there are few changes associated with partial H3.3 deletion.

H3.3 is required for acquisition of the neuronal transcriptome

The timing of post-mitotic H3.3 accumulation coincides with a critical period for developmental acquisition of the neuronal transcriptome (19). H3.3 has been connected to the acquisition of new cellular identity, both in development and reprogramming (103, 108, 152). My differential transcriptomics uncovered large shifts in gene expression in H3.3 dKO mice, in particular in genes that are developmentally upregulated. Many of these genes have bivalent TSSs early on in development that are later resolved to active

chromatin. H3.3 is known to play a role in both establishing and resolving bivalent regions, and these regions have been shown to play important roles in neuronal development (87, 143). Given that the similarity between dKO-E and dKO-N transcriptomes, it appears as though H3.3's role in resolving bivalence post-mitosis is more important for cortical development, or that bivalency at TSSs is already established before E10.5, when *Emx1*^{Cre} becomes active.

Although the similarity between dKO-E and dKO-N was remarkably significant, I did find some differences in the respective transcriptomes. As noted previously, H3.3 is known to play a role in dividing cells as well, although often ascribed to genome integrity functions, and in several study led to relatively little change to the transcriptome despite early embryonic lethality (79, 153). I compared *Emx1*^{Cre} and *Neurod6*^{Cre} conditional knockouts to determine the function of H3.3 in NPCs vs. recently post-mitotic neurons. *Emx1*^{Cre} is active in NPCs around day E10.5 and neurogenesis is largely complete by E17.5. I found no DNA damage or apoptosis in the dKO-E brains, contrasting the severe genome integrity defects described in early knockouts. It is possible that the cytogenic problems in earlier KOs are the result of chronic H3.3 depletion that leads to damage only after many divisions, and that the E10.5 deletion in NPCs in dKO-E has not had enough time or cell divisions for these defects to manifest before the NPCs differentiate into neurons and stop dividing. As NPCs divide a limited number of times, they may retain enough H3.3 to continue sufficient telomere formation until they reach their final division.

H3.3 is required for neuronal development

The establishment of neuronal identity and corresponding axonal connectivity requires precise transcriptional control early in development, including within NPCs (19,

35, 154). This specification continues throughout development, as neurons are further refined to more specific fates (40). Lower-layer neurons co-express L5 and L6 markers at the time of final mitosis, but subsequently refine gene expression to acquire a transcriptome specific to the layer they reside in. This refinement also occurs during the period of H3.3 accumulation observed, and thus may be affected in dKOs. In dKO-N I observed a continued co-expression of deep layer markers BCL11B and TBR1/ZFPM2, suggesting H3.3 might play a role in postmitotic refinement as well. Interestingly upper layer marker expression was largely intact, suggesting that not all refinement requires H3.3.

Neuronal connectivity is correlated to cellular identity, particularly in the cortex (155). The laminar organization also corresponds to where the resident cells will project to, with L2-4 projecting primarily intracortical, and L5-6 subcortically. Alongside the defects found in cellular identity I found sever deficits in axonal tract formation. In both dKO mice there was a complete agenesis of corpus callosum and hypothalamic misrouting of the anterior commissure. Axons successfully projected to the internal capsule but not further into the thalamus, and the cortical-spinal tract was completely absent. Beyond the clear connection between altered cell identity and miswired axons, other factors may also be at play. dKO-N and dKO-E failed to specify subplate neurons, a structure known to assist in axon guidance (156). Furthermore, many subplate specific genes were down-regulated in the RNAseq data. The lack of a subplate or subplate deficits may also be responsible for the white matter defects I saw and would need to be tested with subplate specific deletion of H3.3.

Hippocampal dysplasia

The hippocampus is an extension of the temporal cortex and plays an important role in learning and memory. The hippocampus contains the CA (*Cornu Ammonis*) fields composed of tightly packed projection neurons similar to the cortex and dentate gyrus (DG). Within the DG resides the granule layer, home to dentate granule cells that continue to produce proliferate to create neurons throughout adulthood. In exploring defects to cortical development, I discovered that in dKO-N, there was significant dysplasia of the dentate gyrus, both through DAPI-based morphology and PROX1 staining. In dKO-E I noted even more severe dysplasia with less Prox1 staining and an even greater lack of organization. Additionally, in both dKO-N and dKO-E I noted a loss of distinct laminar organization of the CA fields, similar to that observed in the cortex, and many of the same marker genes were altered in distribution. The differences between dKO-N and dKO-E DG are most likely explained by differences in Cre expression. The DG is home to adult neurogenesis stemming from the DG granule cells found there, a population that is *Emx1* positive but not *Neurod6*. As a result, the DG phenotype I observed is understandably more severe in the dKO-E. Whether H3.3 KO affects neurogenesis from DG granule cells remains to be seen, but given the hypoplasia noted in dKO-E this is a possibility.

Conclusion

One of the defining aspects of neurons is their long-range projections and the cytoplasmic proteins localized to distally along these processes that facilitate their functionality. As such, neurological disease has often been studied in the context of these cytoplasmic genes. Central to disease etiology however, is also cellular identity and differentiation, and these are now being linked to nuclear proteins and chromatin affecting

factors. My work adds to this endeavor, helping to understand the critical importance of chromatin in brain development and function. Here I investigate the role of histone variant H3.3 in brain development and use conditional deletion to assess the consequences of its loss from both NPCs and recently post-mitotic neurons. In the knockouts, I found robust changes to the neuronal transcriptome, possibly driven by an inability to upregulate developmentally important genes and resolve poised, bivalent loci associated with neuronal gene expression. These changes included many neuronal genes associated with cellular identity and axonal projection. These changes were accompanied by altered laminar organization and severe misrouting of white matter tracts. Moreover, these changes were highly similar between NPC deletion in dKO-E and newly post-mitotic deletion in dKO-N. This implied that H3.3's role in the acquisition of the neuronal transcriptome and cellular identity/connectivity takes places primarily in neurons after they have undergone their final division.

Materials and Methods

Mice and mouse husbandry

The conditional-ready *H3f3a* and *H3f3b* alleles (130), and the *Neuord6*^{Cre} (131)*, Emx1*^{Cre} (132), were previously generated. For timed pregnancies, the date of vaginal plug was considered embryonic day (E)0.5. Genotyping was performed using DreamTaq Green 2x Master Mix (Thermo Fisher) and genomic DNA isolated from toe or tail clips. Genotyping Primers are listed in the Key Resources Table. Mice were maintained on a standard 12 h day:night cycle with *ad libitum* access to food and water, and all experiments were carried out in compliance with ethical regulations for animal research. Our study protocol was

reviewed and approved by the University of Michigan Institutional Animal Care & Use Committee.

Single-nuclei RNAseq

The cortex was isolated from an E14.5 embryonic mouse and flash frozen in ethanol and dry ice. Nuceli were then isolated and processed for single-nuclei sequencing in accordance with 10x Genomics recommended protocols. (https://assets.ctfassets.net/an68im79xiti/2IcRfnCKj9MWM4eYZavFnc/47c6023e2987f63ec83173d62124ee7e/CG00055_Demonstrated_Protocol_Dissociation_Mouse_Neural_Tissue_Rev_C.pdf) Briefly, frozen tissue was pulverized using a Dounce homogenizer on ice with 10 strokes of pestle A and 10 strokes of pestle B in 500ul of 0.1x Lysis Buffer. Then the crude lysate was incubated on ice for 7 minutes, followed by the addition of 500ul Wash Buffer and centrifugation for 5 minutes at 500g. The supernatant was filtered through a 40um cell strainer and centrifuged again at 500g for 5 min. Resulting nuclei pellet was resuspended in Diluted Nuclei Buffer. Resulting libraries were sequenced at the University of Michigan sequencing core on the Illumina NovaSeq 6000 platform (150 cycles).

Single-nuclei data processing

Single nuclei RNA-seq (snRNA-seq) reads were pseudoaligned and counted using kallisto-bus tools (100) with kallisto v0.46.2 and bustools v0.40.0. The kallisto indexes used were generated from the GENCODE GRCm38.p6 reference genome and Ensembl 98 annotations with the lamanno workflow option to include introns. Seurat v4.0.3 (42, 101) was used to filter, normalize, cluster, and analyze the data. Regularized

negative binomial regression (Seurat::SCTransform) was used for normalization. Seurat was then used to determine clusters with original Louvain algorithm and marker genes were found using a Wilcoxon Rank Sum test.

Immunostaining and imaging

Brains were isolated and fixed in 4% PFA overnight at 4°C with agitation and embedded in 4% low-melting agarose for sectioning. Brains were vibratome-sectioned at 70 μm using a Leica VT1000S or VT1200S. Free-floating sections were blocked and immunostained in blocking solution containing 5% donkey serum, 1% BSA, 0.1% glycine, 0.1% lysine, and 0.3% Triton X-100 (Triton X-100 was excluded from blocking solution when immunostaining for CSPG). Free-floating sections were incubated with primary antibodies overnight at 4°C followed by washing 3 × 5-min in PBS and incubated with the corresponding fluorescent secondary antibodies and DAPI in blocking solution for 1h at RT. Following secondary antibody staining, sections were mounted with VECTASHIELD Antifade Mounting Medium (Vector Laboratories). Images were acquired using either an Olympus SZX16 dissecting scope with Olympus U-HGLGPS fluorescent source and Q-Capture Pro 7 software to operate a Q-imaging Regia 6000 camera, or using an Olympus Fluoview FV1000 confocal microscope with FV10-ASW software. Primary and secondary antibodies are listed in the Key Resources Table.

Edu incorporation and Staining

EdU was given by intraperitoneal injection at a concentration of 5 μg/g. For EdU staining, sections were permeabilized by incubation for 30 min in 0.5% Triton X-100 in PBS followed by 3 × 5-min washes in PBS. EdU staining solution was made fresh each time, containing 100 mM Tris, 4 mM CuSO4, and 100 mM ascorbic acid diluted in 1× PBS. The

fluorescently labeled azide molecule was added last, and the staining cocktail was immediately added to sections for a 30-min incubation at room temperature (final concentrations of each fluorescent molecule: 4 mM AlexaFluor488-Azide [Click Chemistry Tools, 1275-1], 10 mM Cy3-Azide [Lumiprobe, A1330], 16 mM AlexaFluor647-Azide [Click Chemistry Tools, 1299-1]). After incubation, sections were washed 3 × 5 min in PBS. After EdU labeling, standard protocols were followed for immunostaining.

Western Blot

Mouse cortex was lysed in 1×SDS buffer, proteins were denatured 3 min at 95°C, separated on 4%–12% bis-Tris Gel (NuPAGE), transferred on nitrocellulose membranes, and blocked with 5% non-fat dry milk in Tris Buffer Saline buffer (TBS). Primary incubation was carried out in TBS plus 5% non-fat dry milk, washed 3 times and incubated with anti-rabbit or mouse Peroxidase antibody (1:10,000, Cell Signaling) 1 hour in TBS, followed by washing and ECL Prime chemiluminescence revelation kit (Sigma).

Statistical Analysis

Statistical analyses were performed in GraphPad Prism 8 (GraphPad Software). Values were compared using an unpaired Student's *t* test with Welch's correction, or one-way ANOVA with Tukey's post hoc test.

RNAseq

Embryos were isolated and immediately submerged in ice-cold PBS. Neocortical tissue was dissected and flash-frozen in a dry ice–ethanol bath and stored at −80° until further processing. Tissue was resuspended in 0.5 mL of Trizol and homogenized using metal beads in a bullet blender. Chloroform was added to the sample, and the aqueous phase

was isolated following centrifugation for 15 min at >20,000 g at 4 °C. The sample was transferred to a Zymo Research Zymo-Spin IC column and was processed following the manufacturer's protocol, including on-column DNA digestion. Pure RNA was eluted in DNase/RNase-free water and quantified using a Qubit fluorometer.

RNA-seq libraries were generated by Click-Seq (138) from 600 ng of purified neocortical RNA. Ribosomal RNA was removed from total RNA using NEBNext rRNA Depletion Kit (NEB). ERCC RNA spike-in was included for library quality assessment (Thermo Fisher). SuperScript II (Invitrogen) was used for reverse transcription with 1:30 5 mM AzdNTP:dNTP and 3′ Genomic Adapter-6N RT primer (GTGACTGGAGTTCAGACGTGTGCTCTTCCGATCTNNNNNN). RNaseH treatment was used to remove RNA template and DNA was purified with DNA Clean and Concentrator Kit (Zymo Research). Azido-terminated cDNA was combined with the click adaptor-oligo (/5Hexynyl/NNNNNNNNAGATCGGAAGAGCGTCGTGTAGGGAAAGAGTGTAGATCTCGGTGGTCGCCGTATCATT) and click reaction was catalyzed by addition of ascorbic acid and Cu^{2+}, with subsequent purification with DNA Clean and Concentrator Kit. Library amplification was performed using Illumina universal primer (AATGATACGGCGACCACCGAG), Illumina indexing primer (CAAGCAGAAGACGGCATACGAGATNNNNNNGTGACTGGAGTTCAGACGTGT) and the manufacturer's protocols from the 2× One Taq Hot Start Mastermix (NEB). To enrich for amplification products larger than 200 bp, PCR products were purified using Ampure XP (Beckman) magnetic beads at 1.25× ratio. Libraries were analyzed on TapeStation

(Agilent) for appropriate quality and distribution and were sequenced at the University of Michigan sequencing core on the Illumina NovaSeq 6000 platform (150 cycles).

Chapter 4 H3.3 in Late and Aging Post-Mitotic Neurons

Abstract

Terminally post-mitotic tissue still has a demand for histones. Histone turnover and replacement are thought to play a role in gene transcription and regulation, and histones that are lost or degraded must be replaced to maintain chromatin integrity. I generated a conditional knockout of H3.3 several days after the final mitosis and found that once established, the neuronal transcriptome was largely unaffected by the loss of the H3.3 variant, with the exception of subtle changes to synapse associated genes. Long-term study showed the persistence of pan H3 and H3 PTMs, despite the lack of replacement H3.3, and uncovered the possibility of an as yet unknown source of post-mitotic H3 in quiescent neurons. This work uncovers a role for H3.3 in the long-term maintenance of H3 across the neuronal lifespan that is distinct from its active role in establishing neuronal transcriptome and identity immediately post-mitosis.

Results

H3.3 deletion in *Rbp4*^{Cre}+ neurons days after *Neurod6*^{Cre} deletion

The substantial *de novo* H3.3 accumulation that I found in new cortical neurons occurred in the first few days after terminal mitosis (**Fig. 3.1 & 3.2**). In the absence of this accumulation following *H3f3a*/*H3f3b* co-deletion immediately post-mitosis (dKO-N), cortical neurons were unable to acquire the neuronal transcriptome or undergo

developmental maturation, suggesting an active role for *de novo* H3.3 in the first few postmitotic days. H3.3 can be deposited DNA synthesis-independently (69, 157). In terminally post-mitotic cells such as neurons, H3.3 is thought to be the primary source of new histone H3, thus serving important long-term functions in maintaining overall H3 levels (75). H3.3 has also been shown to be involved in neuronal senescence and plasticity (76). To assess the maintenance roles of H3.3 in cortical neurons, I generated an additional *H3f3a*/*H3f3b* co-deletion model using Tg(*Rbp4-Cre*) (158, 159). Tg(*Rbp4-Cre*) mediates recombination from L5 neurons starting at ~E18.5 (**Fig. 4.1 A**), after substantial *de novo* H3.3 accumulation had occurred in the first few post-mitotic days. Importantly, Tg(*Rbp4-Cre*)*;H3f3a*$^{f/f}$;*H3f3b*$^{f/f}$ (dKO-R), unlike dKO-N, was not affected by peri-natal lethality. Thus, the use of dKO-R (**Fig. 4.1 B**) enabled me to: 1) assess the requirement for *de novo* H3.3 after the initial post-mitotic accumulation; and 2) determine the long-term turnover dynamics of H3.3 in post-mitotic neurons.

First, I sought to determine potential phenotypic differences between *H3f3a*/*H3f3b* co-deletion immediately post-mitosis (dKO-N; prior to initial H3.3 incorporation) versus ~5 days post-mitosis (dKO-R; after initial H3.3 incorporation). For direct comparison, I focused our analysis on L5 neurons, which were affected by both Tg(*Rbp4-Cre*) and *Neurod6-Cre* deletion. In dKO-N, I found robust axonal phenotypes, including a striking absence of corticospinal axons reaching the level of the pons (**Fig. 3.12 D**). Corticospinal tract axons originate from L5 neurons, which express Tg(*Rbp4-Cre*) (158, 159). To assess corticospinal axon development in dKO-R, I used a Cre-dependent tdTomato transgene (*ROSA*$^{CAG\text{-}tdTomato}$) to label corticospinal axons originating from L5 neurons.

In P7 dKO-R, corticospinal tract (CST) axons abundantly innervated the pyramids at the level of the medulla in a manner that was indistinguishable from control (**Fig. 4.2 A**). Furthermore, in dKO-N, I found alterations in layer-dependent neuronal identities; BCL11B staining did not differentiate L5 versus L6 neurons (**Fig. 3.10 B**) and BHLHE22 labeling was lost from L5 neurons (**Fig. 3.10 C**). In P7 dKO-R, however, BCL11B staining differentiated L5 and L6 neurons, and BHLHE22 intensely labeled L5 neurons, each in a manner similar to control (**Fig, 4.2 B**). These data therefore showed that after initial H3.3 deposition, *H3f3a*/*H3f3b* deletion in dKO-R did not disrupt the molecular identity or axon projection of L5 neurons, as *H3f3a*/*H3f3b* deletion prior to initial H3.3 deposition did in dKO-N.

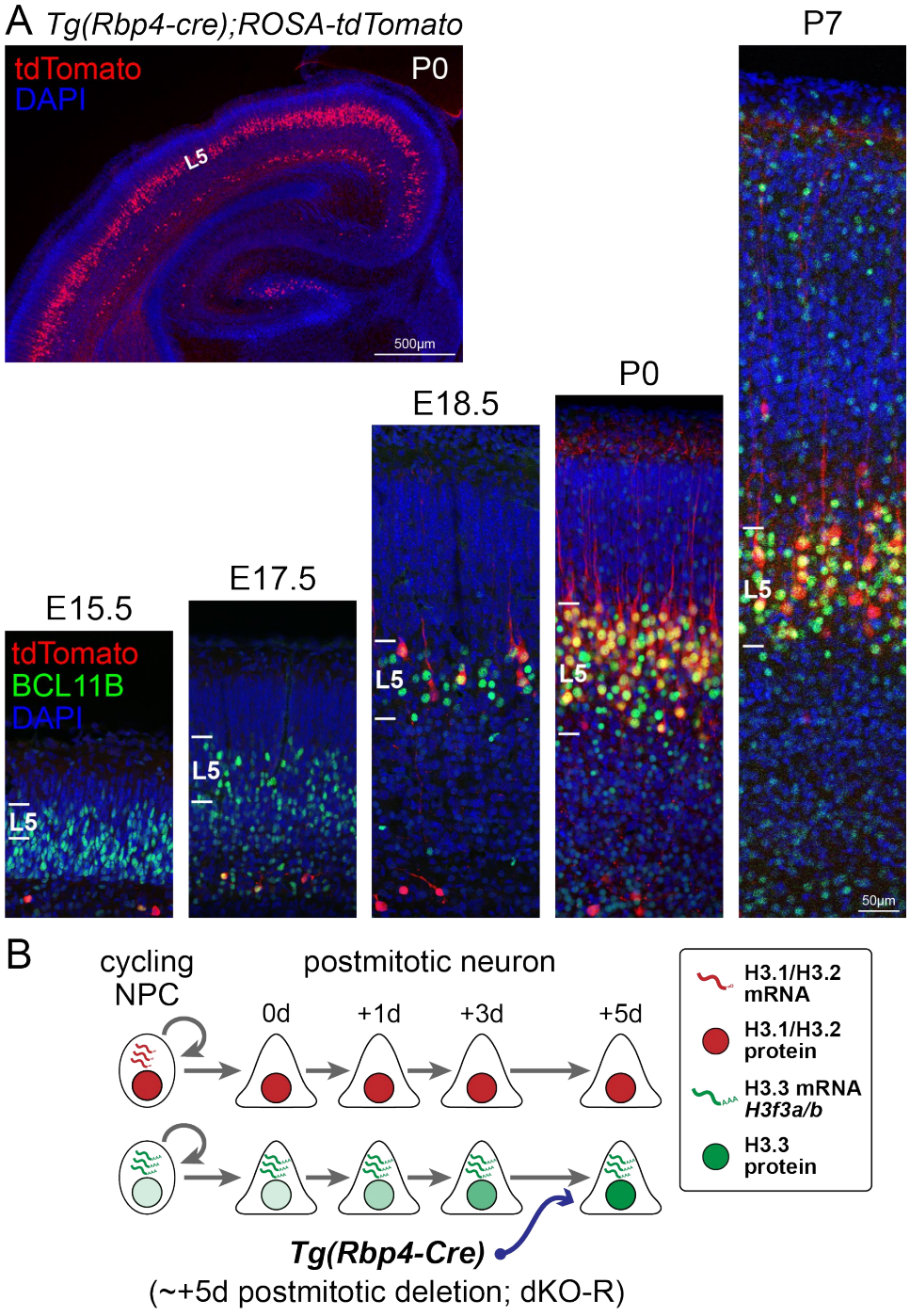

Figure 4.1 Co-deletion of H3.3 genes days after the final mitosis in L5 projection neurons

(A) Tg(*Rbp4*^{Cre})-mediated recombination by Cre-dependent reporter *ROSA-tdTomato* across cortical development. Tg(*Rbp4* ^{Cre})-mediated recombination (red) was present in BCL11B-labeled (green) L5 neurons starting at ~E18.5, approximately 5 days after terminal mitosis. (B) Schematic of H3.3 incorporation and genetic manipulation of *H3f3a* and *H3f3b* by Tg(*Rbp4-Cre*): Tg(*Rbp4-Cre*);*H3f3a*$^{f/f}$;*H3f3b*$^{f/f}$ (dKO-R).

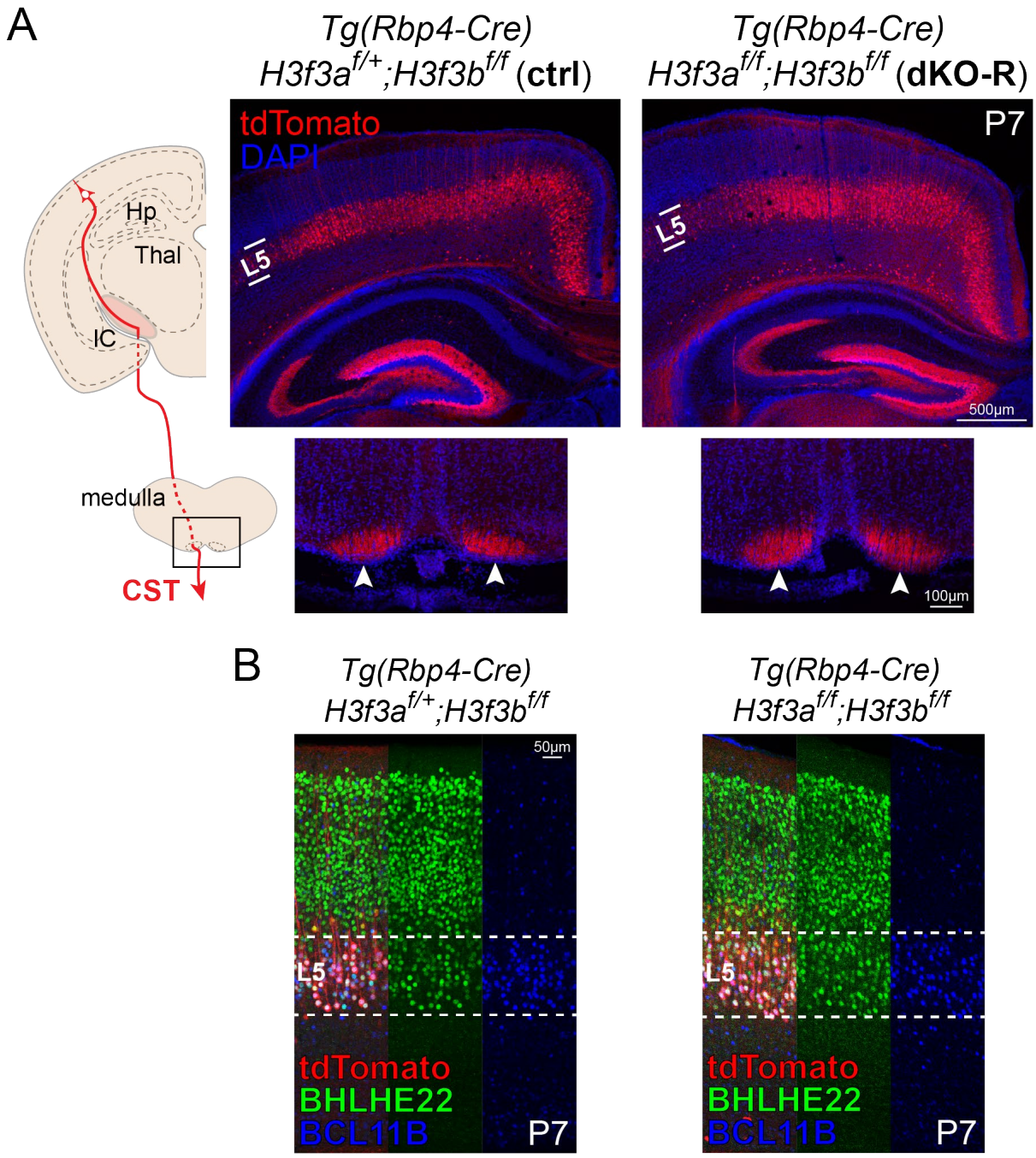

Figure 4.2 Cellular identity and tract formation in P7 dKO-R

(A) At P7, tdTomato-labeled axons (red) arising from L5 neurons abundantly innervated the corticospinal tract (CST) and reached the pyramids (arrowheads) at the level of the medulla in dKO-R in a manner indistinguishable from control. (B) Analysis of BHLHE22 (green) and BCL11B (blue) by immunostaining revealed normal BHLHE22/BCL11B co-expression in tdTomato-labeled L5 neurons (red) in dKO-R.

H3.3 is slowly, progressively replaced in *Rbp4*^{Cre}+ neurons following deletion

Unlike dKO-N mice, dKO-R mice survived into adulthood without premature lethality, enabling me to examine the long-term dynamics of H3.3 turnover in post-mitotic neurons. In dKO-R, Tg(*Rbp4-Cre*) mediated *H3f3a*/*H3f3b* co-deletion after the initial accumulation of H3.3 post-mitosis. Consistent with substantial increase in H3.3 in the first few post-mitotic days (**Fig. 4.1 B**), our analysis of dKO-R at P0 revealed no immediate change in H3.3 levels within Tg(*Rbp4-Cre*)-expressing L5 neurons labeled by *ROSA*$^{CAG\text{-}tdTomato}$ (**Fig. 4.3 A** and **B**). This contrasted dKO-N, in which *H3f3a*/*H3f3b* co-deletion from newly post-mitotic neurons led to a marked loss of H3.3 by P0. To determine how H3.3 levels in dKO-R changed over time in the absence of *de novo* H3.3, I comprehensively analyzed H3.3 in L5 neurons from P0 to 6 months of age. This revealed in dKO-R a slow, progressive loss of H3.3 from L5 neurons (**Fig. 4.3 A** and **B**). These data suggested that in cortical neurons, after initial deposition of H3.3 in the first days post-mitosis, H3.3 was turned over much more slowly, over weeks and months. In addition, the abundance of H3.3-negative neurons in dKO-R at 6 months of age indicated that H3.3 was not required for long-term survival of neurons. Consistent with this, our analysis of DNA double strand breaks by pKAP1 marker staining revealed no increase in DNA damage in dKO-R at six months compared to control.

H3.3 has been proposed to be an important source of H3 protein throughout the lifespan of post-mitotic neurons (76, 160). To assess total H3 levels in dKO-R, I used pan-H3 immunostaining at 6 months, an age at which I observed a ~80% reduction in H3.3 levels in L5 neurons. Surprisingly, despite the marked loss of H3.3, the levels of pan-H3 were not observably different between dKO-R and control (**Fig. 4.3 C**). The presence of

histone H3 was confirmed by immunostaining for H3 that carried post-translational modifications H3K4me3 or H3K27me3 (**Fig. 4.3 C**). These data also suggested that H3 modifications were not eliminated by the lack of *de novo* H3.3 over six months. Together, this data supports that following loss of *de novo* H3.3 synthesis, H3.3 levels progressively decrease over several months. Despite loss of H3.3, total H3 levels were maintained up to six months postnatally, suggesting that H3.3 may not be the sole source of H3 proteins in terminally post-mitotic neurons.

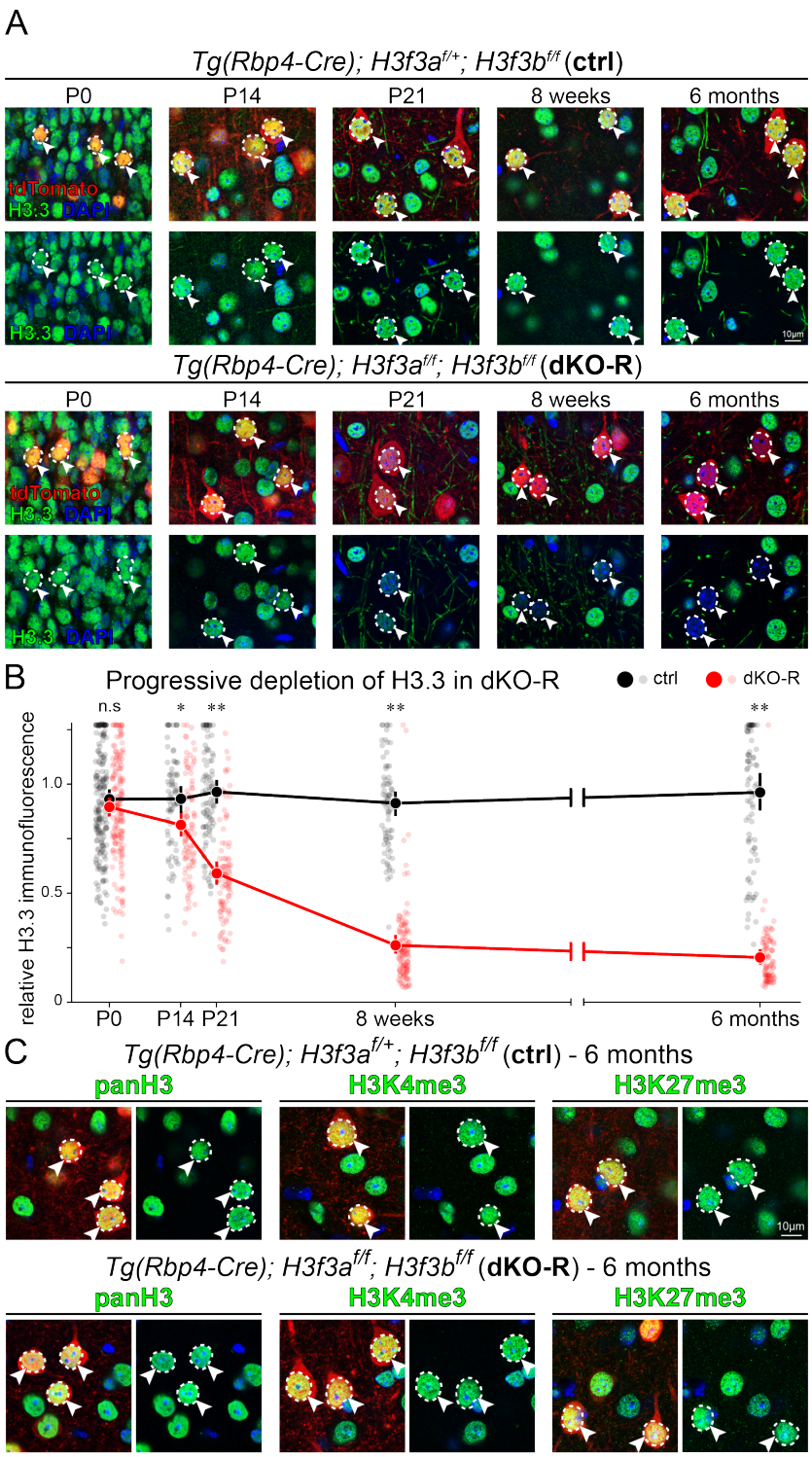

Figure 4.3 Progressive loss of H3.3 from dKO-R neurons

(A) Temporal analysis of H3.3 levels in tdTomato-labeled L5 neurons (red, arrowheads) by immunostaining. In control cortex, H3.3 (green) is maintained in tdTomato-labeled L5 neurons at each analyzed age. In dKO-R, H3.3 levels were unaffected at P0 but showed a progressive loss from L5 neurons over weeks and months. (B) Quantitative analysis of

immunofluorescence (unpaired t-test with Welch's correction, n.s., not significant; ✻, $p < 0.01$; ✻✻, $p < 0.001$). (C) At postnatal 6 months, panH3 and H3 carrying post-translational modifications (PTMs) H3K4me3 and H3K27me3 were assessed by immunostaining. In tdTomato-labeled L5 neurons (red, arrowheads) in dKO-R, despite loss of H3.3 at this age, the levels of panH3 and H3 carrying PTMs were not observably different compared to control.

Neuronal transcriptome of *Rbp4*^{Cre}+ neurons is largely maintained following H3.3 deletion

My results revealed a substantial accumulation of H3.3 in the first days post-mitosis (**Fig. 3.1** & **3.2**) that was required for establishing neuronal transcriptome and identity (**Fig. 3.7** & **3.10**). The timescale of this initial accumulation contrasted long-term H3.3 turnover, which I found to occur over weeks and months in neurons (**Fig. 4.3**). To assess the consequences of H3.3 depletion on the maintenance of neuronal transcription, I used snRNA-seq to analyze control and dKO-R cortex at 5 weeks, after significant loss of H3.3. Clustering by Seurat (121) revealed 34 groups that encompassed the full complement of known cell types in postnatal cortex (**Fig. 4.4 A**). Remarkably, the clustering of ctrl and dKO-R cells showed the same clusters in nearly identical UMAP space (**Fig. 4.4 A**) and substantial overlap of each individual cluster (**Fig. 4.4 B**), including the L5 pyramidal tract (PT) neuron in which Tg(*Rbp4-Cre*) was active (158, 159). This overlap was in striking contrast to the widespread transcriptomic changes I found in dKO-N (**Fig. 3.7**

used differential expression analysis of the L5 PT cluster and specifically assessed whether the differentially-expressed genes (DEGs) in dKO-N were similarly affected in dKO-R L5 PT. I found that all dKO-N DEGs, both up- and down-regulated, were remarkably unaffected, with low log_2FCs (**Fig. 4.4 C**). Together, these data suggest that although the initial accumulation of H3.3 was required to establish the expression of these genes in neurons, once established, *de novo* H3.3 was no longer required to maintain their expression. These data are further consistent with a lack of significant loss of total H3 or H3 PTMs in dKO-R despite loss of H3.3, and the possibility of a non-H3.3 source that can maintain H3 levels in post-mitotic neurons.

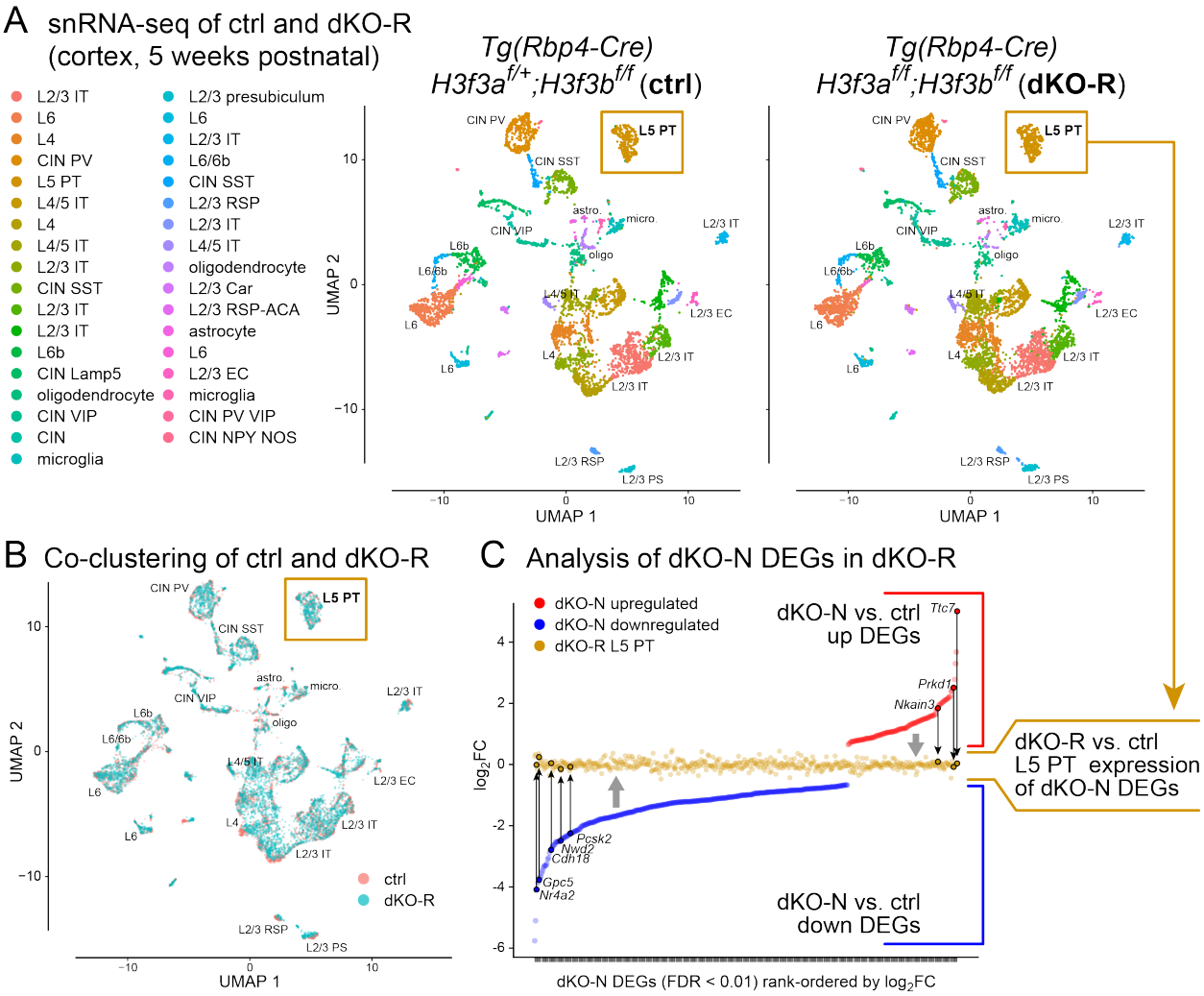

Figure 4.4 single-nuclei RNAseq of adult dKO-R cortex

(A and B) snRNA-seq of control and dKO-R cortex at postnatal 5 weeks visualized by UMAP. Clustering of ctrl and dKO-R cells showed the same 34 cell clusters in UMAP space (A) with substantial overlap of each cluster (B), including the L5 pyramidal tract (PT) neurons (gold boxes) in which Tg(*Rbp4-Cre*) is active. (C) Differentially expressed genes (DEGs) from dKO-N were compared based on log_2FC in dKO-N and in dKO-R L5 PT. Both up- and down-regulated dKO-N DEGs showed a normalization towards a log_2FC of 0 (no change) in dKO-R L5 PT (arrows). (D) Summary of key findings. Cortical neurons undergo substantial *de novo* H3.3 incorporation post-mitosis. *De novo* H3.3 in post-mitotic neurons is required for developmental acquisition of the neuronal transcriptome, establishment of distinct neuronal identities, and formation of axon tracts. The first few post-mitotic days is a critical window for *de novo* H3.3 in neurons. This early H3.3 deposition differs in timescale from long-term H3.3 turnover, which occurs over weeks to months in cortical neurons.

Plasticity/Response genes are altered in L5 PT neurons of adult mice following H3.3 dKO

My analysis did reveal 71 genes that were differentially regulated in dKO-R L5 PT neurons. These genes were largely distinct from the dKO-N DEGs. Interestingly, a number of these genes are associated with neuronal activity or plasticity. This finding is consistent with previous reports that in mature neurons, H3.3 can play a life-long role in neural plasticity (76, 160). In particular, of the top DE genes in L5 PT H3.3 dKO cells there were *Cacna* family calcium channels and Rho-GTPases that were also identified by Maze et. al. as being affected by H3.3 knockdown (76). GO term analysis identified several notable terms: synapse, postsynaptic density, ion channel and cAMP signaling, that further suggest more subtle synaptic function may be altered in these cells, despite the overall lack of overt phenotype (**Fig 4.5**). Further study is required to determine if plasticity or behavior is affected.

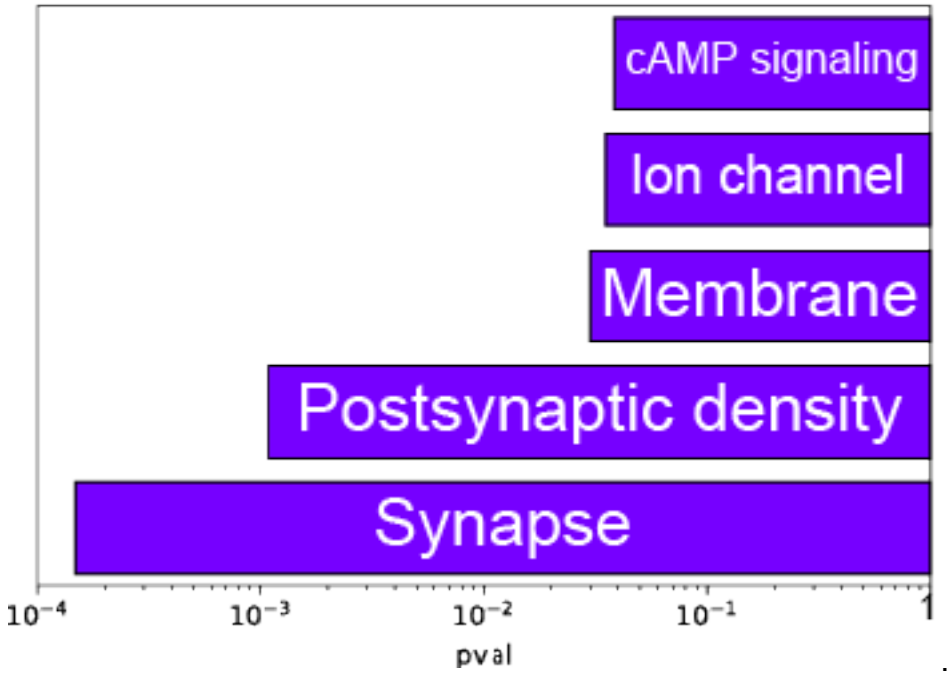

Figure 4.5 GO term enrichment of L5 PT H3.3 dKO DE genes

p-values of select Gene Ontology (GO) terms from differentially expressed genes determined by single-nuclei RNAseq in dKO-R L5 PT cluster. Enrichment calculated using DAVID, p-values displayed using the Bonferroni correction.

Discussion

H3.3 establishes the neuronal transcriptome within the first few days post-mitosis

H3f3a and *H3f3b* are ubiquitously expressed in cell types and throughout the cell cycle, and H3.3 can be deposited DNA synthesis-independently (63, 157). In terminally post-mitotic cells such as neurons, H3.3 is thought to be the primary source of new histone H3 that maintains overall H3 levels long-term. Indeed, previous studies have shown that H3.3 ultimately fully replaces canonical H3, reaching genome-saturating levels several months after birth in the brain and other organs (75). To assess the requirement for *de novo* H3.3 after initial post-mitotic accumulation, I use a Tg(*Rbp4-Cre*) (158, 159) *H3f3a* and *H3f3b* co-deletion model (dKO-R). In dKO-R, *H3f3a* and *H3f3b* are deleted from cortical L5 neurons starting around day E18.5, approximately five days after terminal mitosis and subsequent to substantial H3.3 accumulation in the first few post-mitotic days. Unlike in dKO-N, dKO-R mice were born alive and could nurse, living well into adulthood as fertile adults. This enabled long-term study of H3.3 deletion, something rarely explored in the literature. P0 brains showed no phenotypic differences from control littermates, and this lack of overt phenotype was maintained through P7 and into late adulthood. This lack of phenotype starkly contrasted dKO-N and dKO-E mice, despite the fact that *Rbp4*^{Cre} becomes active only days later. This put a second “bookend” on the critical window of when H3.3 plays an important and active role in shaping neuronal transcription identity. dKO-E and dKO-N showed that before the terminal mitosis, H3.3 played little role in differentiation, and dKO-R showed that once identity was established, H3.3 played little role in its maintenance. Thus, the critical time window for *de novo* H3.3 is in the first few days after terminal mitosis.

H3.3 in maturing neurons

Leveraging the longevity of the dKO-R mouse, I was able to explore H3.3 dynamics over time. In contrast to dKO-N, P0 dKO-R neurons had comparable levels of H3.3 to unaffected neighbor neurons. Despite the large amount of H3.3 accumulation I saw in the first few days post-mitosis, by the time *Rbp4*^{Cre} is active the critical need for *de novo* H3.3 had passed. Over the course of six months, I was able to track and quantify H3.3 levels in *Rbp4*^{Cre} affected cells, observing a steady decrease in H3.3 staining. By six months, L5 cells had lost a majority of H3.3, while maintaining overall levels of panH3 and PTMs. This timeline based on our analysis of dKO-R single cells following *H3f3a* and *H3f3b* co-deletion is consistent with previous wildtype studies of bulk tissues (75, 161). The observation that panH3 levels remained the same despite H3.3 loss was a surprise, as it implies the presence of a compensatory mechanism to maintain overall H3 levels and nucleosome integrity. I further observed no significant increases in DNA damage or cell death associated with dKO-R, again suggesting that genome integrity was maintained in these cells. What this mystery source of H3 is requires further exploration. Canonical histones are largely thought to be expressed exclusively in S-phase, and require DNA-synthesis to be deposited. However, there are some exceptions to these rules (55, 162-164). Additionally, there have been reports of H3-like genes that have escaped annotation that are expressed in the brain (66). Perhaps one of these alternative sources is capable of maintaining H3 in aging cells, but unable to perform H3.3's active function in newly post-mitotic neurons.

Abrogating early H3.3 incorporation in post-mitotic neurons via dKO-N resulted in significant deficits in the acquisition of the neuronal transcriptome. To assess the

consequences of H3.3 loss on the long-term maintenance of the transcriptome, I performed snRNAseq on adult dKO-R cortices. Unlike *Neurod6*^{Cre} and *Emx1*^{Cre} that can alter the entire complement of cortical projection neurons, *Rbp4*^{Cre} affects only a subset L5 cells, and thus requires enrichment of the affected cell type as opposed to bulk sequencing. Clustering identified a clearly marked population of L5 PT cells in both dKO-R and control brains. Overall clustering of dKO-R cells matched that of control remarkably well, with no new cluster identities generated. Additionally, of the 34 clusters identified, dKO-R had roughly the same distribution of cells within these clusters, indicating that there was no significant loss of L5 cells, or molecular confusion that would cause these cells to look transcriptionally similar to another cell type. Together, this suggests that by the time H3.3 is deleted in dKO-R neurons, a) the transcriptome is already established and b) H3.3 is largely dispensable for maintaining the transcriptional regulation required for long-term expression of neuronal identity genes.

H3.3 is largely dispensable for transcriptome maintenance

Previous work has established H3.3's importance in the activation of enhancers (165-167). This activation is proceeded by histone acetylation and binding of transcription factors. Once initiated, these mechanisms are thought to be maintained by feedforward mechanisms, perhaps obviating the need for H3.3. The role of histone turnover could also be at play, as increased turnover in regulatory region may allow for easier access to the enhancer motifs by their cognate binding factors. The mechanisms by which transcriptional programs are enforced over an organism's lifetime are still being explored, but this study would conclude that H3.3 is largely dispensable for maintenance of these programs once they are established.

miRNA silencing of H3.3 in the adult mouse hippocampus was shown to affect plasticity and the transcription of activity-dependent genes (76). While I did not see the widespread transcriptomic changes associated with dKO-R H3.3 deletion, there were a handful of differentially expressed genes in the L5 PT population of dKO-R. This set of genes was enriched for synaptic function and matched some of those identified in the hippocampus shRNA study. This could support the idea that although transcription was not significantly affected overall, activity-dependent transcriptional regulation may rely in part on H3.3. H3.3 contains the unique S31 residue that can be modified, and S31 phosphorylation has been shown to be able to affect transcription. H3.3 can be further modified with transcriptionally active marks, through a variety of mechanisms to induce transcription. Alternatively, it could be the process of H3.3 turnover that is important for activity-dependent gene expression (76). H3.3 can have a substantially lower occupancy time on DNA, and increased turnover of H3.3 containing nucleosomes is connected to transcription and the binding of enhancers and promoters. Whether it is the variant itself that's important or the process of histone turnover is yet to be empirically shown.

Conclusion

This work has clarified a second, maintenance role for H3.3 in aging cells apart from its active role in the acquisition of neuronal fate. Studies using the dKO-R mouse found a broad lack of phenotype in neurons missing H3.3 deleted around day E18.5, particularly when compared to dKO-N and dKO-E. In these mice, panH3 continued to be present into adulthood, despite H3.3 depletion, bringing up the possibility of a previously un-appreciated source of H3 in aging neurons. snRNAseq of adult dKO-R mice further

showed subtle changes to synapse-function relevant genes, suggesting a possible role in fine-tuning neuronal gene expression.

Materials and Methods

Mice and mouse husbandry

The conditional-ready *H3f3a* and *H3f3b* alleles (130), Tg(*Rbp4-Cre*) (158, 159), and *ROSA*^{tdTomato} were previously generated. For timed pregnancies, the date of vaginal plug was considered embryonic day (E)0.5. Genotyping was performed using DreamTaq Green 2x Master Mix (Thermo Fisher) and genomic DNA isolated from toe or tail clips. Genotyping Primers are listed in the Key Resources Table. Mice were maintained on a standard 12 h day:night cycle with *ad libitum* access to food and water, and all experiments were carried out in compliance with ethical regulations for animal research. Our study protocol was reviewed and approved by the University of Michigan Institutional Animal Care & Use Committee.

Single-nuclei RNAseq

Cortices were isolated from three each of 5-weeks postnatal dKO-R and control mice, flash frozen using ethanol and dry ice, and then processed together in a single batch as described below. Nuceli were then isolated and processed for single-nuclei sequencing in accordance with 10x Genomics recommended protocols. (https://assets.ctfassets.net/an68im79xiti/2IcRfnCKj9MWM4eYZavFnc/47c6023e2987f63ec83173d62124ee7e/CG00055_Demonstrated_Protocol_Dissociation_Mouse_Neural_Tissue_Rev_C.pdf) Briefly, frozen tissue was pulverized using a Dounce homogenizer on ice with 10

strokes of pestle A and 10 strokes of pestle B in 500ul of 0.1x Lysis Buffer. Then the crude lysate was incubated on ice for 7 minutes, followed by the addition of 500ul Wash Buffer and centrifugation for 5 minutes at 500g. The supernatant was filtered through a 40um cell strainer and centrifuged again at 500g for 5 min. Resulting nuclei pellet was resuspended in Diluted Nuclei Buffer. Resulting libraries were sequenced at the University of Michigan sequencing core on the Illumina NovaSeq 6000 platform (150 cycles).

Single-nuclei data processing

Single nuclei RNA-seq (snRNA-seq) reads were pseudoaligned and counted using kallisto-bus tools (100) with kallisto v0.46.2 and bustools v0.40.0. The kallisto indexes used were generated from the GENCODE GRCm38.p6 reference genome and Ensembl 98 annotations with the lamanno workflow option to include introns. For the Tg(*Rbp4-Cre*) data, transgenes sequences and annotations were added to the index. Seurat v4.0.3 (42, 101) was used to filter, normalize, cluster, and analyze the data. Briefly, cells passing QC had between 200 and 5000 unique genes and genes were required to be expressed in at least 5 cells. PCA analysis was conducted with nPCAs = 50, and data were log normalized. Seurat was then used to determine clusters with original Louvain algorithm and marker genes were found using a Wilcoxon Rank Sum test. Data from both experiments was integrated using the standard Seurat functions to generate a combined set of cell clusters. Then individual conditions were separated a plotted via UMAP. Differential expression of the L5 PT cluster was determined through pseudo-bulk analysis. Read counts per cell were averaged across

all cells in the L5 PT cluster for each condition individually, and then assessed for differential expression in edgeR.

Immunostaining and Imaging

Brains were isolated and fixed in 4% PFA overnight at 4°C with agitation and embedded in 4% low-melting agarose for sectioning. Brains were vibratome-sectioned at 70 μm using a Leica VT1000S or VT1200S. Free-floating sections were blocked and immunostained in blocking solution containing 5% donkey serum, 1% BSA, 0.1% glycine, 0.1% lysine, and 0.3% Triton X-100 (Triton X-100 was excluded from blocking solution when immunostaining for CSPG). Free-floating sections were incubated with primary antibodies overnight at 4°C followed by washing 3 × 5-min in PBS and incubated with the corresponding fluorescent secondary antibodies and DAPI in blocking solution for 1h at RT. Following secondary antibody staining, sections were mounted with VECTASHIELD Antifade Mounting Medium (Vector Laboratories). Images were acquired using either an Olympus SZX16 dissecting scope with Olympus U-HGLGPS fluorescent source and Q-Capture Pro 7 software to operate a Q-imaging Regia 6000 camera, or using an Olympus Fluoview FV1000 confocal microscope with FV10-ASW software. Primary and secondary antibodies are listed in the Key Resources Table.

Statistical Analysis

Statistical analyses were performed in GraphPad Prism 8 (GraphPad Software). Values were compared using an unpaired Student's *t* test with Welch's correction, or one-way ANOVA with Tukey's post hoc test.

Chapter 5 Discussion

Overview

Chromatin regulation plays critical roles in the cell fate and state transitions that are required for dividing NPCs to become mature neurons. My doctoral research seeks to answer questions about the molecular genetic processes that facilitate this shift in cell state and subsequent refinement of identity, as well as the unique functions of histone variant H3.3 during this period of transition. This work also contributes to the field of histone biology, shedding insight into the behavior of H3.3 in the *in vivo* context of the brain. Conditional deletion of H3.3 from developing NPCs and neurons revealed a striking similarity in phenotypes, while deletion several days after showed relatively little effect. This revealed a previously unknown critical window for H3.3 in the establishment of neuronal identity, connectivity, and gene expression. Transcriptomic analysis gave insights into not only the massive shift in gene expression caused by a lack of *de novo* H3.3, but also may give us clues as to the mechanisms behind this phenomenon.

Additionally, I was able to study the long-term effects of H3.3 loss using dKO-R mice. Although a small population of cells, this is to my knowledge the only *in vivo* study of longitudinal H3.3 loss. This led to the surprising revelation that even without H3.3, histone turnover continues in these cells well into adulthood, and that some previously undescribed source of H3 can maintain overall chromatin integrity. Together, this

research represents an important step forward in understanding the impact of histone variants on neural development.

Histone Turnover

Despite the reputation for giving the genome a rigid structure, chromatin remains fairly fluid in many regions, driven in part by the exchange of histone proteins (96). This process of swapping bound histones for newly synthesized or recycled proteins, known as turnover or exchange, can have meaningful impacts on structure and function of the underlying genomic regions. The exact mechanisms by which histone turnover impacts the genome, however, is still up for debate, and there are several possibilities that are not mutually exclusive and may function in combination.

Increased turnover can facilitate access to the underlying DNA, allowing the binding of regulatory factors or RNA polymerases, while decreased turnover might restrict these processes. This process further allows the incorporation or eviction of specific histone variants or PTMs, both of which can also impact chromatin accessibility. Turnover serves to ensure chromatin integrity by replacing any lost nucleosomes, preventing cryptic transcription or DNA damage at sites of naked DNA. H3.3 turnover has been associated with PRC2 based chromatin remodeling in mouse ESCs, particularly in the establishment of H3K27me3 at bivalent TSSs of developmentally regulated genes (78). Proteostasis is also a significant driver in the regulation of free histone proteins as well. Histones are charged highly basic proteins, and if left unchecked can cause oxidative damage in the cell. As a result, histone synthesis is tightly regulated and newly produced histones are immediately bound by various chaperone factors (96). Alternatively, too few histones are thought to stall turnover affecting transcription, although the exact

mechanisms are still being explored (168, 169). Stalling histone turnover via depletion of soluble H3.3 has been also connected to deficits in neuronal transcription and plasticity (76). Given the ubiquity of histones throughout the genome, their turnover process likely plays many roles. As such, defining the importance of histone turnover remains a challenge. Study is further complicated as turnover and the overall longevity of histones is dependent on histone variants, histone PTMs, and genomic context.

Histones are reported to be some of the longest-lived proteins in the cell, with some reports of half-life averaging 223 days in the brain (170, 171). Canonical H3 has largely been thought to have a much longer half-life compared to H3.3. In *Drosophila*, the H3.3 half-life of chromatin bound H3.3 was estimated to be only a day (172). In adult mouse hippocampus, KCL induced stimulation of activity-dependent genes reduced H3.3 half-life from 3.5 days to 17 hours (76). This study also suggested proteasome-based degradation of histones to be a driving factor behind the rate of H3.3 turnover (76). Soluble, cytoplasmic histone proteins are short-lived, but once incorporated into a nucleosome complex they are significantly more durable (150). Additionally, where they integrate into the genome is a key factor in their longevity. Histones at active regions of the genome are more often turned over, and in many cases degraded (76). Heterochromatic regions also harbor histones, but these regions are tightly condensed and undergo very little turnover, particularly in constitutive heterochromatic regions (153). High rates of histone turnover have been seen at chromatin boundaries, and may be involved in stopping the spread of chromatin marks, keeping individual domains distinct in accessibility (173). Turnover rates also vary greatly between genomic elements, as one study uncovered appreciably different rates for promoter, enhancers, gene bodies and

other elements (68). H3.3 is known to have a high turnover rate at enhancer elements, and particularly high rates at super-enhancers (100). This rate has been observed to be higher even than in active gene bodies, and remains high in elements associated with developmentally regulated genes not yet activated but “poised” for transcription (99, 174). The exact mechanisms behind enhancer-based turnover is still being explored, but DNA binding by transcription factors is often implicated (175). One theory is that regulatory regions are marked for higher turnover, resulting in more transient exposure of the underlying DNA motifs for various factors to bind, resulting in increased recruitment of these proteins to the high turnover regions (95). Alternatively, binding of transcription factors may result in frequent eviction of histones, leading to high turnover rates as histones are continually displaced. Whatever the exact mechanism, the turnover process necessitates new histones, and studying the consequences of removing replacement histones like H3.3 will be important for understanding why histones are removed and replaced at different rates.

My work has provided new insights into histone dynamics in neurons. I found a rapid accumulation of H3.3 in newly born neurons, and slow progressive loss in aging neurons following H3.3 gene co-deletion. Whether these observations reflect turnover, genomic accumulation, or increased non-nucleosome H3.3 during development requires further study. In mature neurons, whether H3.3 depletion leads to widespread stalling of turnover, or if turnover continues with non-H3.3 histones remains to be seen. Given the depletion of H3.3 staining over time, it seems likely that some sort of turnover continues in dKO-R neurons. Ultimately, this would support a model in which turnover rates differ between newly born and aging neurons. This would support previous work positioning

H3.3 and its rapid turnover as important factors in changing the transcriptome concurrent with differentiation (78, 133, 165). The question of why there is histone turnover, particularly high turnover in certain genomic regions, is still open. My use of conditional H3.3 dKO in neurons has helped to determine some of the consequences of reduced turnover. In dKO-N, these neurons are born with a normal amount of H3.3, but cannot produce *de novo* H3.3 post-mitotically. This is potentially a good paradigm for studying the effects of turnover, which requires soluble H3.3 (76).

There remains the possibility that the great increase in H3.3 staining seen in neurons reflects unbound H3.3, rather than a large shift in the genomic composition of histones. Some studies do associate an increase of H3.3 with differentiation, including in neurons (108, 110). However, these studies do not find total saturation at this time point, and longitudinal studies do not show complete replacement of canonical H3 until very late adult hood (75, 76). I observed a sharp increase in H3.3 in new neurons, peaking only a few days after the final mitosis, that didn't increase further in intensity with age (**Fig 3.1**). IHC is limited in its quantification abilities, and it is unlikely that the entire genome becomes saturated by P0. This change might reflect a need for a large amount of unbound H3.3 to participate in histone turnover, a process linked to the accessibility of regulatory regions and successful transcriptional elongation (95, 150, 174, 175). This is however difficult to empirically test. Given that histones are tightly regulated and managed by chaperone proteins, staining for histone chaperones like HIRA, DAXX, ASF1 or NASP may help to explore this hypothesis. NASP in particular might be informative, as this chaperone is thought to bind a "reservoir" of soluble H3 in the nucleus, and an increases in NASP may reflect an increase in soluble H3.3 in neurons (176, 177). .

Alternatives to H3.3 in Post-Mitotic Neurons

Canonical histones outside S-phase

Histones are known to be some of the most stable and longest-lived proteins, with half-life estimates in the range of weeks to months once incorporated into chromatin (170, 171). Unincorporated histones however are relatively short lived, sometimes less than a day (76). Because neurons have permanently exited the cell-cycle, and H3.3 represents the primary source of H3 outside of S-phase, it stands to reason h3.3 would accumulate over time as canonical histones are displaced by transcription, binding of proteins, and other chromatin modifying processes. Indeed, this has been observed in many cases, with H3.3 appearing to saturate the genome over time (75, 76, 160). In dKO-R, I found a progressive loss of H3.3 with age after H3.3 gene deletion without a concurrent decrease in overall levels of H3 (**Fig. 4.3**). This introduces the possibility that there may be some alternative source of H3 compensating for H3.3, as panH3 levels, H3 PTMs, and chromatin integrity seemed to be largely unaffected (**Fig. 4.3**). There are several potential sources for this alternative H3.

Canonical histones are thought to be tightly linked to DNA-synthesis (55, 77). Even the regulatory proteins associated with canonical histone production are actively degraded once the cell exits S-phase (59). However, there are several examples of canonical histone and canonical H3 escaping this narrow definition. The most pertinent examples are from instances of canonical histones being expressed in differentiated tissues (162, 163). Particularly relevant to my work is the discovery of RD histone transcription in aging retinal neurons, including several canonical H3 genes (178).

In addition to the typical stem loop 3' UTR, several histone genes including canonical H3 genes were found to possess cryptic splice sites that led to incorporation of an untranslated exon possessing a polyadenylation signal. Other canonical genes have an underutilized polyA signal upstream of their the stem-loop motif, which may take precedence when the stem-loop processing machinery is absent (179). Moreover, these polyadenylated canonical histone transcripts were only in much higher abundance in differentiated tissue, leading to the speculation that this transcriptional switch may be part of the differentiation program. Alternative 3' processing is not unusual in histone genes, as the well-known H2a.x protein can be produced from a replication dependent stemloop transcript or a replication independent polyA+ transcript, depending on cell cycle (180). Given the need for histone replacement throughout the life of a cell, it seems plausible that other "hybrid" histone genes might exist to provide new histone synthesis independent of S-phase.

Disruption of canonical histone processing factors SLBP, NELF, CBC, CDK9 or Ars2 also resulted in these cryptically spliced and polyadenylated transcripts (179, 181-183). Interestingly, overall transcription of canonical histone genes increased along with removal of the machinery necessary to process the stem-loop containing UTR. This leads to an interestingly possibility where in post-mitotic tissue in which the RD histone machinery is absent, some of these genes can be expressed as polyadenylated transcripts instead. In these studies, the authors often describe the disruption of "correct" 3' processing followed by aberrant polyadenylation, but the fact that this phenomenon is observed in so many cases warrants further exploration as to whether this occurs naturally in post-mitotic tissues (179, 181, 182).

Cellular stress has also been reported to increase canonical H3 polyadenylation. Arsenic exposure resulted in an increase in polyA+ H3.1 transcripts, as well as increased overall H3 levels (164). This process was SLBP dependent and could be reversed by SLBP overexpression, giving further evidence towards the idea that a lack of stem-loop processing results in cryptic polyadenylation of canonical histone genes. Irradiation induced double strand breaks and temperature shock can also cause an increase in polyA+ canonical histone mRNA (163, 184). These studies also saw an increased stability of these polyadenylated transcripts, possibly mediated by HuR. Opinion is split on the functionality of these polyA+ canonical transcripts, which in some instances aggregate in the nucleus (179), whereas others report export to the cytoplasm and association with ribosomes (163, 185). Interestingly, RNA pol II was found through GRO-seq experiments to occupy the promoters of ~60% of canonical histone genes in nondividing tissue (162). In *Drosophila*, there is precedence for compensation by canonical histone of H3.3 disruption. In a H3.3 null flies, H3.2 were found to be upregulated and polyadenylated, likely through alternative 3' end processing (186). Additionally, they found that H3.1/2 could be incorporated outside of replication, possibly using replication-independent chaperones. Whether HIRA can in fact bind and deposit canonical H3 has not been shown conclusively but does pose a tantalizing possibility for the compensation I observed in dKO-R. This upregulation and deposition of H3.1/2 in H3.3 nulls has not been shown in mammals, and further investigation is required. Together, there is a significant body of work converging on the possibility that replication-dependent histones might not be as cell-cycle restricted as previously thought. These are however contextual findings, and would require further investigations in specific contexts, including in post-mitotic neurons.

Post-mitotic canonical histone expression may extend to other histone types beyond H3. H3.3 is well established as the replacement H3, yet H2a, H2b, and H4 have no clear replacement variants. H2a has H2afx and H2afz variants, but each play very specific roles in DNA damage repair and forming unstable nucleosomes, and a more general replacement variant or variants may still exist. Although not formally annotated, there are examples of polyadenylated and replication independent histone variants in the literature. HIST1H4G has been found to also be transcribed as a polyA+ transcript, possibly independent of S-phase. However, this variant was also found elevated in breast cancer and only codes for ~85% of the full H4 protein, is localized to the nucleoli, and may not form fully functional nucleosomes (187). Other studies have identified H4 transcripts that may be polyadenylated, but whether these are translated or if the resulting protein can be incorporated remains to be shown (188, 189). Nonetheless, most H3.3 turnover is associated with $(H3\text{-}H4)_2$ tetramer turnover, which would imply either there is a robust replication-independent H4 variant similar to H3.3, or that the H4 is somehow very well maintained throughout postmitotic life. H3.3 turnover and modifications are also known to affect H4 PTMs, bringing up questions over whether it is H3.3 marks recruiting other chromatin modifiers to affect the adjacent H4 molecules, or whether the H3-H4 tetramer turned over are replaced by newly synthesized H3 and H4 with a blank slate of PTMs.

Poorly-annotated variants

Another possible source of post-mitotic H3 is an unannotated, replication-independent H3.3-like variant. Given that the H3.3 IHC staining was affected by my H3.3 conditional knockouts, this unannotated variant would have to differ substantially from

H3.3 as to not have immunoreactivity with the H3.3 antibody, either at S31 or within the AAIG motif. Differences to these residues would alter the modification potential of the new variant's N' tail or interactions with histone chaperones. There is however precedent for such poorly annotated variants in the genome. Being one of the earliest evolved proteins, histone genes including H3 have undergone duplication and pseudogenization throughout evolution (56). Although H3.3 remains the predominant source of replication independent H3, there has recently been described H3.3-like variants that are expressed and can functionally incorporate into nucleosomes (190). It is possible that these are the product of duplication events that remained active yet escaped annotation. Some of these variants are expressed, and may in fact display preferential expression in the brain (66). While relatively newly discovered, there remains the possibility that these variants are able to compensate for a lack of H3.3 in aging neurons, yet not in recently post-mitotic neurons during establishment of the transcriptome.

In light of the of transcriptomic, cellular identity, and axonal projection phenotypes I observed (Chapter 3) the putative compensatory mechanism is clearly unable to replace H3.3 within the critical window I found during development. That H3.3 replacement happens much more slowly in aging tissue might suggest that this unknown supply of H3 is fairly limited but can produce enough replacement H3 for slower long term maintenance.

Additionally, the lack of changes to H3 PTMs is of note. H3.3 is often found to be enriched for certain marks, mostly associated with transcriptional activity. However, H3.3 is also found in heterochromatic regions with repressive marks. Here I found by immunostaining that loss of H3.3 does not observably change PTM levels on a global

level. While closer inspection is warranted to try and determine more subtle shifts in PTMs and their loci, these findings would add to an emerging idea of H3.3 function. Primarily, that the biochemical structure of H3.3 doesn't confer particular function to the underlying DNA, and that canonical H3 or other H3s have the same capacity for modification to shape chromatin regulation.

Whatever the H3.3 alternative is, it must still be deposited onto the genome to effectively compensate for and replace the missing H3.3. Canonical H3 is deposited by CAF1, but this process is DNA-synthesis dependent, and involves interaction between CAF1 and the clamp complex PCNA, making this an unlikely candidate, even if it is canonical H3 that compensates. HIRA and DAXX are the chief replication independent chaperone proteins, and interact with H3.3 through the AAIG motif unique to H3.3. HIRA has been found to bind and incorporate canonical histones in *Drosophila,* but only after H3.3 depletion (186). This opens up the possibility that mammalian HIRA may also be able to bind canonical H3 if H3.3 is no longer available. In the scenario that an unannotated H3 variant exists in neurons, it would likely have to have favorable enough interactions with HIRA or DAXX for these chaperones to bind and deposit it. Pulldown experiments targeting these two chaperones, followed by mass spectrometry may prove useful in finding new binding partners for these chaperones in H3.3-depleted cells.

H3.3 Interaction with Enhancers

This study found that once the critical developmental window had passed, H3.3 was largely dispensable to maintain the neuronal transcriptome, at least in the context of L5 PT neurons. This is somewhat surprising given widespread evidence of H3.3 being enriched in active genes with activating marks and involved in initiating transcriptional

programs associated with differentiation (108). H3.3 is enriched at enhancer regions and with enhancer related PTMs including H3K27Ac, and found to exhibit increased turnover (100, 165, 191). The exact order of events is however unclear, and whether the high turnover at enhancers is caused by PTMs, or if these marks are a consequence of turnover or enhancer binding is not known. There is also the possibility that binding of these regions by proteins involved in enhancer activation necessitates new histones after displacing old nucleosomes. Here, I cover some of the potential mechanisms by which H3.3 interacts with enhancer regions.

Phosphorylation of S31 is one of key biochemical differences that differentiates H3.3 from canonical histones. This S31Phos has also been recently shown to promote p300/CBP activity, leading to enhancer acetylation (165). Additionally, the S31Phos mark is associated with evicting transcription inhibitor ZMYND11 (192). Depletion of H3.3 led to a reduction in H3K27Ac, and general deficits in the cells' ability to differentiate, similar to dKO-N and dKO-E. However, others have noted a surprising continuance of gene expression following chromatin regulator depletion, including the H3.3 chaperone HIRA, chromatin remodeler CHD1, and H3.3 itself (79, 87, 165, 193). Although I observed large changes to the transcriptome of dKO-N and dKO-E cortex, it seems probable that this is due to a lack of differentiation, rather than an alteration to transcriptional programs. The fact that neurons in dKO-R shows relatively little changes to the transcriptome, that dKO-N and dKO-E transcriptomes largely match each other, and that the affected genes are primarily those upregulated across development all support this idea. Together this would support a role for H3.3 in the activation of developmentally important enhancers associated with genes involved in establishing neuronal identity.

How exactly gene expression is maintained in the absence of H3.3 remains to be seen. Once acetylated by p300 or CBP, enhancers can then recruit further factors as well as stimulate the production of eRNAs (194). These factors are thought to then work independently of H3K27Ac and enhancer-promoter interactions to maintain transcription of their cognate genes (195). It has also been observed that once open, chromatin accessibility can stay in a euchromatic state despite depletion of H3.3K27Ac (196). While the distinctions between activation of enhancers, activation of transcription, and the perdurance of gene expression remain a much larger question, together this work point towards an H3.3 role in cell state transitions, helping to establish the transcriptome during differentiation, after which other processes work to maintain the cell state.

In this work, I found *H3f3a/H3f3b* co-deletion affected the developmental acquisition of the neuronal transcriptome (**Fig. 3.5**). Deficits in highly dynamic histone turnover at enhancers could well explain the deficits in gene expression observed (100). Differentiating between turnover, S31 mediated p300 acetylation, or other mechanisms remains a challenge, but there are likely numerous factors contributing to cell-state transition that H3.3 plays a role in. Given the increased H3.3 turnover rate at enhancers compared to gene bodies, the transcriptional changes I observed could be the result of deficits in enhancer activation rather than transcription per se. H3.3 replacement in gene bodies is also found to be contribute to gene activation (96), making the differentiation of these two processes difficult. The fact that inactive but poised enhancers and promoters have increased turnover rates is also interesting in light of my findings (100). H3.3 deletion may also be affecting the establishment of these poised regions, that then cannot correctly activate gene expression as the cell proceeds though differentiation.

Biochemical Function of H3.3

An open question in H3.3 biology is whether the H3.3 molecule itself plays a specific role in chromatin functionality, or does its presence merely reflect the replication-independent synthesis and deposition pathways it participates in. Histone stability is an important factor in the rate of dissociation and replacement of nucleosomes, as less stable complexes are more readily turned over (95, 99). One study showed H2A.Z-H3.3 containing nucleosomes to be less stable than those containing canonical H3, but other have disagreed that the H3.3 structure lends itself to inherently less stable nucleosomes (197, 198). Crystallography investigation concluded that nucleosomes containing canonical versus non-canonical histones had identical structures and stabilities (199). These studies however cannot disentangle the effects of PTMs versus histone proteins on stability within the *in vivo* cellular context. Whether the H3.3 molecules itself is subject to more or less turnover is difficult to untangle from the combination of chaperone proteins, PTMs, and the genomic enrichment that differentiate H3.3 from canonical histones. Nonetheless, the question of H3.3 turnover remains essential to its functionality in the cell. In this study, I found a small subset of transcriptomic changes in the affected dKO-R neurons that have lost H3.3 (**Fig. 4.5**). Whether these changes are a result of differences in canonical versus H3.3 containing nucleosomes, or an alteration of histone turnover rates remains to be seen.

Future Research

This work has helped define distinct roles for H3.3 in developing and aging neurons, and opened up many more questions about the role of H3.3 and histone turnover in the brain. I revealed a critical window in which H3.3 plays a role in establishing neuronal

identity and gene expression (Chapter 3). Whether it is the H3.3 molecule or the process of histone turnover that is important for this phenomenon has yet to be established. Furthermore, where this large increase in H3.3 is localized, both within the cell and within the genome is also yet to be determined. Additionally, I uncovered evidence for a non-H3.3 source of H3 in aging neurons, and discovering this source will be helpful in understanding what happens when typical replacement mechanisms are disrupted.

The importance of H3.3 versus histone turnover

H3.3 deletion in dKO-N resulted in widespread defects in transcription, axonal projection, and cellular identity, implicating H3.3 in all of these processes. Previous work has called into question whether H3.3 chromatin differs significantly from regions incorporating canonical H3 (135). Nucleosomes containing H3.3 are reported to have the same stability as those containing canonical H3, and it may be the processes of histone eviction and replacement, rather than the variant itself that enables normal acquisition of the transcriptome (199). To disambiguate the role of variant versus turnover, overexpression experiments using canonical and H3.3 expression vectors would be useful. Electroporation or viral transfection of a construct containing Cre and the canonical H3 gene would delete H3.3 but maintain canonical H3 expression past S-phase. Canonical H3 deposition is thought to be mediated by CAF1 and obligately linked to DNA-synthesis, although some counter examples do exist (55, 162, 186). Another option would be to use a mutant H3.3, where the S31 was changed to the canonical A31 to allow for interaction with RI chaperones HIRA and DAXX while still possessing a canonical H3 N-terminal tail. Successful rescue of the phenotypes I observed in dKO-N would suggest

that it is turnover, and not the H3.3 variants itself that is important for acquisition of neuronal transcriptome and identity.

Localization of H3.3

In this work have described global increases and decreases in H3.3 levels, as well as the state of PTMs in H3.3 depleted neurons. A logical next step would be to investigate at the genomic level where these shifts in histone variant levels occur. I found a large increase in H3.3 accumulation during post-mitotic neuronal development (**Fig 3.1**), accompanied by a shift in gene expression that was altered in H3.3 dKOs (**Fig 3.5**). H3.3 ChIP-seq or Cut&Run would be useful tools in determining whether the increase in H3.3 accumulation is accompanied by deposition, and if so which genomic regions are becoming enriched for H3.3. Previous work in cell culture has shown H3.3 enrichment with gene expression and chromatin accessibility, particularly at genes associated with differentiation (108). *In vivo* H3.3 ChIP-seq found a similar enrichment in active genes and their promoters, but found that this enrichment significantly diminished with age as H3.3 began to saturate the genome. Using a conditional H3.3 dKO model like dKO-R would be useful for exploring what happens when the slow replacement of canonical H3 with H3.3 is disrupted. Furthermore, ChIP would be useful in determining to what extent the genomic level of H3.3 is increasing during this period. One possibility is the increase in H3.3 I see in newly born neurons does not represent coating of the genome, but rather an increase in the soluble H3 pool as to facilitate increased and widespread turnover. H3.3 turnover at enhancers is extremely rapid, and differentiation requires the total rewiring of the transcriptome, along with substantial enhancer activation. Exploring the

location of DNA bound H3.3 will help to distinguish whether it is the H3.3 molecule per se or its facilitation of rapid histone turnover that drives these processes.

I found a putative connection between H3.3 and the resolution of bivalent promoters over cortical development. H3.3 is known to be enriched at bivalent TSSs, and mutation of H3.3 to the canonical H3 sequence abolishes this enrichment (87). What role H3.3 plays in the resolution rather than the establishment of these loci, particularly *in vivo* and in the context of the developing brain, is still unexplored. H3K27me3 and H3K4me3 ChIP-seq on the dKO-N mice would be of great interest in determining what happens to bivalent TSSs without H3.3. This would help to establish a mechanistic understanding of the role H3.3 plays in establishing the neuronal transcriptome.

In addition to active regions, H3.3 enrichment has been found in heterochromatinized loci as well, particularly in telomeric repeats (87). H3.3 is further involved in establishment of heterochromatin in centromeric regions, serving as a placeholder for CENP-A until it can be integrated later in G1 (72). It would be of interest to know what happens to these regions over time in neurons that lack *de novo* H3.3. Telomere maintenance in particular is critical to the longevity of all cells. The potential telomeric roles of H3.3 in aging cells remain to be seen.

Compensatory mechanism for H3.3 loss in mature neurons.

My results show a clear and progressive loss of H3.3 in neurons over the span of weeks and months, without overall H3 loss or cellular distress. This would imply that overall nucleosome levels remain constant and general chromatin architecture is grossly intact, despite prolonged absence of *de novo* H3.3 production. This would beg the question, what is replacing H3.3 protein in aging neurons? I have laid out several

possibilities above. Future study should focus on investigating these possibilities and identifying the histone source responsible for this compensation. This includes careful examination of polyA+ RNAseq data for canonical histones transcripts that are polyadenylated and should be further investigated. These reads could then be used to identify cryptic polyadenylation sites that lead to viable mRNAs. Additional validation should include confirmation by qRT-PCR and FISH specific to the polyA version of these transcripts and confirmation of their expression in neurons. Protein pulldown of HIRA or DAXX bound molecules coupled with mass spectrometry may help to identify which, if any, underappreciated histone variants are being deposited outside of S-phase in H3.3 null cells. Should a replacement histone be found, disruption of the gene or genes could be employed to create a completely replacement-deficient model in aging neurons. This would be an interesting paradigm to determine if overall nucleosome levels deplete and genome integrity fails, if histone turnover stalls completely and chromatin remains in stasis, or some other outcome results from more such manipulation.

Concluding Remarks

My dissertation established two distinct roles for H3.3 in neurons; first during a critical developmental window in newly post-mitotic neurons and then later in mature neurons as a source of replacement H3. Through transcriptomic analysis, I defined a large portion of the neuronal transcriptome that is dependent on H3.3 to establish expression as the cell transitions from progenitor to neuron. My data also suggest that H3.3 is involved in more than just the establishment of bivalent loci, but also their developmental resolution. Along with the discovery that H3.3 is involved in upregulating genes associated with neuronal maturation, this work connects H3.3 regulation of gene

expression with the establishment of cortical layer identity and axonal connectivity. I further found that once established, H3.3 is largely dispensable for the maintenance of the neuronal transcriptome and neuronal subtype identity. This is one of very few studies that investigate the long-term impact of H3.3 deletion *in vivo*. Here, I found that in established neurons, there are no observed cellular or transcriptional consequences despite H3.3 depletion. I also found evidence for a non-H3.3 source of H3 in aging neurons, adding to a growing body of literature that converges on the possibility that H3.3 is not necessarily the only post-mitotic source of H3. These findings raise further questions about where and when H3.3 functions to shape development, as well as the biological functions of H3.3 turnover and replacement.

References

1. D. H. Geschwind, P. Rakic, Cortical evolution: judge the brain by its cover. *Neuron* **80**, 633-647 (2013).
2. V. B. Mountcastle, The columnar organization of the neocortex. *Brain* **120 (Pt 4)**, 701-722 (1997).
3. J. Del Río, A. Martínez, C. Auladell, E. Soriano, Developmental history of the subplate and developing white matter in the murine neocortex. Neuronal organization and relationship with the main afferent systems at embryonic and perinatal stages. *Cereb Cortex* **10**, 784-801 (2000).
4. D. H. Hubel, T. N. Wiesel, Anatomical demonstration of columns in the monkey striate cortex. *Nature* **221**, 747-750 (1969).
5. T. M. Preuss, P. S. Goldman-Rakic, Myelo- and cytoarchitecture of the granular frontal cortex and surrounding regions in the strepsirhine primate Galago and the anthropoid primate Macaca. *J Comp Neurol* **310**, 429-474 (1991).
6. D. C. Van Essen, H. A. Drury, S. Joshi, M. I. Miller, Functional and structural mapping of human cerebral cortex: solutions are in the surfaces. *Proc Natl Acad Sci U S A* **95**, 788-795 (1998).
7. E. G. Jones, Neurotransmitters in the cerebral cortex. *J Neurosurg* **65**, 135-153 (1986).
8. J. DeFelipe, Neocortical neuronal diversity: chemical heterogeneity revealed by colocalization studies of classic neurotransmitters, neuropeptides, calcium-binding proteins, and cell surface molecules. *Cereb Cortex* **3**, 273-289 (1993).
9. D. A. McCormick, Z. Wang, J. Huguenard, Neurotransmitter control of neocortical neuronal activity and excitability. *Cereb Cortex* **3**, 387-398 (1993).
10. R. Nieuwenhuys, The neocortex. An overview of its evolutionary development, structural organization and synaptology. *Anat Embryol (Berl)* **190**, 307-337 (1994).
11. S. E. Koester, D. D. O'Leary, Functional classes of cortical projection neurons develop dendritic distinctions by class-specific sculpting of an early common pattern. *J Neurosci* **12**, 1382-1393 (1992).
12. S. J. Butt *et al.*, The temporal and spatial origins of cortical interneurons predict their physiological subtype. *Neuron* **48**, 591-604 (2005).
13. S. H. Hendry, H. D. Schwark, E. G. Jones, J. Yan, Numbers and proportions of GABA-immunoreactive neurons in different areas of monkey cerebral cortex. *J Neurosci* **7**, 1503-1519 (1987).
14. M. Bradl, H. Lassmann, Oligodendrocytes: biology and pathology. *Acta Neuropathol* **119**, 37-53 (2010).
15. S. Hong *et al.*, Complement and microglia mediate early synapse loss in Alzheimer mouse models. *Science* **352**, 712-716 (2016).
16. H. Neumann, M. R. Kotter, R. J. Franklin, Debris clearance by microglia: an essential link between degeneration and regeneration. *Brain* **132**, 288-295 (2009).
17. D. Blackburn, S. Sargsyan, P. N. Monk, P. J. Shaw, Astrocyte function and role in motor neuron disease: a future therapeutic target? *Glia* **57**, 1251-1264 (2009).
18. D. P. Leone, K. Srinivasan, B. Chen, E. Alcamo, S. K. McConnell, The determination of projection neuron identity in the developing cerebral cortex. *Curr Opin Neurobiol* **18**, 28-35 (2008).

19. K. Y. Kwan, N. Sestan, E. S. Anton, Transcriptional co-regulation of neuronal migration and laminar identity in the neocortex. *Development* **139**, 1535-1546 (2012).
20. B. Molyneaux, P. Arlotta, J. Menezes, J. Macklis, Neuronal subtype specification in the cerebral cortex. *Nat Rev Neurosci* **8**, 427-437 (2007).
21. D. D. O'Leary, S. E. Koester, Development of projection neuron types, axon pathways, and patterned connections of the mammalian cortex. *Neuron* **10**, 991-1006 (1993).
22. J. DeFelipe, I. Farinas, The pyramidal neuron of the cerebral cortex: morphological and chemical characteristics of the synaptic inputs. *Prog Neurobiol* **39**, 563-607 (1992).
23. C. Lindwall, T. Fothergill, L. J. Richards, Commissure formation in the mammalian forebrain. *Curr Opin Neurobiol* **17**, 3-14 (2007).
24. T. J. Crow, Schizophrenia as the price that homo sapiens pays for language: a resolution of the central paradox in the origin of the species. *Brain Res Brain Res Rev* **31**, 118-129 (2000).
25. L. Cai, N. L. Hayes, R. S. Nowakowski, Local homogeneity of cell cycle length in developing mouse cortex. *J Neurosci* **17**, 2079-2087 (1997).
26. T. E. Anthony, C. Klein, G. Fishell, N. Heintz, Radial glia serve as neuronal progenitors in all regions of the central nervous system. *Neuron* **41**, 881-890 (2004).
27. T. Miyata *et al.*, Asymmetric production of surface-dividing and non-surface-dividing cortical progenitor cells. *Development* **131**, 3133-3145 (2004).
28. E. S. Anton, J. A. Kreidberg, P. Rakic, Distinct functions of alpha3 and alpha(v) integrin receptors in neuronal migration and laminar organization of the cerebral cortex. *Neuron* **22**, 277-289 (1999).
29. C. Lambert de Rouvroit, A. M. Goffinet, A new view of early cortical development. *Biochem Pharmacol* **56**, 1403-1409 (1998).
30. R. L. Sidman, P. Rakic, Neuronal migration, with special reference to developing human brain: a review. *Brain Res* **62**, 1-35 (1973).
31. P. Rakic, Neurons in rhesus monkey visual cortex: systematic relation between time of origin and eventual disposition. *Science* **183**, 425-427 (1974).
32. M. J. Koenderink, H. B. Uylings, Postnatal maturation of layer V pyramidal neurons in the human prefrontal cortex. A quantitative Golgi analysis. *Brain Res* **678**, 233-243 (1995).
33. H. Wichterle, J. M. Garcia-Verdugo, D. G. Herrera, A. Alvarez-Buylla, Young neurons from medial ganglionic eminence disperse in adult and embryonic brain. *Nat Neurosci* **2**, 461-466 (1999).
34. L. Sussel, O. Marin, S. Kimura, J. L. Rubenstein, Loss of Nkx2.1 homeobox gene function results in a ventral to dorsal molecular respecification within the basal telencephalon: evidence for a transformation of the pallidum into the striatum. *Development* **126**, 3359-3370 (1999).
35. T. Jessell, Neuronal specification in the spinal cord: inductive signals and transcriptional codes. *Nat Rev Genet* **1**, 20-29 (2000).
36. B. Chen *et al.*, The Fezf2-Ctip2 genetic pathway regulates the fate choice of subcortical projection neurons in the developing cerebral cortex. *Proc Natl Acad Sci U S A* **105**, 11382-11387 (2008).
37. R. Hevner *et al.*, Tbr1 regulates differentiation of the preplate and layer 6. *Neuron* **29**, 353-366 (2001).

38. J. M. Weimann *et al.*, Cortical neurons require Otx1 for the refinement of exuberant axonal projections to subcortical targets. *Neuron* **24**, 819-831 (1999).
39. P. Arlotta *et al.*, Neuronal subtype-specific genes that control corticospinal motor neuron development in vivo. *Neuron* **45**, 207-221 (2005).
40. K. Y. Kwan *et al.*, SOX5 postmitotically regulates migration, postmigratory differentiation, and projections of subplate and deep-layer neocortical neurons. *Proc Natl Acad Sci U S A* **105**, 16021-16026 (2008).
41. D. D. O'Leary, S. Sahara, Genetic regulation of arealization of the neocortex. *Curr Opin Neurobiol* **18**, 90-100 (2008).
42. C. MuhChyi, B. Juliandi, T. Matsuda, K. Nakashima, Epigenetic regulation of neural stem cell fate during corticogenesis. *Int J Dev Neurosci* **31**, 424-433 (2013).
43. S. Iwase, D. M. Martin, Chromatin in nervous system development and disease. *Mol Cell Neurosci* **87**, 1-3 (2018).
44. P. Oberst *et al.*, Temporal plasticity of apical progenitors in the developing mouse neocortex. *Nature* **573**, 370-374 (2019).
45. W. L. McKenna *et al.*, Tbr1 and Fezf2 regulate alternate corticofugal neuronal identities during neocortical development. *J Neurosci* **31**, 549-564 (2011).
46. C. Guo *et al.*, Fezf2 expression identifies a multipotent progenitor for neocortical projection neurons, astrocytes, and oligodendrocytes. *Neuron* **80**, 1167-1174 (2013).
47. M. Z. Ozair *et al.*, hPSC Modeling Reveals that Fate Selection of Cortical Deep Projection Neurons Occurs in the Subplate. *Cell Stem Cell* **23**, 60-73.e66 (2018).
48. J. C. Silbereis, S. Pochareddy, Y. Zhu, M. Li, N. Sestan, The Cellular and Molecular Landscapes of the Developing Human Central Nervous System. *Neuron* **89**, 248-268 (2016).
49. I. Olave, W. Wang, Y. Xue, A. Kuo, G. R. Crabtree, Identification of a polymorphic, neuron-specific chromatin remodeling complex. *Genes Dev* **16**, 2509-2517 (2002).
50. J. Lessard *et al.*, An essential switch in subunit composition of a chromatin remodeling complex during neural development. *Neuron* **55**, 201-215 (2007).
51. G. Arents, R. W. Burlingame, B. C. Wang, W. E. Love, E. N. Moudrianakis, The nucleosomal core histone octamer at 3.1 A resolution: a tripartite protein assembly and a left-handed superhelix. *Proc Natl Acad Sci U S A* **88**, 10148-10152 (1991).
52. J. C. Chan, I. Maze, Nothing Is Yet Set in (Hi)stone: Novel Post-Translational Modifications Regulating Chromatin Function. *Trends Biochem Sci* **45**, 829-844 (2020).
53. G. E. Zentner, S. Henikoff, Regulation of nucleosome dynamics by histone modifications. *Nat Struct Mol Biol* **20**, 259-266 (2013).
54. S. Biswas, C. M. Rao, Epigenetic tools (The Writers, The Readers and The Erasers) and their implications in cancer therapy. *Eur J Pharmacol* **837**, 8-24 (2018).
55. W. F. Marzluff, E. J. Wagner, R. J. Duronio, Metabolism and regulation of canonical histone mRNAs: life without a poly(A) tail. *Nature reviews. Genetics* **9** (2008).
56. A. P. Rooney, H. Piontkivska, M. Nei, Molecular evolution of the nontandemly repeated genes of the histone 3 multigene family. *Mol Biol Evol* **19**, 68-75 (2002).
57. Z. Nizami, S. Deryusheva, J. G. Gall, The Cajal body and histone locus body. *Cold Spring Harb Perspect Biol* **2**, a000653 (2010).
58. W. F. Marzluff, K. P. Koreski, Birth and Death of Histone mRNAs. *Trends Genet* **33**, 745-759 (2017).

59. M. M. Koseoglu, L. M. Graves, W. F. Marzluff, Phosphorylation of threonine 61 by cyclin a/Cdk1 triggers degradation of stem-loop binding protein at the end of S phase. *Mol Cell Biol* **28**, 4469-4479 (2008).
60. Q. Mei *et al.*, Regulation of DNA replication-coupled histone gene expression. *Oncotarget* **8**, 95005-95022 (2017).
61. W. F. Marzluff, P. Gongidi, K. R. Woods, J. Jin, L. J. Maltais, The human and mouse replication-dependent histone genes. *Genomics* **80** (2002).
62. R. S. Wu, W. M. Bonner, Separation of basal histone synthesis from S-phase histone synthesis in dividing cells. *Cell* **27**, 321-330 (1981).
63. R. S. Wu, S. Tsai, W. M. Bonner, Patterns of histone variant synthesis can distinguish G0 from G1 cells. *Cell* **31** (1982).
64. D. Brush, J. B. Dodgson, O. R. Choi, P. W. Stevens, J. D. Engel, Replacement variant histone genes contain intervening sequences. *Molecular and cellular biology* **5** (1985).
65. B. Bramlage, U. Kosciessa, D. Doenecke, Differential expression of the murine histone genes H3.3A and H3.3B. *Differentiation* **62**, 13-20 (1997).
66. K. Maehara *et al.*, Tissue-specific expression of histone H3 variants diversified after species separation. *Epigenetics Chromatin* **8**, 35 (2015).
67. S. Martire, J. Nguyen, A. Sundaresan, L. A. Banaszynski, Differential contribution of p300 and CBP to regulatory element acetylation in mESCs. *BMC Mol Cell Biol* **21**, 55 (2020).
68. D. C. Kraushaar *et al.*, Genome-wide incorporation dynamics reveal distinct categories of turnover for the histone variant H3.3. *Genome Biol* **14**, R121 (2013).
69. E. Szenker, D. Ray-Gallet, G. Almouzni, The double face of the histone variant H3.3. *Cell research* **21** (2011).
70. S. J. Elsässer, K. M. Noh, N. Diaz, C. D. Allis, L. A. Banaszynski, Histone H3.3 is required for endogenous retroviral element silencing in embryonic stem cells. *Nature* **522**, 240-244 (2015).
71. M. Udugama *et al.*, Histone variant H3.3 provides the heterochromatic H3 lysine 9 tri-methylation mark at telomeres. *Nucleic Acids Res* **43**, 10227-10237 (2015).
72. E. M. Dunleavy, G. Almouzni, G. H. Karpen, H3.3 is deposited at centromeres in S phase as a placeholder for newly assembled CENP-A in G_1 phase. *Nucleus* **2**, 146-157 (2011).
73. S. B. Hake *et al.*, Serine 31 phosphorylation of histone variant H3.3 is specific to regions bordering centromeres in metaphase chromosomes. *Proc Natl Acad Sci U S A* **102**, 6344-6349 (2005).
74. K. M. Bush *et al.*, Endogenous mammalian histone H3.3 exhibits chromatin-related functions during development. *Epigenetics Chromatin* **6**, 7 (2013).
75. A. Tvardovskiy, V. Schwämmle, S. J. Kempf, A. Rogowska-Wrzesinska, O. N. Jensen, Accumulation of histone variant H3.3 with age is associated with profound changes in the histone methylation landscape. *Nucleic acids research* **45** (2017).
76. I. Maze *et al.*, Critical Role of Histone Turnover in Neuronal Transcription and Plasticity. *Neuron* **87**, 77-94 (2015).
77. D. Bano, A. Piazzesi, P. Salomoni, P. Nicotera, The histone variant H3.3 claims its place in the crowded scene of epigenetics. *Aging (Albany NY)* **9**, 602-614 (2017).
78. L. A. Banaszynski *et al.*, Hira-dependent histone H3.3 deposition facilitates PRC2 recruitment at developmental loci in ES cells. *Cell* **155**, 107-120 (2013).

79. C. W. Jang, Y. Shibata, J. Starmer, D. Yee, T. Magnuson, Histone H3.3 maintains genome integrity during mammalian development. *Genes & development* **29** (2015).
80. S. G. Cox *et al.*, An essential role of variant histone H3.3 for ectomesenchyme potential of the cranial neural crest. *PLoS genetics* **8** (2012).
81. P. A *et al.*, Replication-Independent Histone Variant H3.3 Controls Animal Lifespan through the Regulation of Pro-longevity Transcriptional Programs. *Cell reports* **17** (2016).
82. M. E. Wimmer *et al.*, H3.3 Barcoding of Nucleus Accumbens Transcriptional Activity Identifies Novel Molecular Cascades Associated with Cocaine Self-administration in Mice. *J Neurosci* **39**, 5247-5254 (2019).
83. K. Shibahara, B. Stillman, Replication-dependent marking of DNA by PCNA facilitates CAF-1-coupled inheritance of chromatin. *Cell* **96**, 575-585 (1999).
84. S. E. Polo, D. Roche, G. Almouzni, New histone incorporation marks sites of UV repair in human cells. *Cell* **127**, 481-493 (2006).
85. Y. Shibata, Y. Seki, K. Nishiwaki, Maintenance of cell fates and regulation of the histone variant H3.3 by TLK kinase in. *Biol Open* **8** (2019).
86. C. Gal, K. M. Moore, K. Paszkiewicz, N. A. Kent, S. K. Whitehall, The impact of the HIRA histone chaperone upon global nucleosome architecture. *Cell Cycle* **14**, 123-134 (2015).
87. A. D. Goldberg *et al.*, Distinct factors control histone variant H3.3 localization at specific genomic regions. *Cell* **140**, 678-691 (2010).
88. C. M. Heaphy *et al.*, Altered telomeres in tumors with ATRX and DAXX mutations. *Science* **333**, 425 (2011).
89. M. S. Cosgrove, J. D. Boeke, C. Wolberger, Regulated nucleosome mobility and the histone code. *Nat Struct Mol Biol* **11**, 1037-1043 (2004).
90. E. L. Mersfelder, M. R. Parthun, The tale beyond the tail: histone core domain modifications and the regulation of chromatin structure. *Nucleic Acids Res* **34**, 2653-2662 (2006).
91. J. C. Chan, I. Maze, Nothing Is yet Set in (Hi)stone: Novel Post-Translational Modifications Regulating Chromatin Function. *Trends Biochem Sci* (2020).
92. A. E. Lepack *et al.*, Dopaminylation of histone H3 in ventral tegmental area regulates cocaine seeking. *Science* **368**, 197-201 (2020).
93. P. B. Becker, J. L. Workman, Nucleosome remodeling and epigenetics. *Cold Spring Harb Perspect Biol* **5** (2013).
94. D. C. Hargreaves, G. R. Crabtree, ATP-dependent chromatin remodeling: genetics, genomics and mechanisms. *Cell Res* **21**, 396-420 (2011).
95. S. Henikoff, Nucleosome destabilization in the epigenetic regulation of gene expression. *Nat Rev Genet* **9**, 15-26 (2008).
96. S. Venkatesh, J. L. Workman, Histone exchange, chromatin structure and the regulation of transcription. *Nat Rev Mol Cell Biol* **16**, 178-189 (2015).
97. A. J. Gossett, J. D. Lieb, In vivo effects of histone H3 depletion on nucleosome occupancy and position in Saccharomyces cerevisiae. *PLoS Genet* **8**, e1002771 (2012).
98. N. Sarai *et al.*, WHSC1 links transcription elongation to HIRA-mediated histone H3.3 deposition. *EMBO J* **32**, 2392-2406 (2013).
99. R. B. Deal, J. G. Henikoff, S. Henikoff, Genome-wide kinetics of nucleosome turnover determined by metabolic labeling of histones. *Science* **328**, 1161-1164 (2010).

100. A. M. Deaton *et al.*, Enhancer regions show high histone H3.3 turnover that changes during differentiation. *Elife* **5** (2016).
101. M. C. Tang *et al.*, Contribution of the two genes encoding histone variant h3.3 to viability and fertility in mice. *PLoS Genet* **11**, e1004964 (2015).
102. C. Couldrey, M. B. Carlton, P. M. Nolan, W. H. Colledge, M. J. Evans, A retroviral gene trap insertion into the histone 3.3A gene causes partial neonatal lethality, stunted growth, neuromuscular deficits and male sub-fertility in transgenic mice. *Hum Mol Genet* **8**, 2489-2495 (1999).
103. B. T. Yuen, K. M. Bush, B. L. Barrilleaux, R. Cotterman, P. S. Knoepfler, Histone H3.3 regulates dynamic chromatin states during spermatogenesis. *Development* **141**, 3483-3494 (2014).
104. J. S. Michaelson, D. Bader, F. Kuo, C. Kozak, P. Leder, Loss of Daxx, a promiscuously interacting protein, results in extensive apoptosis in early mouse development. *Genes Dev* **13**, 1918-1923 (1999).
105. C. Roberts *et al.*, Targeted mutagenesis of the Hira gene results in gastrulation defects and patterning abnormalities of mesoendodermal derivatives prior to early embryonic lethality. *Mol Cell Biol* **22**, 2318-2328 (2002).
106. A. Ors *et al.*, Histone H3.3 regulates mitotic progression in mouse embryonic fibroblasts. *Biochem Cell Biol* **95**, 491-499 (2017).
107. J. Jullien *et al.*, HIRA dependent H3.3 deposition is required for transcriptional reprogramming following nuclear transfer to Xenopus oocytes. *Epigenetics Chromatin* **5**, 17 (2012).
108. H. T. Fang *et al.*, Global H3.3 dynamic deposition defines its bimodal role in cell fate transition. *Nature communications* **9** (2018).
109. L. AE *et al.*, Aberrant H3.3 dynamics in NAc promote vulnerability to depressive-like behavior. *Proceedings of the National Academy of Sciences of the United States of America* **113** (2016).
110. W. Xia, J. Jiao, Histone variant H3.3 orchestrates neural stem cell differentiation in the developing brain. *Cell death and differentiation* **24** (2017).
111. J. Schwartzentruber *et al.*, Driver mutations in histone H3.3 and chromatin remodelling genes in paediatric glioblastoma. *Nature* **482**, 226-231 (2012).
112. G. Wu *et al.*, Somatic histone H3 alterations in pediatric diffuse intrinsic pontine gliomas and non-brainstem glioblastomas. *Nat Genet* **44**, 251-253 (2012).
113. S. Behjati *et al.*, Distinct H3F3A and H3F3B driver mutations define chondroblastoma and giant cell tumor of bone. *Nat Genet* **45**, 1479-1482 (2013).
114. A. Santenard *et al.*, Heterochromatin formation in the mouse embryo requires critical residues of the histone variant H3.3. *Nature cell biology* **12** (2010).
115. P. W. Lewis *et al.*, Inhibition of PRC2 activity by a gain-of-function H3 mutation found in pediatric glioblastoma. *Science* **340**, 857-861 (2013).
116. S. Bender *et al.*, Reduced H3K27me3 and DNA hypomethylation are major drivers of gene expression in K27M mutant pediatric high-grade gliomas. *Cancer Cell* **24**, 660-672 (2013).
117. B. T. Yuen, P. S. Knoepfler, Histone H3.3 mutations: a variant path to cancer. *Cancer Cell* **24**, 567-574 (2013).
118. A. Maver, G. Čuturilo, S. J. Ruml, B. Peterlin, Clinical Next Generation Sequencing Reveals an. *Balkan J Med Genet* **22**, 65-68 (2019).

119. V. Di Cerbo *et al.*, Acetylation of histone H3 at lysine 64 regulates nucleosome dynamics and facilitates transcription. *Elife* **3**, e01632 (2014).
120. L. Bjerke *et al.*, Histone H3.3. mutations drive pediatric glioblastoma through upregulation of MYCN. *Cancer Discov* **3**, 512-519 (2013).
121. A. Butler, P. Hoffman, P. Smibert, E. Papalexi, R. Satija, Integrating single-cell transcriptomic data across different conditions, technologies, and species. *Nat Biotechnol* **36**, 411-420 (2018).
122. T. J. Nowakowski *et al.*, Spatiotemporal gene expression trajectories reveal developmental hierarchies of the human cortex. *Science* **358**, 1318-1323 (2017).
123. H. J. Kang *et al.*, Spatio-temporal transcriptome of the human brain. *Nature* **478**, 483-489 (2011).
124. M. Buschbeck, S. B. Hake, Variants of core histones and their roles in cell fate decisions, development and cancer. *Nature Reviews Molecular Cell Biology* **18**, 299-314 (2017).
125. L. Telley *et al.*, Sequential transcriptional waves direct the differentiation of newborn neurons in the mouse neocortex. *Science* **351**, 1443-1446 (2016).
126. R. F. Hevner, R. D. Hodge, R. A. Daza, C. Englund, Transcription factors in glutamatergic neurogenesis: conserved programs in neocortex, cerebellum, and adult hippocampus. *Neurosci Res* **55**, 223-233 (2006).
127. S. Smith, B. Stillman, Stepwise assembly of chromatin during DNA replication in vitro. *The EMBO journal* **10** (1991).
128. T. C. Miller, A. Costa, The architecture and function of the chromatin replication machinery. *Current opinion in structural biology* **47** (2017).
129. C. J. Lin, M. Conti, M. Ramalho-Santos, Histone variant H3.3 maintains a decondensed chromatin state essential for mouse preimplantation development. *Development (Cambridge, England)* **140** (2013).
130. M. C. Tang, S. A. Jacobs, L. H. Wong, J. R. Mann, Conditional allelic replacement applied to genes encoding the histone variant H3.3 in the mouse. *Genesis (New York, N.Y. : 2000)* **51** (2013).
131. S. Goebbels *et al.*, Genetic targeting of principal neurons in neocortex and hippocampus of NEX-Cre mice. *Genesis* **44**, 611-621 (2006).
132. J. A. Gorski *et al.*, Cortical excitatory neurons and glia, but not GABAergic neurons, are produced in the Emx1-expressing lineage. *J Neurosci* **22**, 6309-6314 (2002).
133. P. Chen *et al.*, H3.3 actively marks enhancers and primes gene transcription via opening higher-ordered chromatin. *Genes Dev* **27**, 2109-2124 (2013).
134. C. M. Chow *et al.*, Variant histone H3.3 marks promoters of transcriptionally active genes during mammalian cell division. *EMBO reports* **6** (2005).
135. L. Shi, H. Wen, X. Shi, The Histone Variant H3.3 in Transcriptional Regulation and Human Disease. *Journal of molecular biology* **429** (2017).
136. S. B. Hake *et al.*, Expression patterns and post-translational modifications associated with mammalian histone H3 variants. *The Journal of biological chemistry* **281** (2006).
137. E. McKittrick, P. R. Gafken, K. Ahmad, S. Henikoff, Histone H3.3 is enriched in covalent modifications associated with active chromatin. *Proceedings of the National Academy of Sciences of the United States of America* **101** (2004).
138. A. Routh, S. R. Head, P. Ordoukhanian, J. E. Johnson, ClickSeq: Fragmentation-Free Next-Generation Sequencing via Click Ligation of Adaptors to Stochastically Terminated 3'-Azido cDNAs. *J Mol Biol* **427**, 2610-2616 (2015).

139. L. Shi, A. Qalieh, M. M. Lam, J. M. Keil, K. Y. Kwan, Robust elimination of genome-damaged cells safeguards against brain somatic aneuploidy following Knl1 deletion. *Nat Commun* **10**, 2588 (2019).
140. J. M. Keil *et al.*, Symmetric neural progenitor divisions require chromatin-mediated homologous recombination DNA repair by Ino80. *Nat Commun* **11**, 3839 (2020).
141. M. D. Robinson, D. J. McCarthy, G. K. Smyth, edgeR: a Bioconductor package for differential expression analysis of digital gene expression data. *Bioinformatics* **26**, 139-140 (2010).
142. E. P. Consortium, An integrated encyclopedia of DNA elements in the human genome. *Nature* **489**, 57-74 (2012).
143. B. E. Bernstein *et al.*, A bivalent chromatin structure marks key developmental genes in embryonic stem cells. *Cell* **125**, 315-326 (2006).
144. M. Sachs *et al.*, Bivalent chromatin marks developmental regulatory genes in the mouse embryonic germline in vivo. *Cell Rep* **3**, 1777-1784 (2013).
145. J. Liu, X. Wu, H. Zhang, G. P. Pfeifer, Q. Lu, Dynamics of RNA Polymerase II Pausing and Bivalent Histone H3 Methylation during Neuronal Differentiation in Brain Development. *Cell reports* **20** (2017).
146. R. J. Mullen, C. R. Buck, A. M. Smith, NeuN, a neuronal specific nuclear protein in vertebrates. *Development (Cambridge, England)* **116** (1992).
147. B. G. Rash, E. A. Grove, Area and layer patterning in the developing cerebral cortex. *Curr Opin Neurobiol* **16**, 25-34 (2006).
148. R. McEvilly, M. de Diaz, M. Schonemann, F. Hooshmand, M. Rosenfeld, Transcriptional regulation of cortical neuron migration by POU domain factors. *Science* **295**, 1528-1532 (2002).
149. S. P. Wise, The laminar organization of certain afferent and efferent fiber systems in the rat somatosensory cortex. *Brain research* **90** (1975).
150. W. Wenderski, I. Maze, Histone turnover and chromatin accessibility: Critical mediators of neurological development, plasticity, and disease. *Bioessays* **38**, 410-419 (2016).
151. M. S, B. LA, The roles of histone variants in fine-tuning chromatin organization and function. *Nature reviews. Molecular cell biology* **21** (2020).
152. L. A. Banaszynski, C. D. Allis, P. W. Lewis, Histone variants in metazoan development. *Developmental cell* **19** (2010).
153. W. LH *et al.*, Histone H3.3 incorporation provides a unique and functionally essential telomeric chromatin in embryonic stem cells. *Genome research* **19** (2009).
154. M. Heiman *et al.*, A translational profiling approach for the molecular characterization of CNS cell types. *Cell* **135**, 738-748 (2008).
155. G. Tau, B. Peterson, Normal development of brain circuits. *Neuropsychopharmacology* **35**, 147-168 (2010).
156. D. Z. Doyle *et al.*, Chromatin remodeler Arid1a regulates subplate neuron identity and wiring of cortical connectivity. *Proc Natl Acad Sci U S A* **118** (2021).
157. S. Henikoff, M. M. Smith, Histone variants and epigenetics. *Cold Spring Harbor perspectives in biology* **7** (2015).
158. L. DP *et al.*, Satb2 Regulates the Differentiation of Both Callosal and Subcerebral Projection Neurons in the Developing Cerebral Cortex. *Cerebral cortex (New York, N.Y. : 1991)* **25** (2015).

159. C. R. Gerfen, R. Paletzki, N. Heintz, GENSAT BAC cre-recombinase driver lines to study the functional organization of cerebral cortical and basal ganglia circuits. *Neuron* **80** (2013).
160. B. Piña, P. Suau, Changes in histones H2A and H3 variant composition in differentiating and mature rat brain cortical neurons. *Developmental biology* **123** (1987).
161. M. K. Urban, A. Zweidler, Changes in nucleosomal core histone variants during chicken development and maturation. *Developmental biology* **95** (1983).
162. S. M. Lyons *et al.*, A subset of replication-dependent histone mRNAs are expressed as polyadenylated RNAs in terminally differentiated tissues. *Nucleic Acids Res* **44**, 9190-9205 (2016).
163. V. Kari *et al.*, A subset of histone H2B genes produces polyadenylated mRNAs under a variety of cellular conditions. *PLoS One* **8**, e63745 (2013).
164. J. Brocato *et al.*, Arsenic induces polyadenylation of canonical histone mRNA by down-regulating stem-loop-binding protein gene expression. *J Biol Chem* **289**, 31751-31764 (2014).
165. S. Martire *et al.*, Phosphorylation of histone H3.3 at serine 31 promotes p300 activity and enhancer acetylation. *Nature genetics* **51** (2019).
166. A. Tafessu, L. A. Banaszynski, Establishment and function of chromatin modification at enhancers. *Open biology* **10** (2020).
167. M. S, N. J, S. A, B. LA, Differential contribution of p300 and CBP to regulatory element acetylation in mESCs. *BMC molecular and cell biology* **21** (2020).
168. A. Gunjan, A. Verreault, A Rad53 kinase-dependent surveillance mechanism that regulates histone protein levels in S. cerevisiae. *Cell* **115**, 537-549 (2003).
169. S. Jimeno-González *et al.*, Defective histone supply causes changes in RNA polymerase II elongation rate and cotranscriptional pre-mRNA splicing. *Proc Natl Acad Sci U S A* **112**, 14840-14845 (2015).
170. B. H. Toyama *et al.*, Identification of long-lived proteins reveals exceptional stability of essential cellular structures. *Cell* **154**, 971-982 (2013).
171. S. L. Commerford, A. L. Carsten, E. P. Cronkite, Histone turnover within nonproliferating cells. *Proc Natl Acad Sci U S A* **79**, 1163-1165 (1982).
172. B. E. Schwartz, K. Ahmad, Transcriptional activation triggers deposition and removal of the histone variant H3.3. *Genes Dev* **19**, 804-814 (2005).
173. O. J. Rando, H. Y. Chang, Genome-wide views of chromatin structure. *Annu Rev Biochem* **78**, 245-271 (2009).
174. C. Huang *et al.*, H3.3-H4 tetramer splitting events feature cell-type specific enhancers. *PLoS Genet* **9**, e1003558 (2013).
175. C. Huang, B. Zhu, H3.3 turnover: a mechanism to poise chromatin for transcription, or a response to open chromatin? *Bioessays* **36**, 579-584 (2014).
176. A. J. Cook, Z. A. Gurard-Levin, I. Vassias, G. Almouzni, A specific function for the histone chaperone NASP to fine-tune a reservoir of soluble H3-H4 in the histone supply chain. *Mol Cell* **44**, 918-927 (2011).
177. M. J. Apta-Smith, J. R. Hernandez-Fernaud, A. J. Bowman, Evidence for the nuclear import of histones H3.1 and H4 as monomers. *EMBO J* **37** (2018).
178. A. R. Banday *et al.*, Replication-dependent histone genes are actively transcribed in differentiating and aging retinal neurons. *Cell cycle (Georgetown, Tex.)* **13** (2014).

179. K. D. Sullivan, T. E. Mullen, W. F. Marzluff, E. J. Wagner, Knockdown of SLBP results in nuclear retention of histone mRNA. *RNA* **15**, 459-472 (2009).
180. E. Griesbach, M. Schlackow, W. F. Marzluff, N. J. Proudfoot, Dual RNA 3'-end processing of H2A.X messenger RNA maintains DNA damage repair throughout the cell cycle. *Nat Commun* **12**, 359 (2021).
181. T. Narita *et al.*, NELF interacts with CBC and participates in 3' end processing of replication-dependent histone mRNAs. *Mol Cell* **26**, 349-365 (2007).
182. J. J. Gruber *et al.*, Ars2 promotes proper replication-dependent histone mRNA 3' end formation. *Mol Cell* **45**, 87-98 (2012).
183. J. Pirngruber *et al.*, CDK9 directs H2B monoubiquitination and controls replication-dependent histone mRNA 3'-end processing. *EMBO Rep* **10**, 894-900 (2009).
184. I. Ryu *et al.*, HuR stabilizes a polyadenylated form of replication-dependent histone mRNAs under stress conditions. *FASEB J* **33**, 2680-2693 (2019).
185. V. Romeo, E. Griesbach, D. Schümperli, CstF64: cell cycle regulation and functional role in 3' end processing of replication-dependent histone mRNAs. *Mol Cell Biol* **34**, 4272-4284 (2014).
186. A. Sakai, B. E. Schwartz, S. Goldstein, K. Ahmad, Transcriptional and developmental functions of the H3.3 histone variant in Drosophila. *Curr Biol* **19**, 1816-1820 (2009).
187. M. Long *et al.*, A novel histone H4 variant H4G regulates rDNA transcription in breast cancer. *Nucleic Acids Res* **47**, 8399-8409 (2019).
188. L. SM *et al.*, A subset of replication-dependent histone mRNAs are expressed as polyadenylated RNAs in terminally differentiated tissues. *Nucleic acids research* **44** (2016).
189. T. S. Rai *et al.*, HIRA orchestrates a dynamic chromatin landscape in senescence and is required for suppression of neoplasia. *Genes Dev* **28**, 2712-2725 (2014).
190. M. K *et al.*, Tissue-specific expression of histone H3 variants diversified after species separation. *Epigenetics & chromatin* **8** (2015).
191. P. Chen *et al.*, H3.3 actively marks enhancers and primes gene transcription via opening higher-ordered chromatin. *Genes & development* **27** (2013).
192. A. Armache *et al.*, Histone H3.3 phosphorylation amplifies stimulation-induced transcription. *Nature* **583**, 852-857 (2020).
193. A. Gaspar-Maia *et al.*, Chd1 regulates open chromatin and pluripotency of embryonic stem cells. *Nature* **460**, 863-868 (2009).
194. R. Raisner *et al.*, Enhancer Activity Requires CBP/P300 Bromodomain-Dependent Histone H3K27 Acetylation. *Cell Rep* **24**, 1722-1729 (2018).
195. N. T. Crump *et al.*, BET inhibition disrupts transcription but retains enhancer-promoter contact. *Nat Commun* **12**, 223 (2021).
196. T. Zhang, Z. Zhang, Q. Dong, J. Xiong, B. Zhu, Histone H3K27 acetylation is dispensable for enhancer activity in mouse embryonic stem cells. *Genome Biol* **21**, 45 (2020).
197. C. Jin, G. Felsenfeld, Nucleosome stability mediated by histone variants H3.3 and H2A.Z. *Genes Dev* **21**, 1519-1529 (2007).
198. A. Thakar *et al.*, H2A.Z and H3.3 histone variants affect nucleosome structure: biochemical and biophysical studies. *Biochemistry* **48**, 10852-10857 (2009).
199. H. Tachiwana *et al.*, Structures of human nucleosomes containing major histone H3 variants. *Acta Crystallogr D Biol Crystallogr* **67**, 578-583 (2011).